MODEL-SCALE TESTS IN TURBULENT WIND

PART I

PHENOMENA DEPENDENT ON THE WIND SPEED

Shelter at Houses - Dispersal of Smoke

MARTIN JENSEN AND NIELS FRANCK

The Danish Technical Press
COPENHAGEN
1963

ATLASTRYK KØBENHAVN

PREFACE

The wind laboratory of the Technical University of Denmark was established by Professor Nøkkentved in 1936. The objects of the laboratory were to investigate natural wind conditions on the basis of model tests as well as tests in nature.

Until 1941 measurements were made of the shelter at screens both in nature and in wind tunnel, the work being particularly concentrated on the shelter given by systems of screens and hedgerows. The model tests and the measurements made in nature were not in satisfactory conformity and in course of time it became evident that the discrepancy was due to a difference in turbulence in the natural wind and the flow of air in the wind tunnel.

After a standstill due partly to the war the work on the problem of shelter at hedgerows and screens was resumed in 1946. A model technique was now successfully developed by use of a turbulent boundary layer in the wind tunnel, and by basing a model law on the roughness parameter of the logarithmic velocity profile conformity was obtained between the measurements in nature and the model tests.

These investigations of the shelter of hedgerows and screens were concluded in 1952 and were together with the model law published in Martin Jensen, Shelter Effect, Copenhagen, 1954.

After 1952 the wind laboratory continued investigations into the shelter at houses and the problem of the dispersal of smoke from chimneys. In connections with these investigations the model law was tested on ever-decreasing scale models.

This paper deals with the work of the wind laboratory from 1952 to 1957. From a theoretical point of view the model laws are, of course, the factor of prime importance. For practical purposes the results with regard to shelter at houses and the dispersal of smoke may be presumed to be of some interest. It must, however, be considered of greater importance that a model technique supported on

theory and tested in practice has become available making it possible in a suitably equipped aerodynamic laboratory to solve a number of important problems within these fields.

Almost all previous investigations within the fields here dealt with were carried out as model tests, and matters will frequently go wrong when the results of such model tests are transferred to nature. Except for those mentioned in Chapter 4 all the investigations reported on in this paper were checked by measurements in nature.

All the investigations mentioned deal with phenomena either depending directly on the speed of the wind, such as shelter, or directly connected with the speed, such as the dispersal of smoke. In the years 1957 to 1960 the wind load on houses and structures was investigated. Also in this respect regard must be paid to the turbulence of the wind in the model tests. A publication dealing with these investigations is in course of preparation and will be issued as Part II of this paper.

In 1960 the research work ceased as the wind laboratory was abolished.

E. Güntelberg, Ph.D. rendered valuable assistance in preparing the empirical method for the measurement of the CO_2-content of atmospheric air used in the quantitative model tests of smoke dispersal.

The economic basis for the investigations into shelter at houses and dispersal of smoke was provided by the Danish National Institute of Building Research.

The translation into English was performed by Mr. P. Prom.

Figures and tables are numbered according to the page on which they are printed. Thus, Figure 18 is to be found on page 18.

CONTENTS

Figures and tables are numbered according to the page on which they are printed. Thus, Fig. 18 is to be found on page 18.

1. APPARATUS AND EXPERIMENTAL TECHNIQUE

1.1 Cup-anemometer. Lattice-masts

Cup-anemometer. The speed of the wind in nature was measured by means of a cup-anemometer. The apparatus was designed to measure the mean speed of the wind over a given period, say, one minute.

As natural wind is changing speed all the time, the measurement of the mean value presents certain difficulties. A cup-anemometer cannot follow the pulsations of the wind but will give a damped variation. The mean value of this damped rotation is different from the mean value of the wind. In order that the optimum results may be obtained, the apparatus must be so designed as to follow the pulsations of the wind as closely as possible. The object is, in the first place, to obtain a great turning moment from the wind, in the second place, a small moment of inertia of the mass of the rotating parts and, in the third place, the minimum friction in bearings, gears and contact path.

A series of experiments with different shapes of cups proved that hemispherical cups gave the maximum turning moment in proportion to the weight of the cup.

In a second series of experiments the number of cups was varied. 2 and 3 cups gave almost the same turning moment in proportion to the moment of inertia of the mass, but 2-cup-anemometers had dead points at which they could not start by themselves and this was not the case when 3 cups were used. When 4 or more cups were used the moment of inertia increased far more than the turning moment. It is therefore better to use 3 cups.

Finally, a third series of experiments proved the most favorable ratio between the diameter of the cup and its radius to the axis of rotation to be about 1÷1.

The apparatus resulting from the abovementioned experiments has the following technical data, see also Figures 2 and 3. It has 3 hemispherical cups, r = 2.4 cm. The cups are pressed on a spinning lathe out of 0.04 cm aluminium sheeting with a 0.2 cm bulb along the edge. Weight per cup 4.3 g. The cups are riveted to arms of aluminium of circular cross-section, diameter 0.3 cm. Radius to the centre of cup 4.8 cm. The plane of the cup's

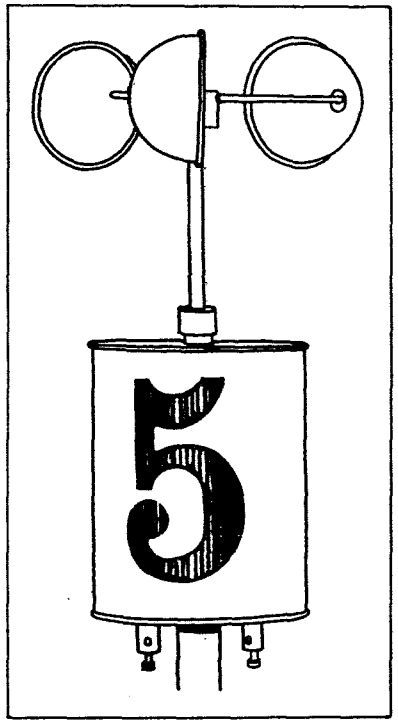

Fig. 2. Cup-anemometer.
The total height of the apparatus is 25 cm. The casing is 11 cm high and 8.3 cm in diameter.
The anemometer closes the contact for each 6.4 revolutions and the count is made by an electrical counter.

opening contains the axis of rotation. The arms carrying the cups are by means of Araldite glued to an aluminium head, diameter 1.3 cm, screwed to the top of the axle. The axle is of brass, of diameter 0.5 cm, and runs on two ball-bearings, SKF No.13 300. The bearings are cleaned of grease and kept lubricated with a very thin oil. The lower end of the axle carries a gear with 15 teeth driving a gear with 96 teeth. The axle of the large gear is provided with a contact cylinder, diameter 0.5 cm, one-half of the circumference of which is of the insulation material Araldite and the other half of brass connected to one terminal of the apparatus. A spring of phosphor - bronze connected to the other terminal presses against the contact cylinder with a force of 15 g. The circuit in the anemometer will be closed when the set of cups has made 6.4 revolutions and the number of contacts is registered by a counter connected with the apparatus. The moment of inertia of the mass of the rotating parts is 0.38 g cm s^2.

The measuring panel is for each cup-anemometer provided with an electrical impulse counter with four digits, 24 V, 500 Ohm. The counters can register a maximum of 10 impulses per second.

In the circuit between the cup-anemometer and the counter a clockwork switch has been inserted for automatic control of the measuring time.

The laboratory has 12 cup-anemometers of the type described above.

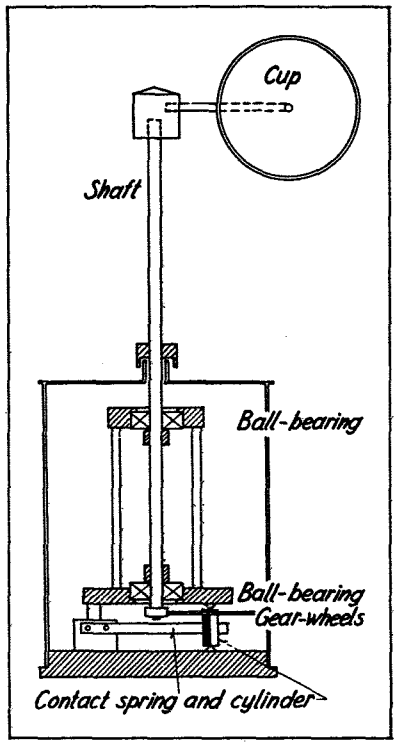

Fig. 3. Cup-anemometer.

The cup - anemometers were adjusted in the 60·60 cm wind tunnel of the laboratory. If the speed of the wind, v, is plotted in terms of the number of impulses per minute, N, a straight line will be obtained, common to all twelwe apparatus. The line has the equation

$$v = 0.084\ N + 0.6$$

v m/s, N impulses per minute. The lower limit for the use of the apparatus is that during measurements the speed of the wind must not get below 1.5 m/s, so the mean value should probably not be less than 2.5 m/s. The upper limit is determined by the fact that the counter can cope with 10 impulses per second, that is N = 600, to which corresponds v = 50 m/s as the maximum speed in the gusts. The maximum value of the mean speed ought not exceed 30 m/s.

Lattice-masts. For the installation of the cup-anemometers for measurements in nature two lattice - masts were built. They were designed with a view to lightness, rigidity and strength.

The masts consist of sections, 2 m in length. As shown in Figure 4a they are of triangular cross-section. They are built of three mahogany battens connected by a lattice of aluminium tubes. At the joints the tubes are squeezed flat and fastened with screws.

The sections are joined together by Fish-plates of aluminium and 1/4" brass bolts.

Otherwise the data of the two stands are as follows:

		16 m	12 m
Length			
Cross-sections of battens		4.0/2.0 cm	3.0/2.0 cm
Tubes for lattice	D/d	1.2/1.0 cm	1.0/0.8 cm
Weight		2.5 kg/m	2.0 kg/m

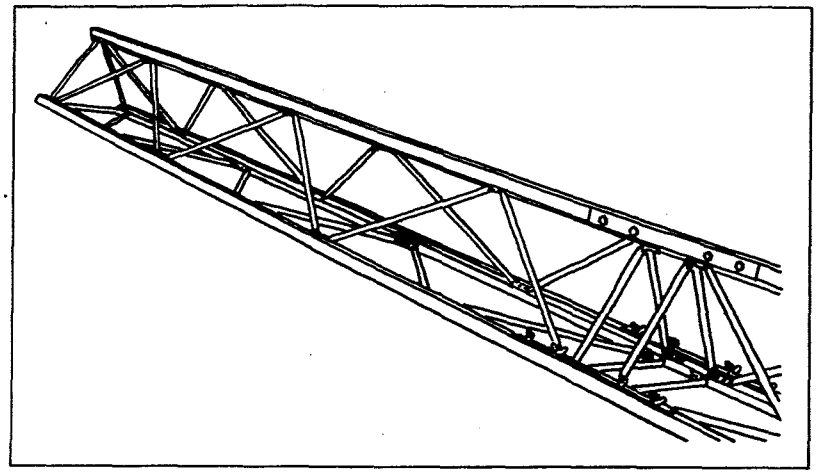

Fig. 4a. Section of a lattice-mast.
The mast may be assembled in a total length of 16 m and weighs only 40 kg.

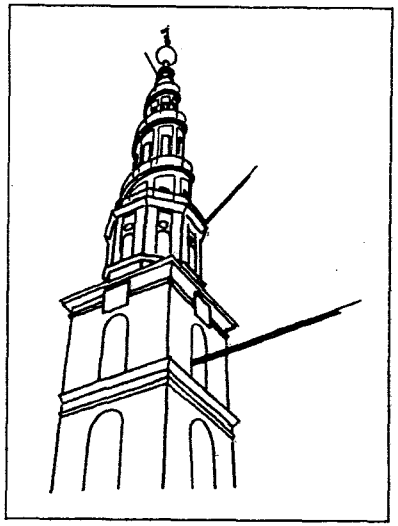

Fig. 4b. The spire of the Church of Our Saviour in Copenhagen.
3 cup-anemometers are mounted for the measurement of the velocity profile over the central part of Copenhagen. The two lowermost anemometers are mounted on light lattice-masts like that shown in Fig. 4a. The uppermost anemometer is seen to the left below the ball on the top af the spire.

Figure 4b shows the stands in use for measurements at the 80 m spire of the Church of Our Saviour in Copenhagen. The stands are placed horizontally and carry a cup-anemometer at their outer ends.

1.2 Wind tunnel. Pitot-static tubes. Manometer

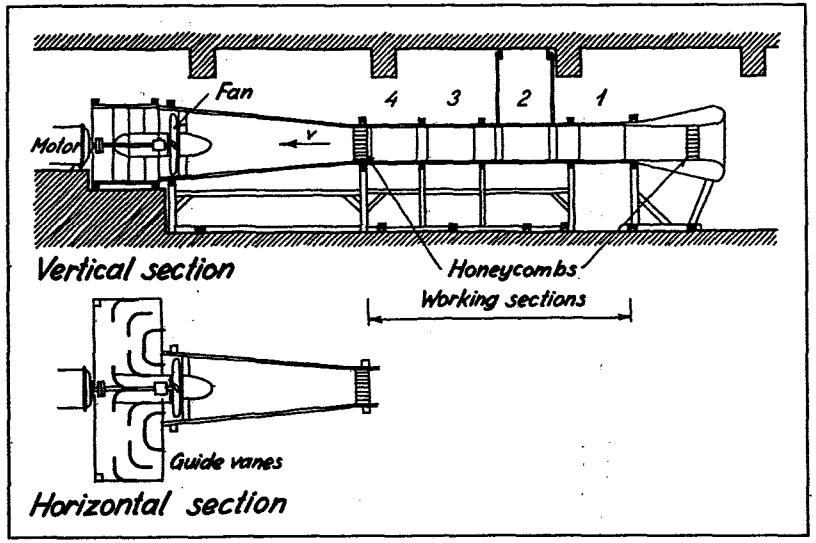

Fig. 5. Wind tunnel in the wind laboratory of the Technical University of Copenhagen.
The tunnel is of closed working section type. Its cross-section is square, 60·60 cm, the full length 10 m.

Wind tunnel. The laboratory tests were made in a wind tunnel of the type with enclosed working section and open return flow. The tunnel, which is shown in Figure 5, is 60·60 cm in cross-section and has a total length of 10 m.

A detailed description of the tunnel is to be found in Martin Jensen: 'Shelter Effect', Copenhagen, 1954.

The 4 sections of the experiment stage are of a total length of 5.5 m and at each end provided with honeycombs.

In a number of the tests carbon dioxide or smoke was dispersed in the tunnel. In order to obviate an increasing contamination of the air in the room, an interimistic partition was built across the laboratory, separating the inlet and outlet openings of the tunnel. During the experiments the spaces on both sides of the partition were open to the air, so that pure atmospheric air was sucked into the tunnel.

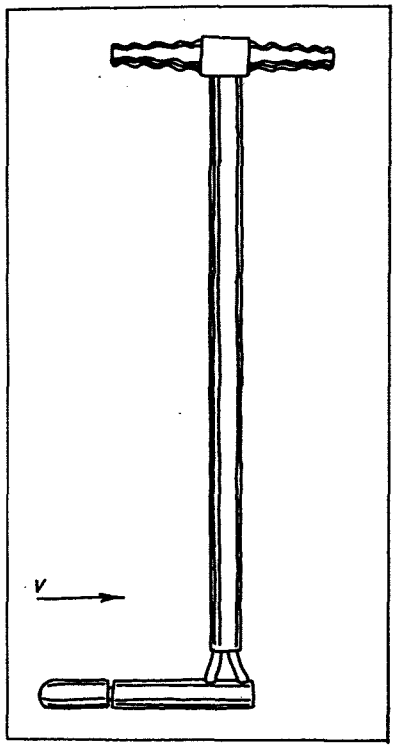

Fig. 6a. Pitot-static tube of Prandtl type.
The length of the lower horisontal branch is 9 cm.

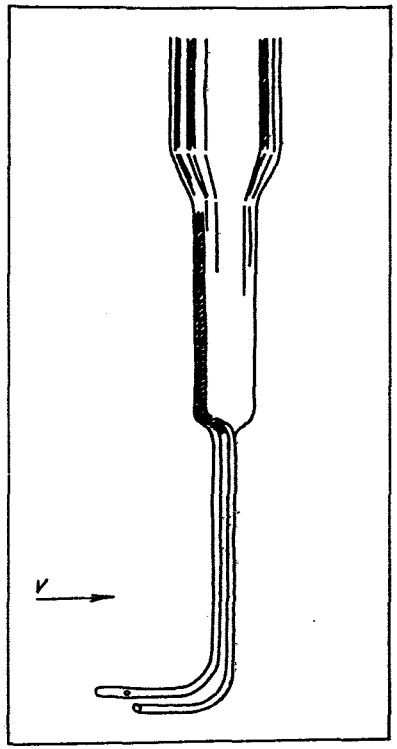

Fig. 6b. Pitot-static tube for precision measurements.
The length of the longer horizontal branch is 1.2 cm.

Pitot-static tubes. The velocity of the wind in the tunnel was measured by means of pitot-static tubes and a manometer.

A pitot-static tube of Prandtl-type is shown in Figure 6a. The total pressure is taken from a hole at the point of the horizontal branch and the static pressure from a slit situated 3 times the diameter of the tube from the point of the branch.

For finer measurements of velocity profiles in the different boundary layers in the tunnel, the pitot - static tube shown in Figure 6b was used.

The two branches are tubes of external diameter 0.1 cm.

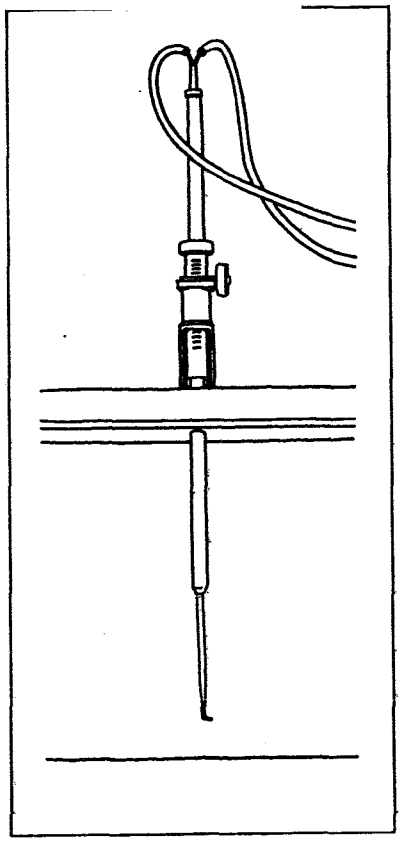

Fig. 7. Holder for the pitot-static tube in Fig. 6b.
By means of the holder the pitot-static tube may be placed at any point of the vertical symmetrical plane of the tunnel.

The short branch is open at the end so that the pressure there will be the sum of the dynamic and static pressures.

The longer branch protrudes 0.3 cm forward of the short branch and is closed at the end but provided with two lateral holes, d = 0.009 cm, abreast of the point of the short branch. From these holes the static pressure is taken.

The velocity pressure will thus be registered by a manometer, the two sides of which are connected with the two branches of the pitot - static tube.

The pitot - static tube was mounted in the manner shown in Figure 7, so that it might be moved in the vertical, symmetrical plane of the wind tunnel and adjusted with an accuracy of 0.01 cm.

Manometer. The air pressure was measured by means of a manometer of FUESS manufacture with sloping scale.

The manometer liquid was alcohol of specific gravity 0.800, and the scale, graduated in mm, may be inclined corresponding to factors of 0.4, 0.2, 0.1 and 0.05 of the pressure of mm water column.

The manometer is shown in Figure 8.

In the measurement of velocity pressure the pressure pulsations were damped by the insertion of a 100 cm capillary tube, of internal diameter 0.1 cm, between the

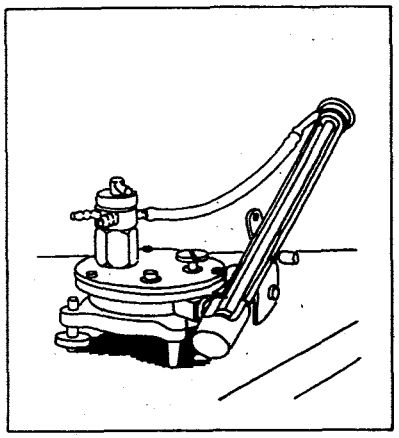

Fig. 8. FUESS manometer with sloping scale.
Length of manometer tube: 20 cm.

total pressure side of the pitot-static tube and the manometer. The flow in the capillary tube due to the pulsations is of so low velocity as to be laminary, so that the damping will give the correct mean value.

1.3 Hot-wire anemometer

By measurements in the wind tunnel of the speed of the wind in areas in which the direction of the wind could be determined only with approximation, for instance at screens or around models of houses, use was made of a hot-wire anemometer the detector of which is almost insensitive to the direction of the wind. Under such circumstances pitot-static tubes are less suitable due to their sensitiveness to direction.

The righthand side of Figure 9 shows the hot-wire detector used.

The actual hot-wire is a platinum wire of diameter 0.03 mm and 3 mm in length. In a few experiments wires 6 mm long were used. The ends of the wire are welded to two heavier platinum wires, d = 0.1 mm, which in turn are soldered to two manganin wires, d = 0.75 mm. The manganin wires are taken through two glass tubes, glued by means of Araldite to an acryl head, to two terminals fastened to the acryl head.

The welding of the platinum wires was performed in the following manner: One end of the detector wire, in the following called A, is wound tightly once around one of the

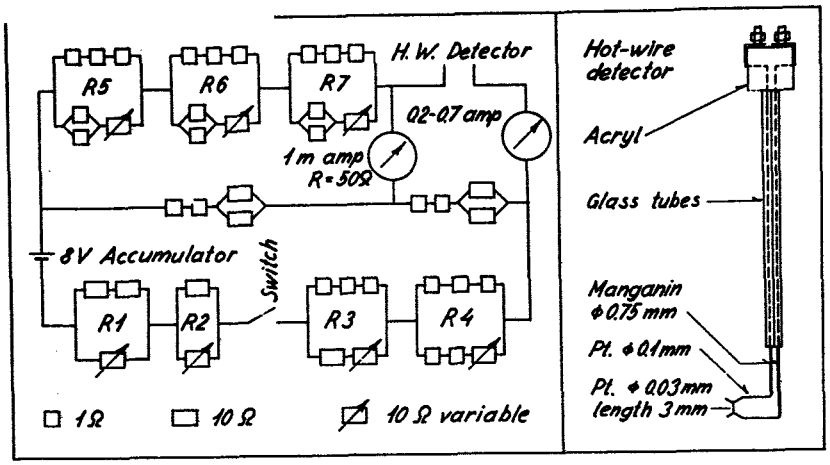

Fig. 9. Hot-wire anemometer on the constant-resistance principle.
To the left a diagram of the metering bridge. To the right a detector with a 3 mm long hot-wire.
The total height of detector: 13 cm.

heavier platinum wires, in the following called B, in the desired position about 1 mm from the end of B.

A carbon rod is placed in contact with the same end of B. The other end of the carbon rod is connected with one pole of a 4 V storage battery the other pole of which is through B connected with terminal B on the acryl head.

If the circuit is closed for about one second, B will be heated to bright redness and this heating will be sufficient to weld wires A and B together.

Wire A should be so mounted as to be under a slight tension sufficient to keep A tight during the tests. This may be done by bending wires B suitably from each other during the mounting.

The detector is so designed that it will give little disturbance of the flow of air while at the same time its suspension is sufficiently rigid to prevent vibrations of the wire. In the wind tunnel the detector was mounted on a portable stand so that it might be placed anywhere in the tunnel.

The hot-wire detector was connected with one side of a Wheatstone bridge as shown in the diagram in the lefthand side of Figure 9.

Measurements of the velocity of the wind were made

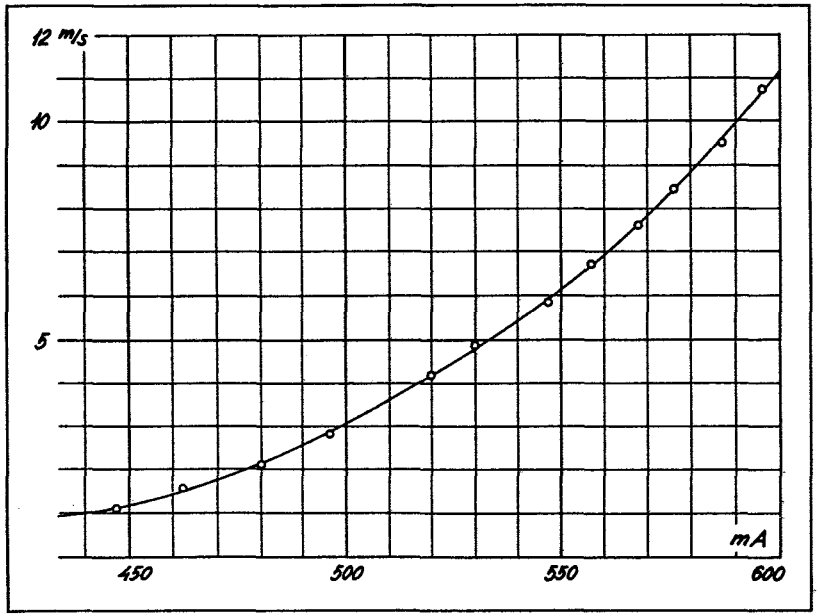

Fig. 10. Calibration curve for hot-wire anemometer with 3 mm long hot-wire.
The abscissa is the amperage through the hot-wire in mA, the ordinate the speed of the wind in m/s.

according to the constant – resistance method, that is to say that the resistance of the wire is kept constant during measurements so that the amperage required may be taken as a measure of the velocity of the wind at the wire.

The zero instrument of the bridge is an ammeter with an internal resistance of 50 Ohm and full deflection of the needle at 1 mA.

For wind velocity v = 0 the other resistances in the bridge are so adjusted that the resistance and thus the temperature of the wire will be of a suitable value. In these experiments a temperature of about 500° C was used, i.e. the wire was just about to become incandescent.

If the hot-wire is exposed to a speed of wind it will give off an increasing amount of heat and its resistance will decrease. To return the temperature and resistance of the hot-wire to the original values and thereby stabilise the bridge, the current through the wire must be increased

and this is done by reducing the resistances R_1 R_2 R_3 and R_4. The amperage through the detector is measured on an ammeter with a range of 0.2 – 0.7 A and suppressed zero position.

Calibration of the hot-wire was performed in the free flow of air in the wind tunnel by means of a pitot-static tube. Thereby the correlated values of the wind velocity and the current through the hot-wire were determined.

Calibration was performed before and after each experiment.

Figure 10 shows a typical calibration curve for a 3 mm hot-wire. The device described is capable of measuring wind velocities of up to 15 m/s with an error of less than 0.5 m/s. The sensitiveness of the apparatus is highest for small wind velocities.

1.4 Tunnel coatings

To produce different turbulent boundary layers in the wind tunnel the bottom was provided with coatings of different roughness.

In all cases the coating extended from the honey comb at the inlet end to the 4th experiment section, i.e. over a length of 5.5 m. The coating extended over the entire width of the tunnel which is 60 cm.

Glazed cardboard. Sheets of glazed cardboard were fastened to the bottom of the tunnel with screws. A velocity profile is shown in Figure 49. The roughness parameter is $1.5 \cdot 10^{-3}$ cm. The thickness of the boundary layer in the 4th section was 10 cm.

Smooth masonite plates. Figure 13a. 0.3 cm thick plates of hard masonite were screwed to the bottom of the tunnel with the smooth side upwards. Examples of velocity profiles are shown in Figures 29 and 40. The roughness parameters are $1.8 \cdot 10^{-3}$ and $0.9 \cdot 10^{-3}$ cm respectively, and the thickness of the boundary layer in the 4th section 10 cm.

Sandpaper, Figure 13b, was glued to masonite plates screwed to the tunnel bottom. A velocity profile is shown in Figure 54. The roughness parameter is $2.5 \cdot 10^{-2}$ cm. The boundary layer was 12 cm thick in the 4th section.

Corrugated paper, Figure 14a, was glued to masonite plates screwed to the bottom of the tunnel. The height from the bottom of the corrugations to their crests was 0.35 cm, the distance between the crests 0.9 cm. Examples

of velocity profiles are given in Figures 29 and 40. The roughness parameters are 0.041 and 0.067 cm, respectively. Maximum thickness of boundary layer 14 cm.

2.5·2 cm fillets, Figure 14b. Wooden fillets, 2.5 cm in height and 2 cm in width were fastened to the bottom of the tunnel. First the fillets were placed at right angles to the longitudinal axis of the tunnel and spaced 20 cm apart. They were then turned at random up to 20°, and the space was likewise varied at random between 15 and 25 cm. A velocity profile will be seen in Figure 40. The roughness parameter is 0.41 cm and the thickness of the boundary layer 20 cm.

Small broken stones, Figure 15a. Cubical stones of sizes between 1.5 and 2 cm were distributed over the bottom of the tunnel. A velocity profile is shown in Figure 29. The roughness parameter is 0.37 cm and the maximum thickness of the boundary layer 15 cm.

Large broken stones, Figure 15b. Cubical stones of sizes from 3 to 6 cm were distributed over the tunnel bottom. A velocity profile is shown in Figure 29. The roughness parameter is 0.86 cm and the maximum thickness of the boundary layer 22 cm.

Model of a city. To meet the desire of obtaining a roughness corresponding to that of a model of a densely built-up area, attempts were made to place models of houses at random on the bottom of the tunnel. The velocity profiles of a series of arrangements of this kind, all of the same density, were measured.

It appeared that the velocity profiles might differ to a considerable extent, inasmuch as the arrangement of houses just in front of the point of measurement exerted a great influence.

Accordingly, it was evident that a model arrangement could not be made by putting up houses at random, but that it would be necessary to use a schematic location of the houses. After some initial experiments the arrangement of the houses described below was fixed and used in the further experiments.

The models were placed as shown in Figure 16 in rows across the tunnel at angles of 70 to 90° with the longitudinal axis of the tunnel. The angles were varied at random. The space between the rows of houses corresponded to the desired density of building. To avoid the possibility of a 'rythm' in the turbulence the spaces between the houses were varied slightly and casually.

Fig. 16.
Model of a city.

Fig. 14a.
Corrugated paper.

Fig. 14b.
2.5·2 cm fillets.

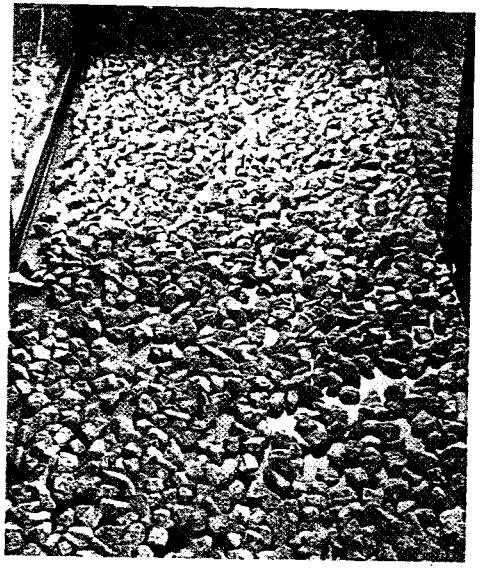

Fig. 15a.
Small broken stones.

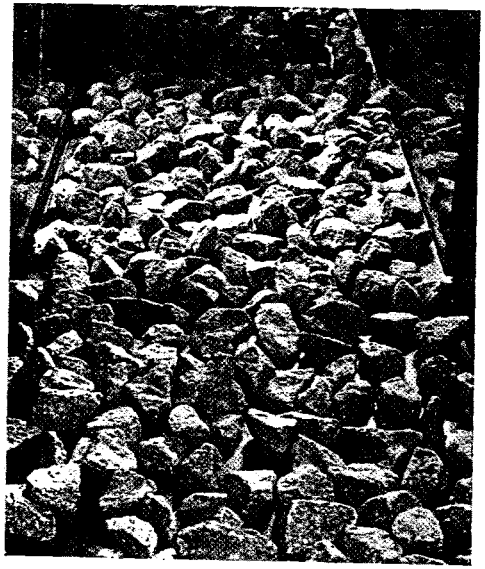

Fig. 15b.
Large broken stones.

Fig. 13b
Sandpaper.

Fig. 13a
Smooth masonite plates.

The house models were 2.9 cm wide and 7.0 cm high to the ridge of the roof. Roof slope 1÷1. They were glued to the rough side of the hard masonite plates described above. The density of the built-up area was 0.25. On a scale of about 1÷300 this will correspond to a densely built- up area of five-storey houses. The velocity profile is shown in Figure 29 . The roughness parameter was 3.5 cm and the maximum thickness of the boundary layer 30 cm.

In some experiments a turbulence grid was placed at the inlet end of the tunnel for the purpose of producing a thicker boundary layer. This did not have much effect on the roughness parameter and the velocity profile remained logarithmic. The boundary layer, however, became somewhat thicker, for corrugated paper and the city model up to 45 cm.

1.5 Smoke plant. Photographic technique

Smoke plant. For the performance of qualitative smoke tests in the tunnel a smoke plant was constructed as shown in the diagram in Figure 18.

The smoke was produced in a smoke generator of steel. Compressed air is supplied to the top of the generator and the smoke is forced out through the lower pipe into a large bottle operating as a precipitator. Thence the smoke passes through a venturi meter provided with a manometer to control the velocity of the smoke. The smoke then passes on to, for instance, a chimney model in the tunnel.

The smoke powder used, which gives off a dense, white smoke, is composed of 15 g sawdust with an admixture of a solution of 4 g KNO_3 and 1.5 g calcic soda in 18 ml water. After drying 18 cm^3 solar oil with asphalt is admixed.

The quantity of oxidiser, KNO_3, is thus slightly deficient, so that by supplying compressed air to the powder in a closed container the combustion may be controlled.

The powder is filled into a tinplate box with perforated bottom. This box is placed in the smoke generator where the powder is ignited by a gas flame. The smoke generator is then closed and compressed air admitted.

The smoke venturi meter is of brass. A longitudinal section is shown at the bottom of Figure 18. The venturi meter is adjusted by means of a gasometer.

From the smoke generator to the precipitator the smoke is taken through a copper tube, otherwise rubber hoses were used.

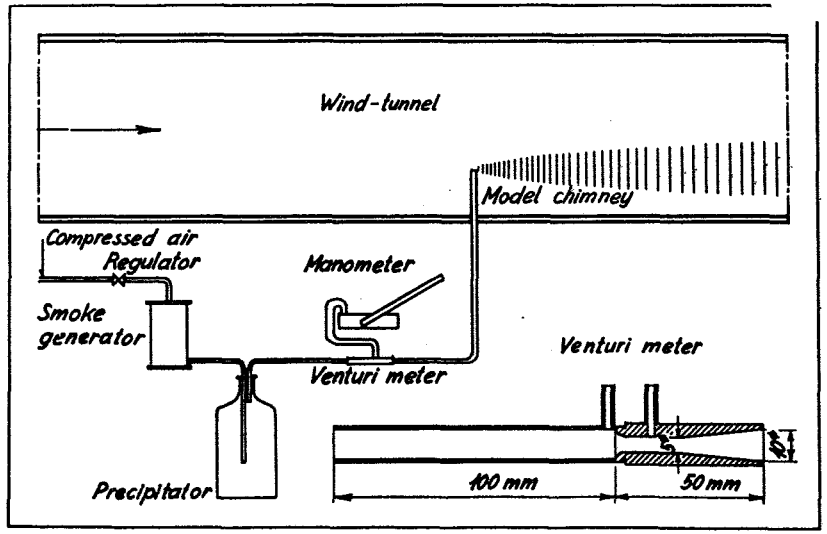

Fig. 18. Arrangement for visual smoke experiments.
The smoke is produced by combustion in the generator. The quantity of smoke is controlled by regulating the quantity of compressed air for the combustion. The quantity of smoke is measured by the venturi meter.

Photographic technique. Photographs of smoke plumes in the tunnel were mostly taken in the 4th section which was provided with a plate-glass window in one side and on the other side provided with an internal cover of black velvet.

In the ceiling of the 4th section a window was installed together with a case containing 3 photo-lamps each of 11.000 lm, so screened as to keep the light within a 50 cm wide field around the vertical, symmetrical plane of the tunnel.

For the photographic work use was made of a Leica camera and films ADOX KB 14, exposed corresponding to DIN 17/10 and somewhat overdeveloped.

1.6 CO_2 dosage. CO_2 analysis

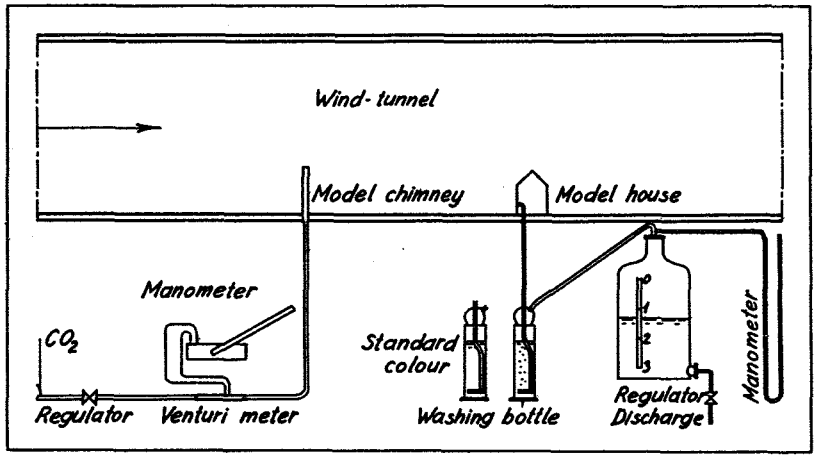

Fig. 19. Arrangement for quantitative smoke experiments.
The dosage is shown in the lefthand side of the figure. CO_2 is blown out of the chimney model. The quantity is measured by the venturi meter shown in detail in Fig. 18.
The analysis is shown in the righthand side of the figure. The CO_2-contaminated air is sucked out at the wall of a house model, passes through a washing bottle containing $Ba(OH)_2$ and an indicator.

For the model tests of smoke dispersal, CO_2 was used to represent smoke in the quantitative tests. The equipment for these measurements comprised a dosage plant and an analysis plant.

CO_2 dosage, lefthand side of Figure 19. From the CO_2 cylinder, which is provided with a reduction valve for fine adjustment, the CO_2 passes through a venturi meter of the same type as that used in the smoke plant. The venturi meter is connected to a FUESS manometer whereby the quantity of CO_2 flowing through it may be determined.

From the venturi meter the CO_2 is taken through a chimney model into the wind tunnel.

CO_2 analysis, righthand side of Figure 19. The quantity of CO_2 emerging from the chimney model at a given place in the wind tunnel is taken to express the contamination of the air at that place.

To make it possible to determine the CO_2 content of the air at any place in the tunnel use was made of the plant outlined in the righthand side of Figure 19. The suction of air from the tunnel might, for instance, as shown in Figure 19, take place from the front of a house model. In other cases, when it was desired to determine the CO_2 concentration at a point in the open air outside the house models, a thin copper pipe with its mouth placed at that point was used as a sampler.

The quantity of air sucked from the wind tunnel was in all cases of a magnitude which did not influence the main flow through the wind tunnel.

The sample of air from the wind tunnel was taken through a poly-vinyl hose to a wash bottle in which it was sucked through a solution of $Ba(OH)_2$. From the wash bottle the air was sucked into a flask. The vacuum required to suck the air through the system is produced by reducing the quantity of water in the suction flask. The quantity of water drained off corresponds to the quantity of air which has passed through the wash bottle.

The $Ba(OH)_2$ solution used in the experiments was a standard solution of 150 ml containing $3.5 \cdot 10^{-5}$ g mol $Ba(OH)_2$. To the solution was added a small quantity of the indicator thymol blue.

The method for the determination of the CO_2 content of the air sucked out depends upon the measurement of the quantity of air to be taken through the wash bottle to cause the indicator in the solution to change from blue to a yellowish colour.

The $Ba(OH)_2$ solution was prepared immediately before each test in order to prevent the CO_2 content of the atmospheric air from affecting the very weak solution.

For each test a double dose of the solution was made, i.e.300 ml, 150 ml of which was placed in the wash bottle while 150 ml was titrated with 0.01 n HCl to control the strength of the solution.

To the 300 ml solution was added 2 ml thymol blue, consisting of 0.2 g thymol blue + 14.5 ml NaOH dissolved in 400 ml distilled water. The range of change of the indicator is taken to be between p_H = 7.9 and 9.6. At 7.9 the colour is almost a pure yellow, at 9.6 almost a pure blue.

Furthermore, 7.5 g $BaCl_2,2H_2O$ was added to the 300 ml solution. This addition was necessary to reduce the CO_3^{--} concentration and thus the HCO_3^- concentration of the solution saturated with $BaCO_3$ formed by the passage through the wash bottle. $Ba(OH)_2 + CO_2 \rightarrow BaCO_3 + H_2O$.

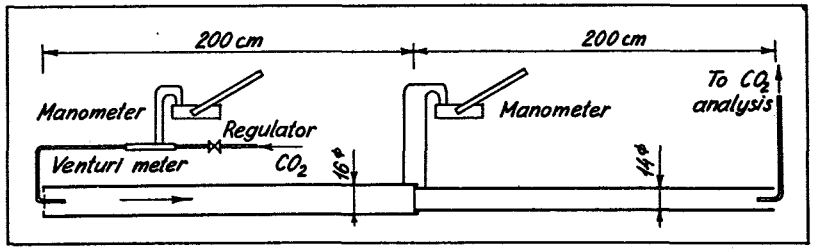

Fig. 21. Adjustment of CO_2-analysis.
Through the 4 m long steel tube atmospheric air is supplied in a quantity which may be measured by means of the venturi contraction of the tube. At the inlet end CO_2 is added in quantities controlled and measured by the small venturi meter. At the outlet end of the large tube the CO_2-contaminated air is sucked out for analysis in the plant shown in the righthand side of Fig. 19.

All tests were stopped when the indicator had assumed a given yellowish colour, a measuring glass containing a solution of that colour being placed beside the wash bottle as a standard of comparison.

The absorption of CO_2 in the wash bottle is not perfect. In the tests air was analysed containing up to 4 per mille added CO_2, and it applies to these mixtures that about 70% of the CO_2 content will be absorbed in the wash bottle when the rate of flow is about 1 l per hour.

Rather than calculating the quantity of CO_2 in the air on the basis of the strength of the $Ba(OH)_2$ solution, the quantity of air flowing through the apparatus and the absorption percentage, it was chosen to standardize the entire measuring process and by empirical means to find an adjustment curve for the CO_2 analysis.

The adjustment curve indicates the per mille of CO_2 added to the air in terms of the quantity of air that must be sucked through the bottle in order to make the indicator in the standard solution change colour.

Direct air mixtures containing known quantities of added CO_2 were produced, the mixture was sucked through the standard solution and determination was made of the volume of air flowing through it before colour changes gave the points of the adjustment curve.

For the adjustment the plant shown in Figure 21 was used. By means of the wind tunnel atmospheric air was sucked through the large steelpipe, the quantity being measured by the venturi contraction at the middle. At the same

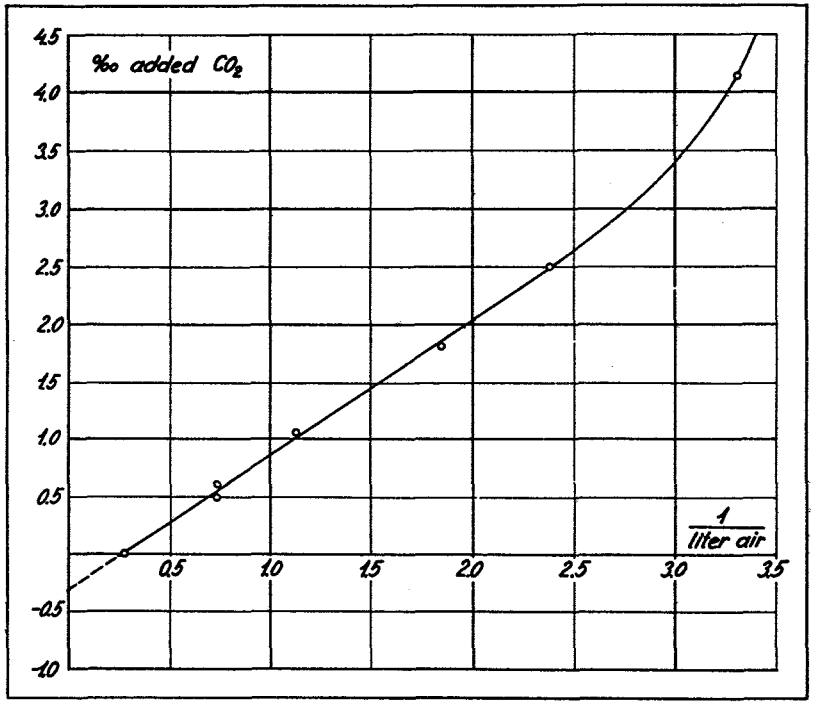

Fig. 22. Calibration of the standardized CO_2-analysis.
The abscissa is the reciprocal value of the quantity of air required for a change of colour of the indicator, measured in litres; the ordinate is the quantity of CO_2 added in per mille.
The natural quantity of CO_2 contained in the air is 0.3 per mille, which corresponds to the point at which the calibration line intersects the ordinate axis.

time CO_2 was added at the inlet end of the pipe in quantities measured on the small venturi meter. In this way air of a given content of CO_2 could be taken off at the outlet.

Figure 22 shows the adjustment curve. The method gives a suitable accuracy by measurements of concentrations of between 0.3 per mille and 4 per mille added CO_2.

The use of this empirical method requires that during the tests the same conditions are maintained as those obtained during the adjustment.

Thus, the standard solution must be very carefully made. The rate of flow through the wash bottle must be kept

almost constant, and this is done by regulating the flow from the suction flask and thereby the vacuum in the wash bottle. The pressure may by read on the manometer inserted in the connection between the wash bottle and the suction flask, see Figure 19. Finally, the natural CO_2 content of the air must be assumed to remain constant, so the laboratory must always be effectively aired before and during the tests.

2. THE MODEL LAWS

2.1 Laminary and turbulent flows. Velocity profile

Laminary flow. In a laminary flow in the direction of the X-axis with a velocity gradient in the direction of the Z-axis, a shearing stress τ_z will occur in a section parallel to the XY-plane and at a distance z therefrom,

$$\tau_z = \mu \frac{du}{dz}$$

in which u is the velocity and μ the dynamic viscosity. The kinematic viscosity ν is defined by

$$\nu = \frac{\mu}{\rho}$$

in which ρ is the density.

The viscosity of a laminary flow is due to the random movement of the molecules. Molecules from one layer will move into another layer carrying with them a momentum in the direction of flow corresponding to that of the layer from which they departed.

The diffusion of momentum as well as of all other qualities in a laminary flow is due solely to the irregular movements of the molecules.

Turbulent flow. In a turbulent flow of, for instance, air, entire volumes of air will move in irregular eddies in the direction of the main flow.

The flow may be taken to be the mean of a motion, namely the main flow superposed with a complicated secondary motion whose velocities are casual as regards direction and value.

Normally, turbulent flows are dealt with statistically, mean values being used in the description, usually in terms of time.

The momentary velocity at a given point has the components u v and w, and the mean velocity through the time interval Δ will then be

$$\bar{u} = \frac{1}{\Delta} \int_{T - \frac{\Delta}{2}}^{T + \frac{\Delta}{2}} u\,dt$$

and the two corresponding equations.

If the mean velocity $\bar{u}$ is deducted from the total velocity u at a given point of time, a velocity u', the eddy velocity, will be obtained, representing the irregular part of the turbulent flow. Thus

$$u = \bar{u} + u', \quad v = \bar{v} + v' \quad \text{and} \quad w = \bar{w} + w'.$$

Over a period of time of sufficient length the mean value of the eddy velocity will be zero,

$$\bar{u}' = \bar{v}' = \bar{w}' = 0.$$

The flow may thus be taken to be described by $\bar{u}$ $\bar{v}$ and $\bar{w}$ with u' v' and w' as a supplementary quality, and it will thus be possible to speak of a steady, stationary turbulent flow when at all points $\bar{u}$ $\bar{v}$ and $\bar{w}$ are independent of time.

The irregularity of the turbulent flow produces an eddy viscosity far greater than the molecular viscosity in the laminary flow. In the turbulent flow entire part volumes of the medium move across the main flow, while in the laminary flow it is only a case of irregularities due to movements of molecules.

Correspondingly the interchange of all quantities between one layer of the flow and another will be far greater in the turbulent flow than in the laminary flow.

The flow of natural wind close to the surface is generally a turbulent flow. Only at low wind velocities in connection with inversion laminary flows may occur.

This paper deals only with phenomena occurring in turbulent wind.

Turbulent boundary layer. If in a parallel flow, for instance in a wind tunnel, a plane sheet is mounted parallel to the flow, this sheet will affect the flow. The particles of air closest to the surface will be braked and at increasing distances from the windward edge this braking effect will be transmitted farther and farther out into the flow.

The layer of the flow influenced by the surface is called the boundary layer and its thickness will increase with the distance from the windward edge of the sheet.

Above the boundary layer the flow is independent of the sheet.

In the boundary layer the velocity varies with the distance from the surface; the velocity is zero at the surface and increases with the height above it.

Both the height and character of the boundary layer are to a material extent determined by the roughness of the surface. A surface can be aerodynamically smooth or aerodynamically rough to different degree.

A surface is aerodynamically smooth if immediately above it there is a sublayer with laminary flow, i.e. a layer in which laminary viscosity predominates. In this layer the velocity gradient will be very great. Above this laminary sublayer we have the turbulent boundary layer in which eddy viscosity prevails.

Above an aerodynamically rough surface no thin laminary layer will be formed, but the flow will be turbulent right down to the actual surface. The flow is therefore called a pure roughness flow.

The factor determining whether a surface will be aerodynamically rough is that its obstacles are so great as to be able to prevent the formation of the laminary sublayer.

Reynolds' number. In his classical examinations of the flow of water in smooth pipes, Reynolds demonstrated that the change from laminary to turbulent flow depended solely on the non-dimensional number

$$Re = \frac{\bar{u}d}{\nu}$$

in which $\bar{u}$ is the mean velocity through the cross-section, d the diameter of the pipe and ν the kinematic viscosity.

The flow will become laminary when Re is less than about 2000.

Reynolds' number may be defined correspondingly for flows not passing through pipes, some characteristic length being chosen to represent d.

The thickness of the laminary sublayer depends on the value of Reynolds' number, the thickness decreasing as Re increases. This means that a given surface may be aerodynamically smooth at low wind velocities and aerodynamically rough at higher wind velocities. At low wind velocities the obstacles of the surface will be entirely submerged in the laminary sublayer, whereas at the higher velocities of the wind the obstacles will be large enough to destroy the laminary layer.

Almost all surfaces in nature will be aerodynamically rough. Only surfaces such as those of large ice-fields may be aerodynamically smooth at low wind velocities. Therefore, natural wind close to the ground will normally be turbulent right down to the surface and thus be a pure roughness flow.

Eddy viscosity. The shearing stresses in the turbulent flow may be defined on an analogy with the shearing stresses in the laminary flow.

If we consider a flow in the direction of the X-axis

with gradient in the direction of the Z-axis at $\bar{u} = \bar{u}(z)$ ($\bar{v} = \bar{w} = 0$), the shearing stress in a horizontal section at height z may thus be defined by

$$\tau_z = A \frac{d\bar{u}}{dz} .$$

Coefficient A, the exchange coefficient, is analogous with the molecular viscosity μ and is of the same dimension.

Corresponding to the kinematic viscosity ν the eddy viscosity may be defined by

$$K = \frac{A}{\rho}.$$

The shearing stress for z approaching zero is called τ_o. In the natural wind it is the friction stress at the surface. τ_o must depend on the roughness of the surface and on $\bar{u}$.

Friction velocity. Prandtl introduced the term friction velocity which he defined by

$$u_* = \sqrt{\frac{\tau_o}{\rho}}$$

in which τ_o is the friction stress for z = 0 and ρ the density of the air. u_* is used as a unit of velocity at the different levels, and it will thereby be possible to obtain a non-dimensional expression for the velocity distribution. Like τ_o u_* depends on the roughness of the surface and on $\bar{u}$.

Velocity profile. The variation of the velocity with the height in the turbulent boundary layer $\bar{u}(z)$ is to be determined from the equation

$$\tau_z = A \frac{d\bar{u}}{dz} = \rho K \frac{d\bar{u}}{dz}.$$

Insofar as it is possible to ignore the pressure gradient changes in the direction of the mean wind, τ_z may in a stationary flow be taken to be independent of the height. This will for natural wind blowing over an ordinary terrain hold good up to a height of 100 m, a particularly important zone with regard to technical problems.

If we therefore take

$$\tau_z = \tau_o,$$

the differential equation for the variation of velocity with the height will be

$$\frac{d\bar{u}}{dz} = \frac{\tau_o}{\rho K}.$$

In the turbulent boundary layer the velocity gradient decreases with the height, K must therefore increase with the height. Let us introduce the simple assumption that K is varying linearly with the height.

$$K = \varkappa u_* (z + z_o)$$

in which z_o represents a length dependent upon the roughness of the surface, and we obtain the differential equation

$$\frac{d\bar{u}}{dz} = \frac{\tau_o}{\rho \varkappa u_* (z + z_o)} = \frac{u_*}{\varkappa (z + z_o)}, \quad \text{whence}$$

$$\frac{\bar{u}}{u_*} = \frac{1}{\varkappa}(\log_e (z + z_o) - \log_e z_o).$$

At the given roughness used by Nikuradse in his fundamental experiments on the flow in rough pipes, the ratio between the size of grain and the roughness parameter is 30. At other forms of irregularities this ratio will have other values, at soil bearing grass or low grain crops it may be 4. Over an urban district with a density of buildings of 0.25 the ratio between the height of the houses and the roughness parameter is 2, if the density is 0.14 the ratio will be 3.

The result to be derived from the above, is in other words, that the wind velocity will vary with the height according to the logarithmic formula

$$\frac{u(z)}{u_*} = \frac{1}{\varkappa} \log_e \frac{z + z_o}{z_o},$$

$u(z)$ is the velocity at height z, u_* the friction velocity, which for a given z_o will generally depend only on the velocity of the free wind. $\varkappa$, Kármán's constant, is a universal constant of numerical value 0.4. z_o is the roughness parameter and depends solely on the roughness of the surface; if two surfaces have similar irregularities in a ratio of f, their z_o values will likewise be of ratio f. The lefthand side of the equation represents the non-dimensional velocity, and correspondingly the term following $\log_e$ is the non-dimensional height. The formula cannot be used at levels close to the obstacles, for there a strong influence will be exerted by the nearest parts of the roughness, a local effect for which the formula cannot, of course, make allowance; it is therefore usual in the counter after $\log_e$ to delete z_o. In many cases the reference point for z in the formula does not coincide with, for instance, the surface of the ground. If a plane surface is covered with a dense layer of balls, the point of departure for the measurement of z will, of course, not be the plane but a place on the level of the centres of the balls or perhaps sligthly higher. z must be measured from the level at which the wind velocity is theoretical zero. In the measurements of the velocities another zero point for z may have been used, for instance a point displaced by the disance d. The formula will then read

$$\frac{u(z)}{u_*} = \frac{1}{\varkappa} \log_e \frac{z - d}{z_o}$$

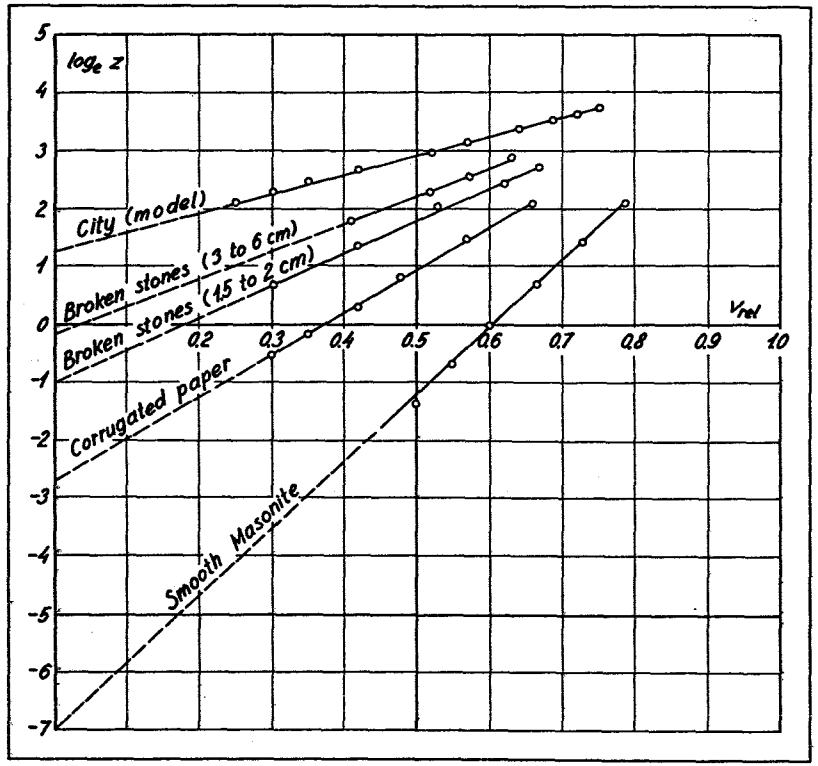

Fig. 29. Velocity profiles over different coatings of the bottom of the tunnel.

The abscissa is the relative speed of wind, the speed at 100 cm level having been fixed at 1.00; the ordinate is the logarithm of the height above the surface.

corresponding to an upward displacement of zero of $d + z_0$.

Figures 29 40 49 and 54 show some examples of velocity profiles over different surfaces in the wind tunnel. The smoothest surface is that of the masonite plates in Figure 29 with $z_0 = 9.1 \cdot 10^{-4}$ cm, the roughest surface that of the model of a city in Figure 29 with $z_0 = 3.5$ cm.

Figures 31 35 and 48 show some examples of velocity profiles measured in nature. The harrowed field in Figure 31 corresponds to the smoothest surface that may be found in agricultural areas, it has $z_0 = 8.2 \cdot 10^{-2}$ cm. At the top of Figure 31 the velocity profile over the central part of Copenhagen is shown. In this case the points of measurement were not sufficiently high to obtain the rectilinear part of the profile. The unbroken, thin line is the tangent to the profile and shows a value of $z_0 = 750$ cm. This corresponds to the city model on scale $3.5 \div 750 = 1 \div 214$, which is very close to the ratio between the height of the houses, namely 7.0 cm to about 15 m.

In the derivation of the formula for the velocity profile it was assumed that

$$K = \varkappa u_* (z + z_0).$$

From Figures 29 31 35 40 48 49 and 54 it will be seen that this assumption was justified as the logarithmic velocity profile obviously covers a very comprehensive field. It is, however, a condition for a rectilinear velocity profile in a logarithmic depiction that the temperature varies with the height in such manner that the air will be in neutral equilibrium.

Thickness of boundary layer. Nikuradse found that a surface is aerodynamically smooth if

$$\frac{u_* z_0}{\nu} < 0.13$$

and aerodynamically rough if

$$\frac{u_* z_0}{\nu} > 2.5.$$

The thickness δ of the turbulent boundary layer over an aerodynamically rough surface may be calculated from

$$\delta = z_0^{0.2} \; 0.341 \; x^{0.8} \quad \text{when} \quad 2 \cdot 10^3 < \frac{x}{z_0} < 5 \cdot 10^5,$$

in which x is the distance to the windward to the place where the boundary layer begins to form.

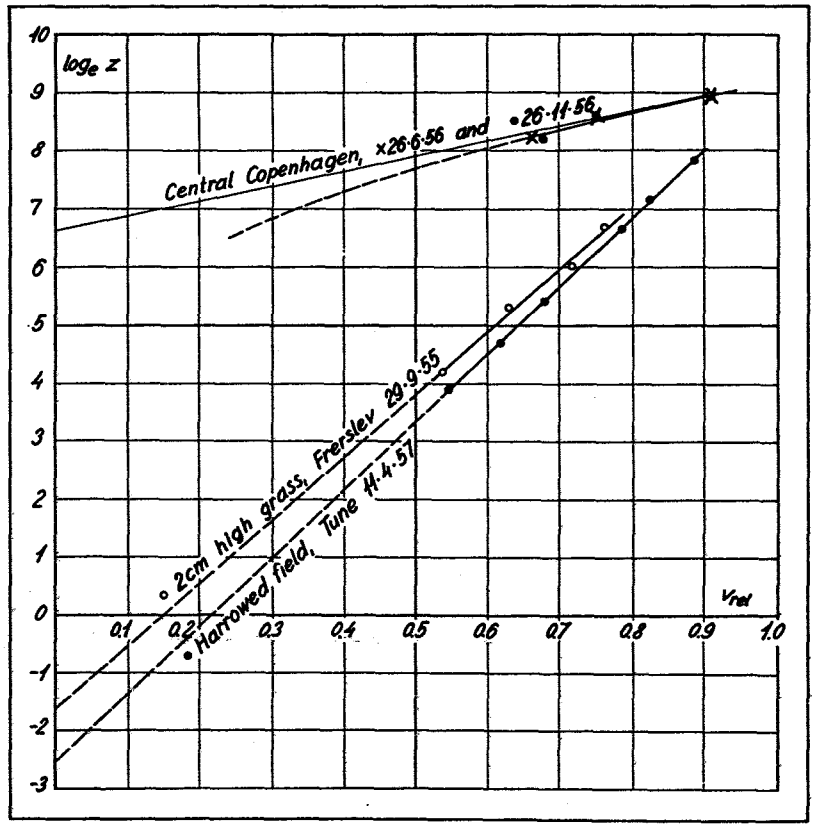

Fig. 31. Different velocity profiles measured in nature.
The abscissa is the relative speed, the speed at 10,000 cm level having been fixed at 1.00; the ordinate is the logarithm of the height above the surface.

2.2 Model law based on the roughness parameter

The investigations elsewhere available on the subject dealt with in this paper were made either without regard to the model law or were based on the notion that the law of identical Reynolds' numbers in nature and model should actually be maintained.

Reynolds' number for an object is

$$Re = \frac{v_o d}{\nu}$$

in which v_o is the undisturbed velocity, d a measure of length in the object and ν the kinematic viscosity.

In other words, the model law demands that the product of velocity and size of the object is to be identical in the model experiment and in nature. It will, of course, hardly ever be possible to fulfil this model law require - ment within the fields here dealt with. If it is a matter of wind conditions at a 20 m high house at a speed of wind of 20 m/s, the product will be $4 \cdot 10^6$ cm^2/s. In a wind tunnel this would require a model of a height of 4 m and a wind speed of 100 m/s. A wind tunnel of sufficient capacity for this experiment would probably not be available.

For by far the greater part of the conditions prevailing in the aerodynamics of natural wind there is, however, no problem at all involving Reynolds' number. The model law is an entirely different one, namely a law based solely on turbulence.

The wind blowing over the surface of the earth is turbulent. Its mean velocity increases with the height above the surface. These are the two most remarkable features of natural wind and they are essential with regard to the movements of the wind not only over open land but also over cultivated and built-up areas.

Despite the fact that the two abovementioned characteristics of the wind, the turbulence and the velocity profile, are very much in evidence - as far as the velocity profile is concerned, of course, only qualitatively, most laboratory experiments curiously enough become invalid because air currents of an entirely different character are used.

Most wind tunnels have a very short working section, frequently a free jet, by which out of regard to investigations of aeronautics it is endavoured to maintain a constant velocity throughout the cross-section. Besides, everything is being done to keep a low turbulence in the flow of air. Such tunnels are unsuitable for investigations of the phenomena in natural wind at the surface of the ground, and the many experiments made can by used only with great caution. This applies also to most experiments made in wind tunnels having a long working section.

If model experiments are made of shelter conditions at a solid screen and the model is mounted on the bottom of the tunnel, its lowermost part will be within the boundary layer which is to be found over the bottom of the

tunnel, no matter how smooth it may be. According as this boundary layer extends to a greater or higher level of the model, the conditions of flow will change. This fact has alarmed many investigators and different tricks have been used to avoid getting the model down into this boundary layer. The model has been suspended in the middle of the tunnel, and in order to avoid false results due to air that may flow under the model and into the sheltered area, the suspended models were provided with a base plate as a substitute for the surface of the earth. A boundary layer will be formed also over this plate; if the plate projects only a short distance to the windward of the model, this boundary layer will, of course, only be thin. To have boundary layers entirely eliminated use has at times been made of symmetrical double models suspended in the middle of the tunnel.

Unfortunately, these efforts to eliminate the boundary layer will in most cases lead to serious errors when the results of the model experiments are applied to real objects standing on the ground.

To demonstrate these conditions measurements was made in nature of the shelter behind a screen, and in the wind tunnel measurements on a model of this screen were performed.

The arrangement in nature appears from Figure 34. The screen was solid, 0.95 m high and 35 m long, and was mounted at right angles to the wind. The speed of the wind was measured in the vertical plane in the direction of the wind abreast of the middle of the screen. Within the area included in the measurement of the shelter the flow may be considered two-dimensional. The speed of the wind was measured by means of cup-anemometers as described in Chapter 1.1. The terrain was a stubblefield extending over a long distance to the windward.

An 8 m tall mast with 4 cup-anemometers was erected 35 m to the windward of the southern end of the screen, here the velocity profile was measured. At the same dist - ance from the northern end of the screen a cup-anemometer was mounted at a height of 0.95 m. The recordings there together with the recordings at the mast were used as a basis for the calculation of the shelter given by the screen.

Measurements within the shelter zone of the screen were made by means of 5 cup-anemometers mounted on a portable pole.

During the experiment which was made in the course of the night between October 25th and 26th, 1959, the wind was

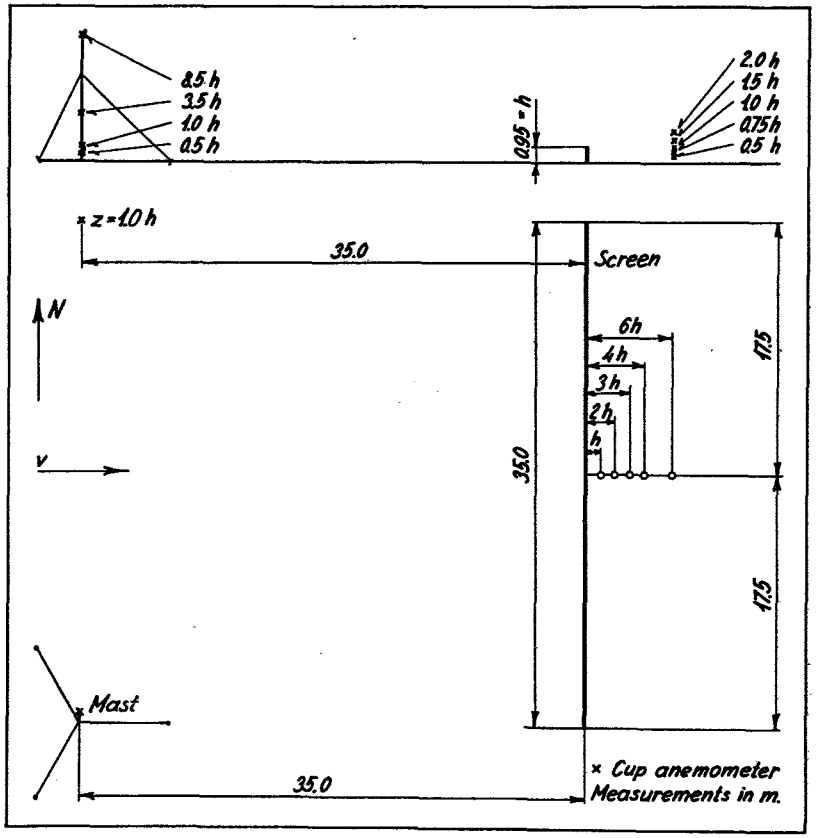

Fig. 34. Arrangement for the measurement of the shelter behind a screen in nature.

The screen was solid, 0.95 m tall and 35 m long, and placed in direction N–S. The velocity profile was measured at an 8 m tall mast erected 35 m to the west of the southern end of the screen. The measurements of the speed of the wind there and at an apparatus mounted 35 m to the west of the northern end of the screen at 0.95 m level were used as the speed of the undisturbed wind in the calculation of the shelter value. The shelter was measured abreast of the middle of the screen at 5 different levels.

from the west and its speed at a level of 8 m was 8 – 10 m/s. The weather was overcast without precipitation.

The velocity profile measured is shown in Figure 35. The roughness parameter was 0.74 cm. Figures 36 and 37

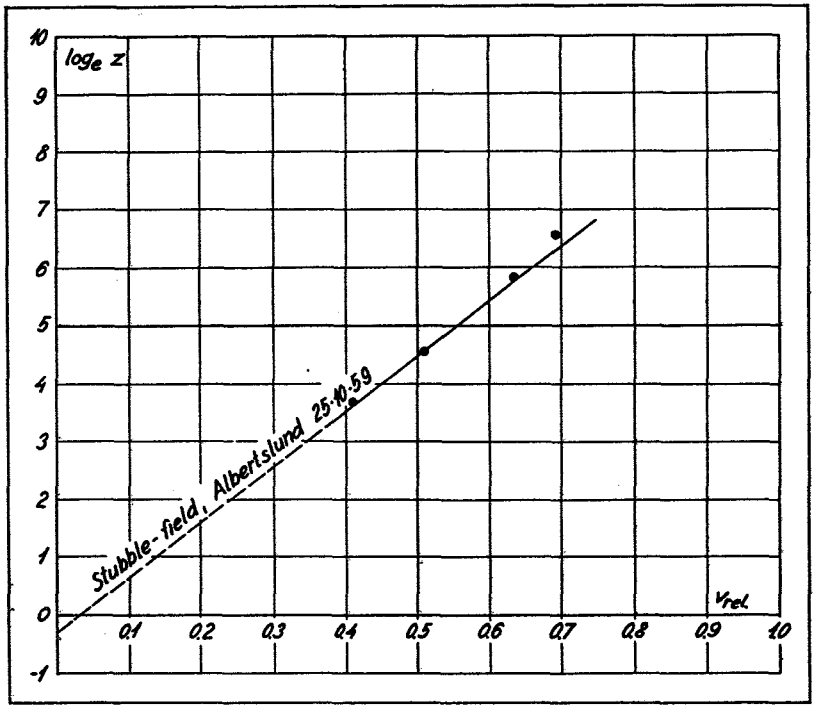

Fig. 35. Velocity profile over a stubble field.

The abscissa is the relative speed of wind, the value being fixed at 1.00 at a level of 10,000 cm; the ordinate is the logarithm of the height above the surface of the ground.

The profile was measured at the 8 m mast shown in Fig. 34.

show two sections of the shelter zone behind the screen, namely the shelter in a horizontal line at a level of 0.4 times the height of the screen above the ground, and the shelter in a vertical line at a distance of 4 times the height of the screen from the screen, respectively. In both figures the shelter curve is shown in solid line and designated by the number 128.

The shelter s in a point at a screen is defined by

$$s = \frac{v_o - v_s}{v_o}$$

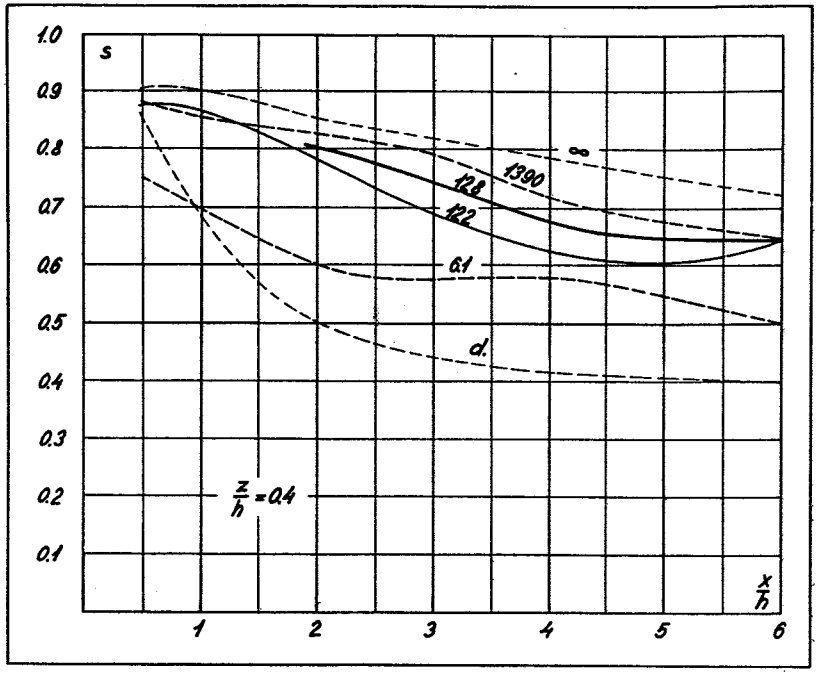

Fig. 36. Shelter behind a solid screen in nature and in model experiments.

The ordinate is the shelter s; the abscissa the distance x from the screen made non-dimensional by division with the height of screen h. The shelter curves shown correspond to a level of z = 0.4 h.

The fat curve represents the measurement in nature shown in Fig. 34. The height of the screen was 128 times the roughness parameter z_0. The other curves correspond to different model experiments. ∞ is a model experiment with the screen erected on a smooth plate of moderate extent; the plate was suspended in the middle of the tunnel. d is a model experiment with the screen freely suspended in the middle of the tunnel; it represents 'poised double models'. 1390 122 and 6.1 are model experiments in which the screen was standing in the turbulent boundary layer developed over different coatings of the bottom of the tunnel; the figures indicate the ratio between the height of screen and the roughness parameter.

It appears that the condition for a true model experiment is that the experiment is performed in a turbulent boundary layer with a roughness parameter true to scale.

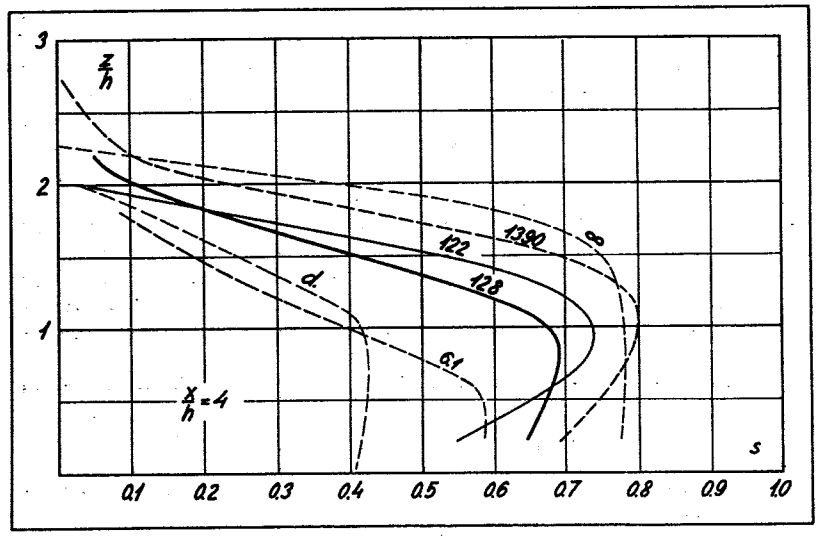

Fig. 37. Shelter behind a solid screen in nature and in model experiments.

The abscissa is the shelter s; the ordinate the level z above the ground made non-dimensional by division with the height h of the screen. The shelter curves correspond to the distance x = 4 h from the screen.

For further information see text of Fig. 36.

in which v_0 is the speed of the wind at the point when there is no screen, and v_s the speed of the wind when the screen has been put up.

The speed v_0 of the unobstructed wind at the different levels was determined by interpolation between the measurements at the mast. All determinations of the speed of the wind represent the mean value for 10 minutes.

In the wind tunnel experiments were made on a symmetrical double model of the screen suspended in the smooth flow in the middle of the cross-section of the tunnel. The screen was 2.5 cm high and of infinite length. The speed of the wind was measured by means of the hot-wire anemometer described in Chapter 1.3. The shelter curves in the two sections are designated by d and shown in broken lines in Figures 36 and 37. It will be seen that the shelter behind the suspended double model is quite different from that obtained in nature.

In the case of body in double flow, like the freely suspended model screen, the free flow, the potential field, on the windward side will extend all the way in to the thin boundary layer surrounding the body. There will always be a stagnation point in front of the body at the place where the current divides to flow in two currents, one to each side of the body, and where the velocity will be zero.

When it is a body in single flow, like the screen standing in the field, a shelter zone will form on the windward side, this zone being bounded towards the free flow by a vortex layer which in a rounded curve connects the ground with a point on the body, in this case the upper edge of the screen. There will therefore be no point at which the velocity of the unobstructed flow is zero.

When a body is in double flow, the flow behind it will vary with ever-recurrent eddies forming and breaking into the eddy region from alternate edges, so that the whole eddy region will move up and down without symmetry on the symmetry axis of the body. This is the wellknown Kármán Vortex Street.

At a body in single flow a rear vortex layer will form bounding the shelter zone. The vortex layer will certainly oscillate somewhat in the vertical plane, all discontinuity surfaces being unstable, but these small motions will cause only minute variations in velocities. Particles of air from the unobstructed flow will only to a limited extent enter the vortex layer and pass on into the shelter zone which, on the whole, will be subject to minimal changes because it is supported by the solid boundary constituted by the ground.

If we are to have any chance of obtaining from model experiments conditions resembling those measured in nature, the model screen must thus be mounted on a base plate which can support the vortex layer to the windward of the model and the shelter zone behind it in the same way as in nature.

As previously mentioned, many model experiments have been made with model suspended in the middle of the tunnel and provided with a base plate of moderate extent. A determination of the shelter of such an arrangement was therefore made. The screen was 2.5 cm in height and of infinite length and it was mounted on a masonite plate extending 15 cm forward of and 40 cm to the rear of the screen.

Figures 36 and 37 show the results in broken lines and designated ∞. A comparison with the measurement made in nature, shown in solid line and designated 128, indicates appreciable deviations.

Natural wind is practically always turbulent all the way down to the surface of the ground. It is thus a roughness flow, and Reynolds' number does not apply to the velocity profile of a turbulent flow. The flow is determined by the roughness, or perhaps rather by the turbulence, but this makes no difference as the turbulence is determined solely by the roughness when the atmosphere is in a neutral state, i.e. when there are no positive or negative thermic contributions to the turbulence.

It now begins to emerge that conditions for model experiments must aim at making the flow in the wind tunnel turbulent in a manner similar to the turbulence of the wind.

In a wind tunnel with the bottom covered with smooth masonite plates a boundary layer will be formed having the velocity profile shown in Figure 40 with a roughness parameter $z_o = 1.8 \cdot 10^{-3}$ cm. A covering of corrugated paper will give $z_o = 4.1 \cdot 10^{-2}$ cm, and a cover of 2 cm wide and 2.5 cm high fillets gives $z_o = 0.41$ cm. The corresponding velocity profiles are also shown in the figure.

With the tunnel bottom dressed in these manners the shelter behind the model screen was measured. The screen stood on the bottom of the tunnel and the turbulent boundary layer was of a height of more than 4 times the height of the screen. The results are shown in Figures 36 and 37. The experiment in nature is shown in solid line, the model experiment with corrugated paper covering in thin, solid line designated 122, whereas the experiments on the smooth masonite are represented by the broken curve designated 1390, and that on the covering with fillets by the broken line designated 6.1.

The three model experiments, curves 6.1 122 and 1390 correspond to three different degrees of turbulence of the wind. Over the smooth surface the turbulence is less than that over the rough surfaces. It is clearly apparent from the figures that it is of decisive importance for the shelter behind the screen whether the bottom of the tunnel is rough or smooth, or in other words, whether the turbulence is great or small.

At the present time it is impossible to give a mathematical description of the turbulence in a flow in such a manner as to be sufficiently detailed and at the same time also practicable in its wider application. Thus, it will be impossible in this way to cope with the problem of the model law for more or less turbulent flows. It is not necessary, however, to include a description of the actual turbul-

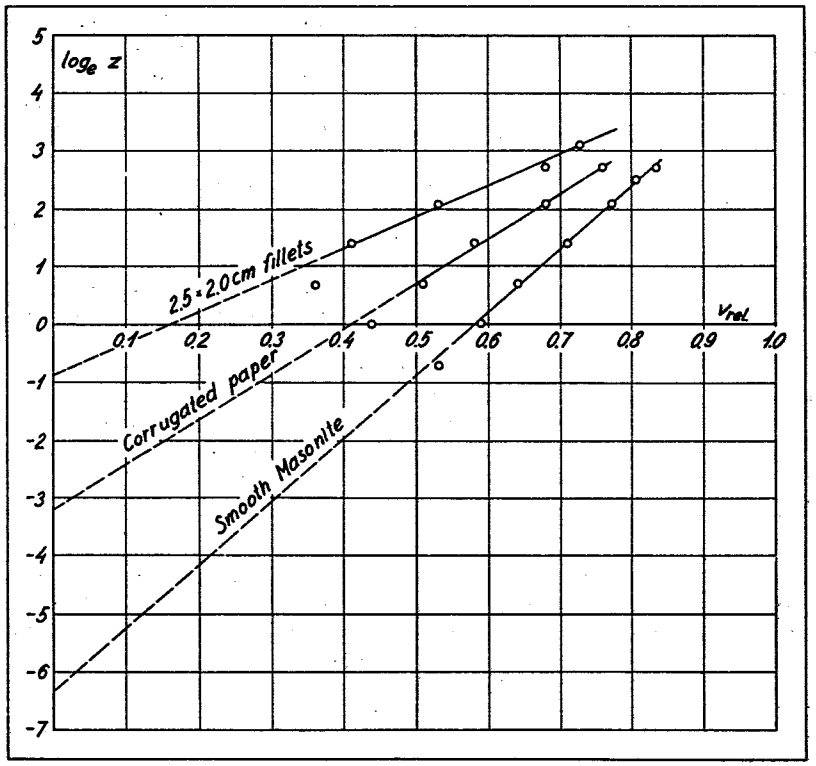

Fig. 40. Velocity profiles in wind tunnel.
The abscissa is the relative speed of the wind, the speed at 100 cm level having been fixed at 1.00; the ordinate is the logarithm of the level above the surface.

ence, we need only stick to the fact that phenomena in a pure roughness flow depend upon the roughness.

The problem of the model condition for natural wind is reduced to a model condition for the roughnesses of the surfaces. Theoretically the easiest procedure would be to reproduce the terrain to be investigated in the proper scale in the wind tunnel. In practice this will often be very difficult, more particularly in case of cultivated surfaces of the earth. It may, however, be done in a much easier way.

In Chapter 2.1 the formula was derived for the velocity profile in a turbulent flow over a rough surface

$$\frac{v(z)}{v_*} = \frac{1}{\kappa} \log_e \frac{z + z_o}{z_o},$$

in which the roughness parameter z_o represents a length characteristic of the roughness.

The velocity profile is the most outstanding feature of a pure roughness flow, and there is every reason to expect that the other phenomena of the flow must depend upon the same physical values as those entering into the formula for the velocity profile, and in respect of our problem concerning the roughness this will mean the roughness parameter z_o.

We have thus arrived at the condition for model experiments that the velocity profile in the wind tunnel must be similar to that in nature on the scale selected, or more simply, that the roughness parameter of the tunnel bottom shall be on a scale with the roughness length in nature.

$$\frac{Z_o}{z_o} = \frac{D}{d},$$

in which Z_o is the roughness parameter in nature, z_o the roughness parameter in the tunnel, D end d a measurement of the object in nature and in tunnel, respectively. The model must, of course, be entirely submerged in the turbulent boundary layer of the tunnel.

Figures 36 and 37 show all the shelter curves. At each curve the value of the ratio between the height of screen and the roughness parameter has been stated. In the model experiment in which the screen was standing on a smooth plate of moderate extent the boundary layer was quite thin and the model was thus exposed to a flow of a constant velocity independent of the height. Viewed on the basis of the new model law this may be characterized by the statement that the roughness parameter was infinitesimal small or $h \div z_o = \infty$.

Figures 36 and 37 make it apparent that symmetrical double models give entirely wrong results. Otherwise there is a gradual change in the shelter curves from the very rough model experiment having $h \div z_o = 6.1$ to the very smooth one having $h \div z_o = 1390$. The experiment with the model on a short plate enters reasonably as an even smoother case.

Finally the figures show the excellent conformity between conditions in nature and model experiments when the values of $h \div z_o$ are approximately equal, i.e. 128 in nature and 122 in the model experiment over corrugated paper.

The above conditions for true model experiments make certain new requirements as regards technique and equipment.

The model law in this form requires that it is possible to dress the wind tunnel with rough coverings giving a wide range of roughness parameters, in order to accomodate both variations in roughness parameter and the different scales of models. Chapter 1.4 contains descriptions of a number of roughnesses.

Furthermore, the experiment must be made in the boundary layer of the tunnel bottom. The boundary layer increases rather slowly, particularly over smooth surfaces, so a considerable length of tunnel will be required.

2.3 Experiments to check the model law

In addition to the experiments mentioned in Chapter 2.2 on the shelter behind a solid screen several control experiments were made to check the scope of application of the model law.

Figure 43 shows the results of shelter measurements behind artificial screens in nature and in model experiments. The shelter was measured at a level of 0.4 h above the ground, h being the height of the screen. The screens consisted of horizontal boards spaced so as to give a hole percentage of 38. The experiments were two-dimensional. The abscissa in Figure 43 is the distance from the screen to the point of measurement made non-dimensional by division with the height of screen. The ordinate is the shelter s defined by

$$s = \frac{v_o - v_s}{v_o}$$

in which v_o is the speed of the wind at the point without the screen, v_s its speed at the point with the screen mounted.

The full-line curve shows the shelter behind a 3.5 m tall screen in a terrain with a roughness parameter of 4.5 cm. The short-dash curve shows the shelter behind a 5 cm tall model screen when the tunnel bottom is dressed with corrugated paper giving a roughness parameter of 0.09 cm. Finally, the long-dash curve represents the shelter in a model experiment with smooth tunnel bottom having $z_o = 1.1 \cdot 10^{-3}$ cm. In nature the ratio between the height of screen and the roughness parameter is 78, and in the two model experiments 56 and 4500, respectively. The figure

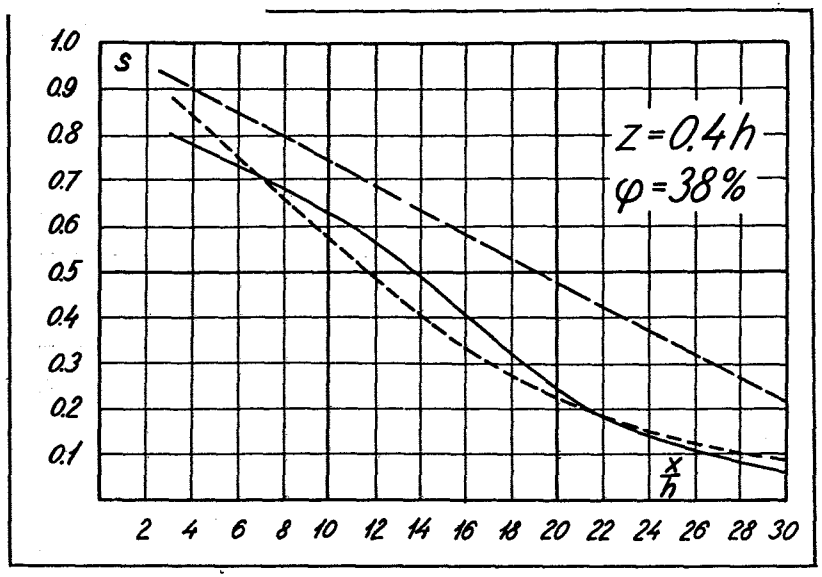

Fig. 43. Comparison between shelter curves from measurements in nature and in model experiments.

The abscissa is the distance x from the screen made non-dimensional by division with the height h of the screen; the ordinate is the shelter s; the measurements were made at a level of z = 0.4 h. The percentage of hole area of the screen was 38.

The solid curve represents the shelter behind a 3.5 m tall screen in nature. The short-dash line is the shelter behind a model screen in the turbulent boundary layer over corrugated paper. The long-dash curve originates from a model experiment in smooth tunnel.

show a good conformity between model experiment and nature when the roughness parameter is according to scale, whereas the smooth tunnel bottom will give an entirely different shelter curve.

The velocity profiles for measurements in nature and in the tunnel are to be found in 'Shelter Effect' by Martin Jensen, Figures 177 and 179.

Figure 44 shows the results of some other shelter experiments. Board screens with a hole area of 45% were used. The screen in nature was of a height of 2.5 m and was placed in a very smooth terrain, namely in the tidal flats outside the sea-wall at Højer in Southern Jutland. Here a several kilometre wide marshland covered with grass and

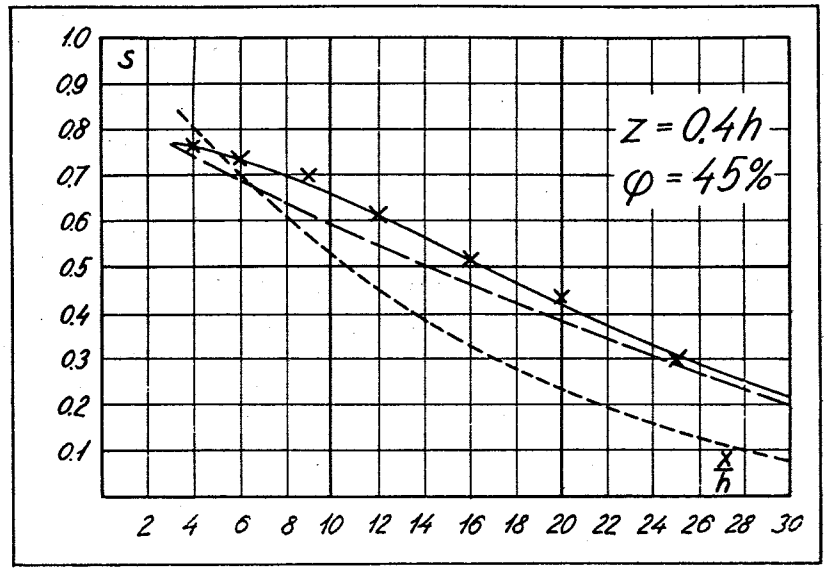

Fig. 44. Comparison between shelter curves from measurements in nature and from model experiments.

The abscissa is the distance x from the screen made non-dimensional by division with the height h of the screen; the ordinate is the shelter s. The measurements were made at a level of z = 0.4 h. The hole percentage of the screen was 45.

The solid curve represents the shelter behind a 2.5 m tall screen in an extremely smooth terrain. The long-dash curve shows the shelter behind a model screen on a smooth tunnel bottom. The short-dash curve shows the shelter behind a model screen in the turbulent boundary layer over corrugated paper.

submerged at high tide extends to the seaward. At suitable water levels the grass will rise vertically from the bottom to the surface of the sea on which it will lie horizontally and prevent all wawe formation. The roughness parameter was $1.8 \cdot 10^{-2}$ cm. The model experiment was made with screen models of a height of 5 cm on a smooth tunnel bottom with $z_o = 1.1 \cdot 10^{-3}$ cm as well as on a bottom covered with corrugated paper and having $z_o = 0.09$ cm.

In Figure 44 the shelter behind the screen in nature is shown in full-line curve. The model experiment on smooth bottom is shown by the long-dash curve, while the short-dash curve represents the shelter measured over the rough tunnel bottom.

In nature the ratio between height of screen and roughness parameter was 14 000, in the smooth-bottom model experiment 4 500 and in that on rough bottom 56. It again appears that there is a fine conformity between model experiment and nature when the roughnesses are reasonably similar, whereas otherwise the model experiments do not give a suitable representation of what happens in nature.

Finally, measurements were made of the shelter in nature at a three-wing school at Frerslev on the Island of Zealand, and a shelter measurement in wind tunnel of a model on a scale of 1÷140 of the same school.

The Frerslev school is situated in a flat terrain. To the west and north of the school are open fields and the playground is asphalted. At the time of measurement in 1955 there were no hedgerows offering any shelter, so shelter conditions were determined solely by the school buildings.

The measurement in nature comprised in the first place a determination of the velocity profile at a mast erected in the sports ground of the school as shown in Figure 46. On the pole 4 cup-anemometers were mounted at levels 1.2 2 4 and 8 m. A series of values of the simultaneous speed of wind at these levels was measured.

Cup-anemometers were thereupon mounted at a level of 1.2 m at the five points marked in Figures 46 and 47. Simultaneous measurements were made at all these points of a number of mean values of the speed of wind for one minute. The shelter was calculated by taking the measurements at 1.2 m level on the mast in the sports ground as the speed of the undisturbed wind.

Figure 47 shows the results of measurements made on September 3rd between the hours of 13^{30} and 16^{30}. The weather was half overcast and the wind was blowing from 255° from north through east, changing within an arc of 10° during the time of observation. At the level of 1.2 m the speed of the undisturbed wind was 7 - 8 m/s.

The sports ground was grown in grass of a height of 2 cm, in front of the school to the windward lay grass fields. Figure 48 shows the velocity profile, the roughness parameter $z_o = 0.30$ cm.

The shelter in the playground was determined as a mean of 15 measurements, the results are indicated by the upper numbers in Figure 47.

In the tunnel the bottom was covered with glazed cardboard sheets. The velocity profile, which was measured in the 4th section by means of the small pitot-static tube, is shown in Figure 49. Roughness parameter $z_o = 1.5 \cdot 10^{-3}$ cm.

Thus, the ratio between the roughness parameters was

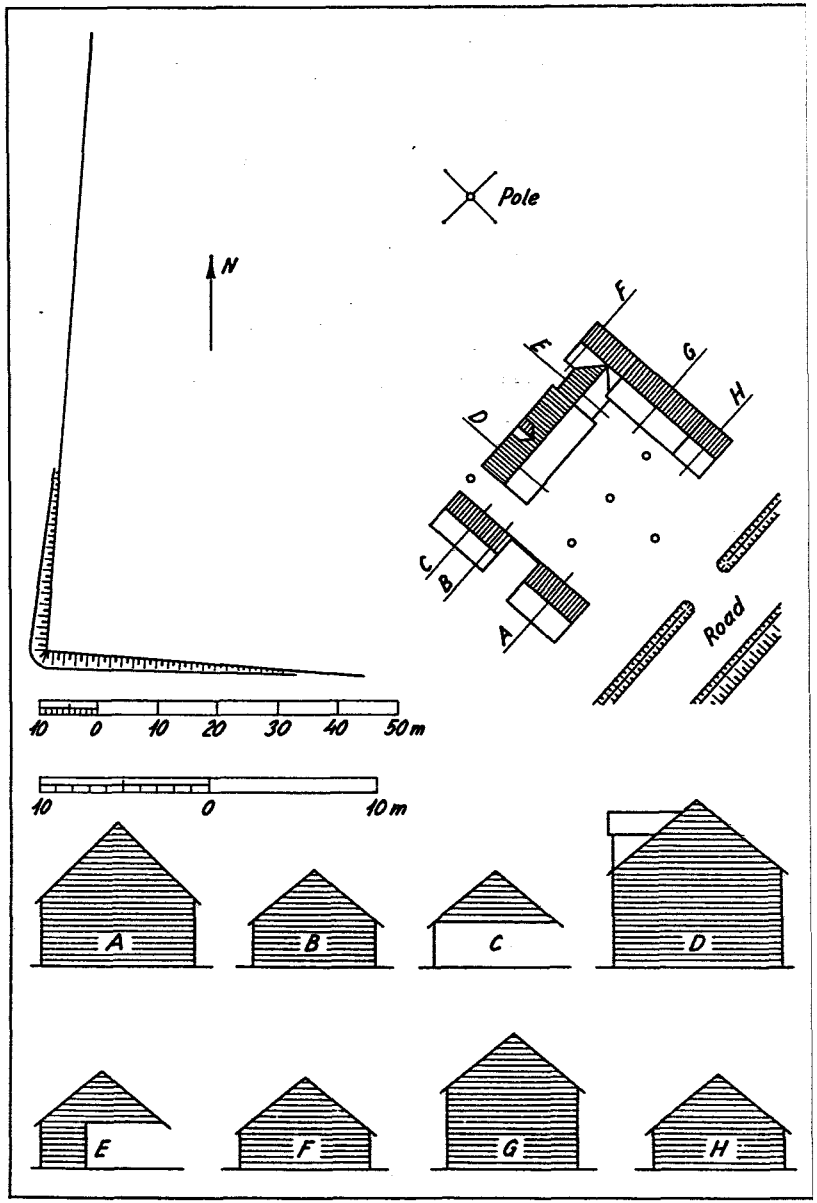

Fig. 46. Comparison between the shelter in nature and in model experiments.

The upper parts shows the plan of a school situated in an entirely open terrain. At westerly wind a velocity profile was measured from the mast shown, which was 8 m high. At the same time the speed of the wind was measured at the 5 points marked between the buildings at a level of 1.2 m above the surface.

The lower part shows a cross-section of the buildings.

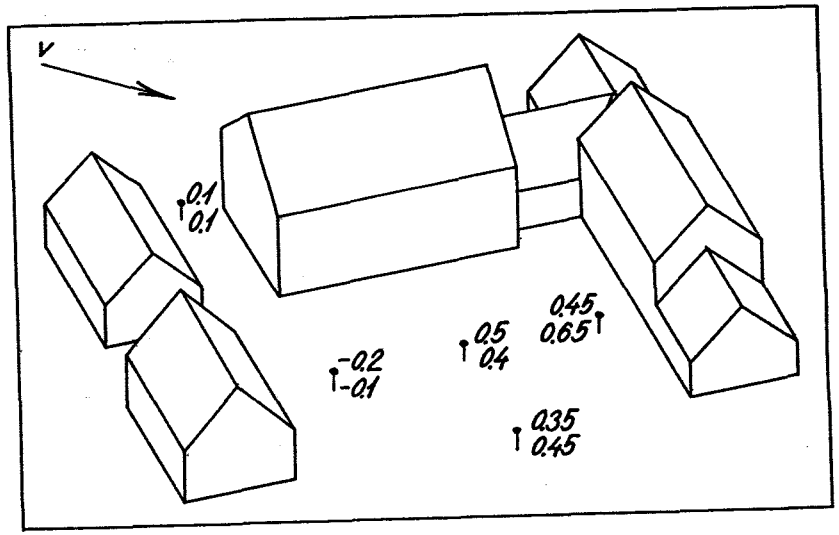

Fig. 47. Comparison between the shelter in nature and in model experiments.

The shelter values from the measurements made at the school shown in Figure 46 are noted as the upper figure at each point of measurement. The lower figure indicates the shelter from the model experiment in the wind tunnel.

1÷200, and the model was on a scale of 1÷140. This conformity is sufficient to fulfil the model requirements.

In the model experiment the speed of the wind at the different points was measured by means of the hot-wire anemometer. The hot-wire was vertical and 0.3 cm in length. Its centre was 0.84 cm above the tunnel bottom, corresponding to the level of the cup-anemometers in nature.

The results of the model experiments are indicated by the lower numbers in Figure 47.

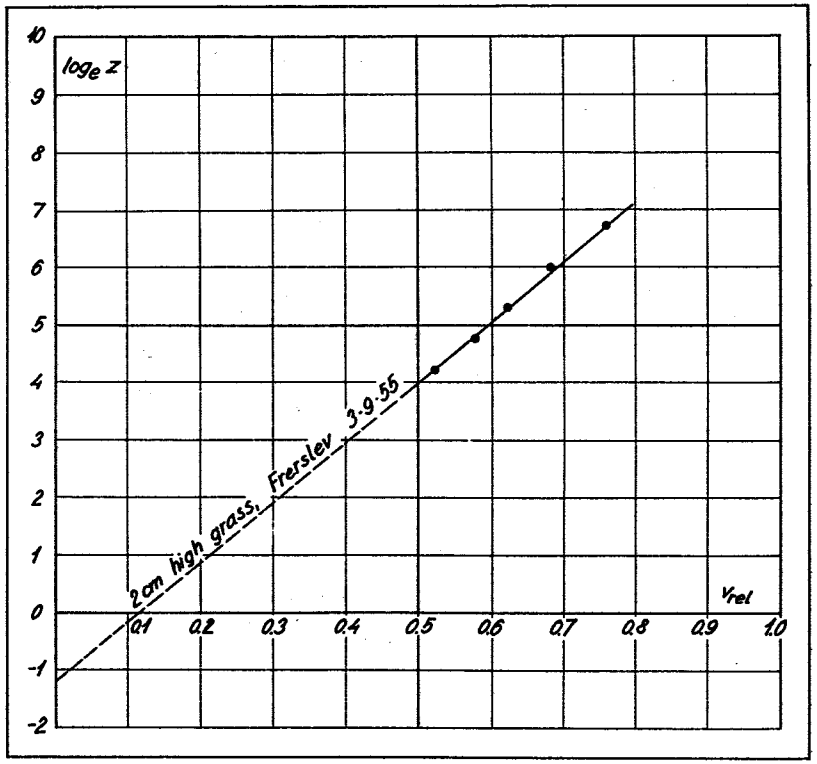

Fig. 48. Velocity profile over a field with short grass.
The abscissa is the relative speed of wind, the speed at 10,000 cm level having been fixed at 1.00; the ordinate is the logarithm of the level above the surface. The profile was measured at the mast shown in Fig. 46.

Table 49 contains a record of the speed of the wind at the different points both in nature and in the model experiment. The speeds have been converted to correspond to an undisturbed speed of 10 m/s. The table shows a satisfactory conformity between nature and model experiment.

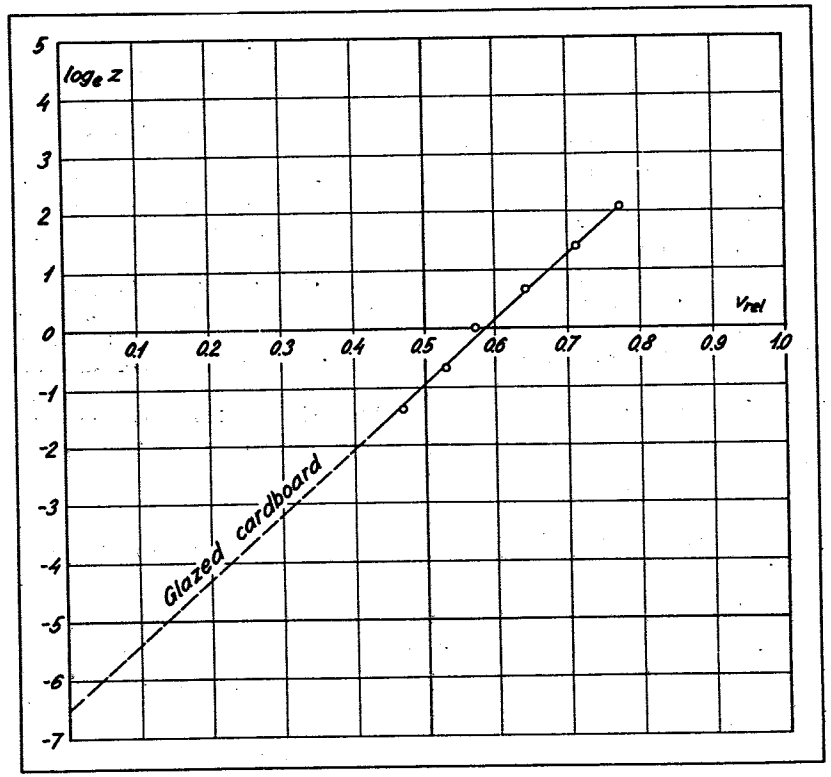

Fig. 49. Velocity profile over glazed cardboard in wind tunnel.
The abscissa is the relative speed of wind, the speed at 100 cm level having been fixed at 1.00; the ordinate is the logarithm of the height above the surface.

Table 49. Comparison between the speed of wind in nature and in model experiments at the school shown in Fig. 46.
Measurements were made at 1.2 m level in nature and the corresponding level in tunnel. The speed of the unobstructed wind at this level was fixed at 10 m/s.

Nature, m/s	Model, m/s	Error, m/s
9.0	9.0	0.0
5.5	3.5	2.0
5.0	6.0	-1.0
6.5	5.5	1.0
12.0	11.0	1.0
	Average	0.6 m/s

2.4 Model law for the dispersal of smoke

A chimney is assumed to emit Q cm^3 per second of a gas or a fine suspension. This matter is distributed in the plume of smoke and at a certain distance from the chimney it may pass down between houses or down to the ground. The matter of interest to us is the concentration of gas q at a given point. q represents cm^3 gas per cm^3 contaminated air.

Let us consider a closed curve around the point. Through this curve streamlines are drawn thus forming a tube in which the point is situated. The curve and thus also the stream-tube are chosen of so small dimensions that the velocity v may be considered constant throughout the cross-section F containing the point. The quantity of gas passing through the stream-tube is $\beta' Q$, β' being a constant smaller than 1. We thus have

$$\beta' Q = qFv.$$

The velocity v is proportional to the friction velocity v_*

$$\beta'' v = v_*,$$

and the area F is proportional to the square of some characteristic length, for instance the roughness length z_o

$$\beta''' F = z_o^2.$$

If the two last equations are inserted in the first equation and it is solved in relation to q, and β' β'' and β''' are taken together as b, we have

$$q = b \frac{Q}{z_o^2 v_*}$$

in which q is the concentration of gas in cm^3/cm^3, Q the strength of the source in cm^3/s, z_o the roughness parameter in cm, v_* the friction velocity in cm/s, and b a non-dimensional coefficient indicating the variation from place to place in the given arrangement

$$b = q \frac{z_o^2 v_*}{Q},$$

b may be termed the non-dimensional concentration.

It may at times be more convenient to use the reciprocal value of the non-dimensional smoke concentration

$$\frac{1}{b} = \frac{Q}{z_o^2 v_* q};$$

and as $\frac{1}{b}$ is proportional to Q, $\frac{1}{b}$ may be termed the non-dimensional strength of source.

3. SHELTER AT HOUSES

3.1 Introduction. Experimental technique

When buildings are situated in open country it will frequently be of great interest to establish an efficient shelter, partly out of regard to the people living there, and partly, in certain cases, out of regard to the vegetation in adjacent gardens.

Especially in the case of rural school buildings it is of importance to provide good shelter in the playground.

The experiments referred to in this chapter were made on models of different types of school buildings for the purpose of obtaining information with regard to the shelter effect of the actual school buildings.

In the course of the experiments a total of 5 different schools was investigated. In all cases the school buildings were 1 or 2-storey houses. The simplest specimen consists of a one-wing building, the model of which is shown in Figure 53. In addition the experiments comprised a two-wing, a three-wing and a four-wing school building and a school consisting of three low, parallel buildings.

In each case the shelter measurements of the models of these five schools comprised only the area of the school grounds arranged as a play-ground.

In some of the types of schools the models include lean-tos and hedgerows about the play-ground.

All the models were on a scale of 1:200.

The models were arranged in the fourth section of the tunnel. There a turntable had been built into the floor of the tunnel, so that the model might be turned in relation to the direction of the wind. Figure 53 shows a model mounted on the turntable. The turntable was smooth, while the rest of the bottom of the tunnel was coated with sandpaper with $z_o = 2.5 \cdot 10^{-2}$ cm. Figure 54 shows the velocity profile over this coating.

The roughness used in the tunnel corresponds to a roughness in nature of $z_o = 5$ cm.

Measurements of the speed of the wind in the tunnel were made by the hot-wire anemometer described in detail in Section 1.3.

The hot-wire used was 0.3 cm in length. The wire was mounted vertically at the point of measurement. All measurements were made with the centre of the hot-wire at a level

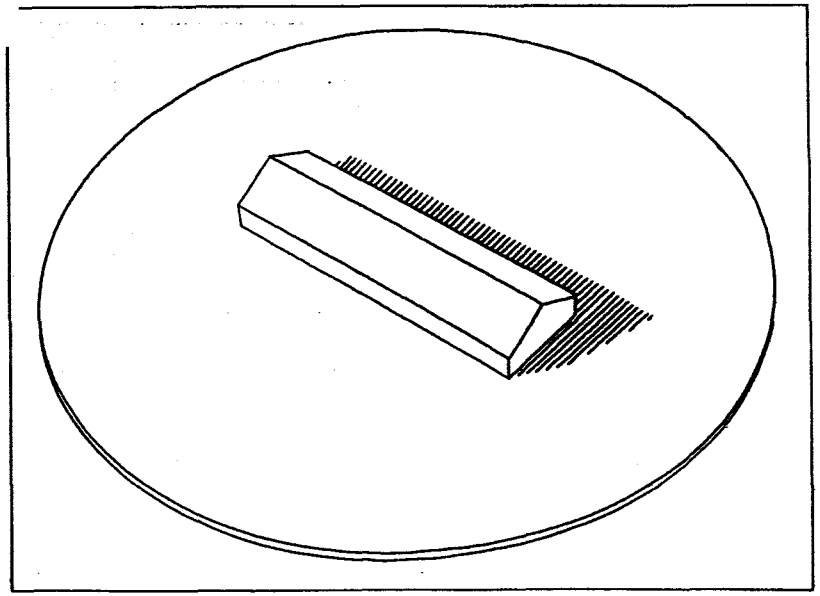

Fig. 53. Model for investigation of the shelter at a house.
In the wind tunnel the model was mounted on a turntable so that the shelter might be investigated at different angles of incidence of the wind.

of 0.75 cm above the floor coating, which corresponds to 1.5 m above the ground.

The result of having the hot-wire placed vertically is that measurements will be independent of turns of the wind in the horizontal plane; at the same time measurements will be independent of vertical turns of the wind of up to 45°.

Before measurements were made at any point, the direction of the wind was, however, ascertained by means of a bit of thread affixed to a pin at the point of measurement.

In the second section of the tunnel a pitot-static tube was mounted in the free flow above the boundary layer to control the velocity of the wind in the tunnel during the experiments.

For each of the 5 school models shelter conditions were investigated at a number of points in the play-ground at different wind directions.

The results of these measurements are shown in Figures 55 to 73, in which the shelter is given in per cent.

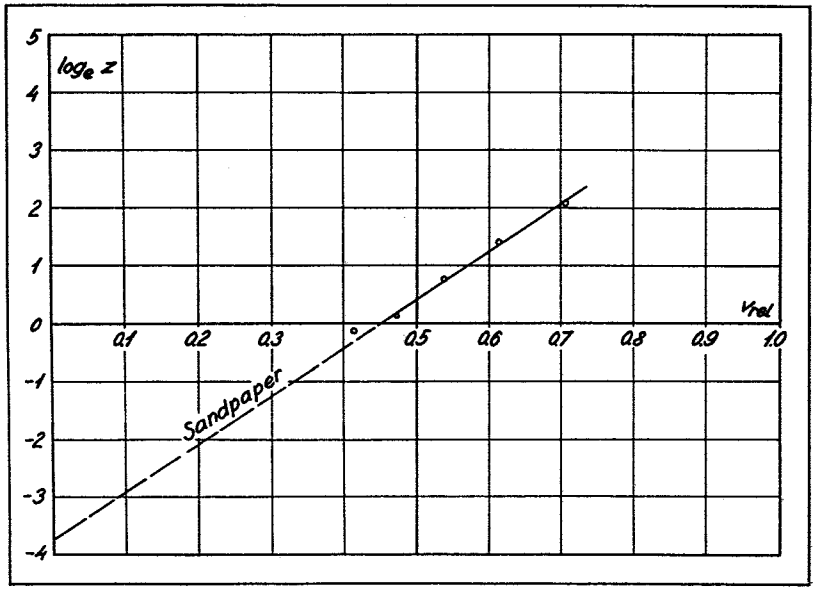

Fig. 54. During the experiments on shelter at houses the tunnel was dressed with sandpaper and had the velocity profile shown in the figure.

The abscissa is the relative speed of wind, the speed at 100 cm level having been fixed at 1; the ordinate is the logarithm of the height above the surface.

$$s = \frac{v_o - v_s}{v_o} 100$$

in which s is the shelter in %, v_o the velocity at the point of measurement when the sheltering arrangements were removed, and v_s the velocity measured in the shelter zone.

A shelter of s = 25% at a given point thus means that at the point the speed of wind is reduced by 25% because of the sheltering arrangements. A shelter of s = −10% means that the speed of the wind at the point has been increased by 10%.

As it is the object of the shelter to create more comfortable conditions for human beings, a shelter of less than, say, 50% will not be of much interest. Corresponding to this evaluation, isoskepes have been drawn in the figures for 50, 60, 70, and 80% shelter (skepe = shelter), and for the sake of lucidity areas of more than 50% shelter have been hatched on a graduated scale increasing in density with the amount of shelter, as shown in the lower parts of the figures.

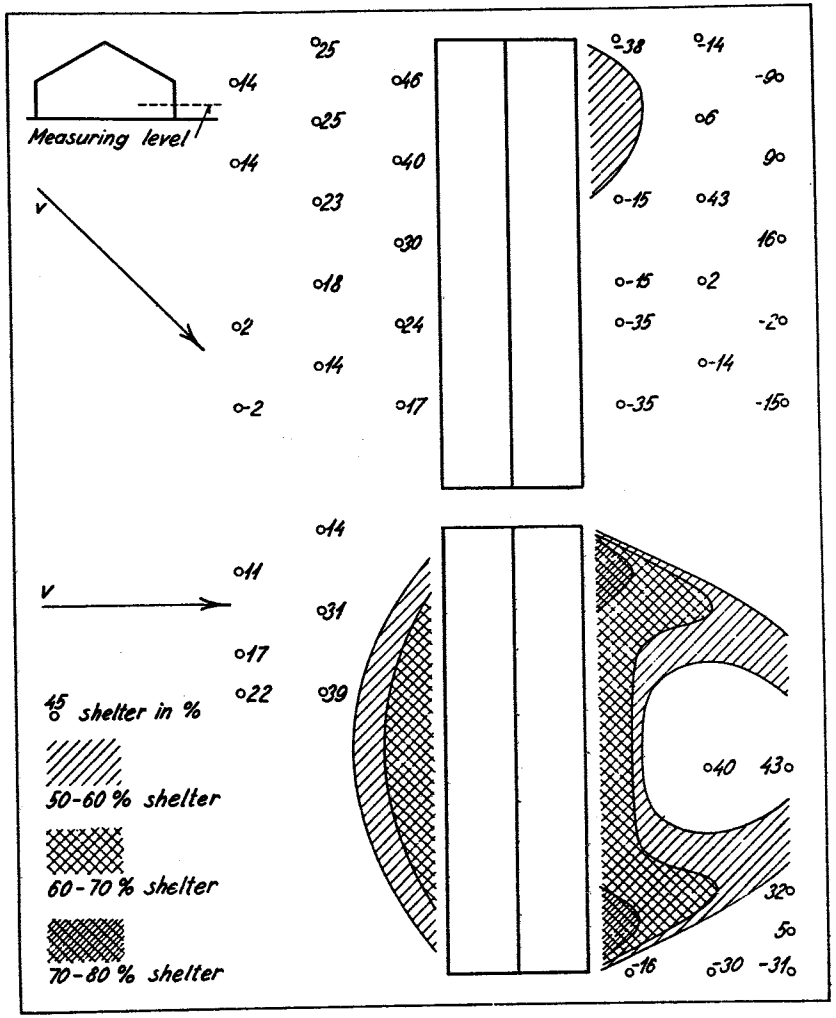

Fig. 55. Shelter at an isolated house.

At the top of the figure the shelter is shown at a wind blowing at an angle of 45° with the longitudinal axis of the house. In the lower part the shelter is shown at winds at right angles to the house. Isoskepes have been drawn for 50 60 and 70% shelter, and areas having more than 50% shelter are hatched with a density increasing with the shelter. In the remaining areas the shelter is given in %.

3.2 Shelter at groups of houses

Figure 55 shows the shelter zone around a single house at angles of incidence of 45° and 90° with the longitudinal axis of the house. The cross-section of the house is shown in the upper lefthand corner. The vector v indicates the direction of the wind. At an angle of incidence of the wind of 45° it will be seen that there is only a very small area having more than 50% shelter.

Figures 57 to 60 shows the shelter at a building consisting of two adjoining wings. Measurements were made only in the area within the angle between the two wings.

The shelter in the area between the wings of a 3-wing building appears from Figures 61, 62 and 63.

The shelter within the space of a four-wing building is shown in Figures 64 - 67.

Figures 68 and 69 show the shelter at a school consisting of three parallel buildings and a lean-to parallel thereto.

Figures 70 and 71 show the shelter in the play-ground of the last-mentioned school, but with lean-tos to the east and west of the playground.

Figure 72 shows the shelter at the same school, but with lean-to only to the west of the play-ground.

Figure 73 shows the shelter when hedgerows are planted along the eastern and western sides of the play-ground. The hedgerows had a perforation of 66%.

Figs. 57 58 59 and 60. Shelter at a two-wing building.
Isoskepes have been drawn for 50 60 70 and 80% shelter. Areas having more than 50% shelter have been hatched with a density increasing with the shelter. In the remaining areas the shelter is given in %.

Figs. 61 62 and 63. Shelter at a three-wing building.
Isoskepes have been drawn for 50 60 and 70% shelter. Areas having more than 50% shelter have been hatched with a density increasing with the shelter. In the remaining areas the shelter is given in %.

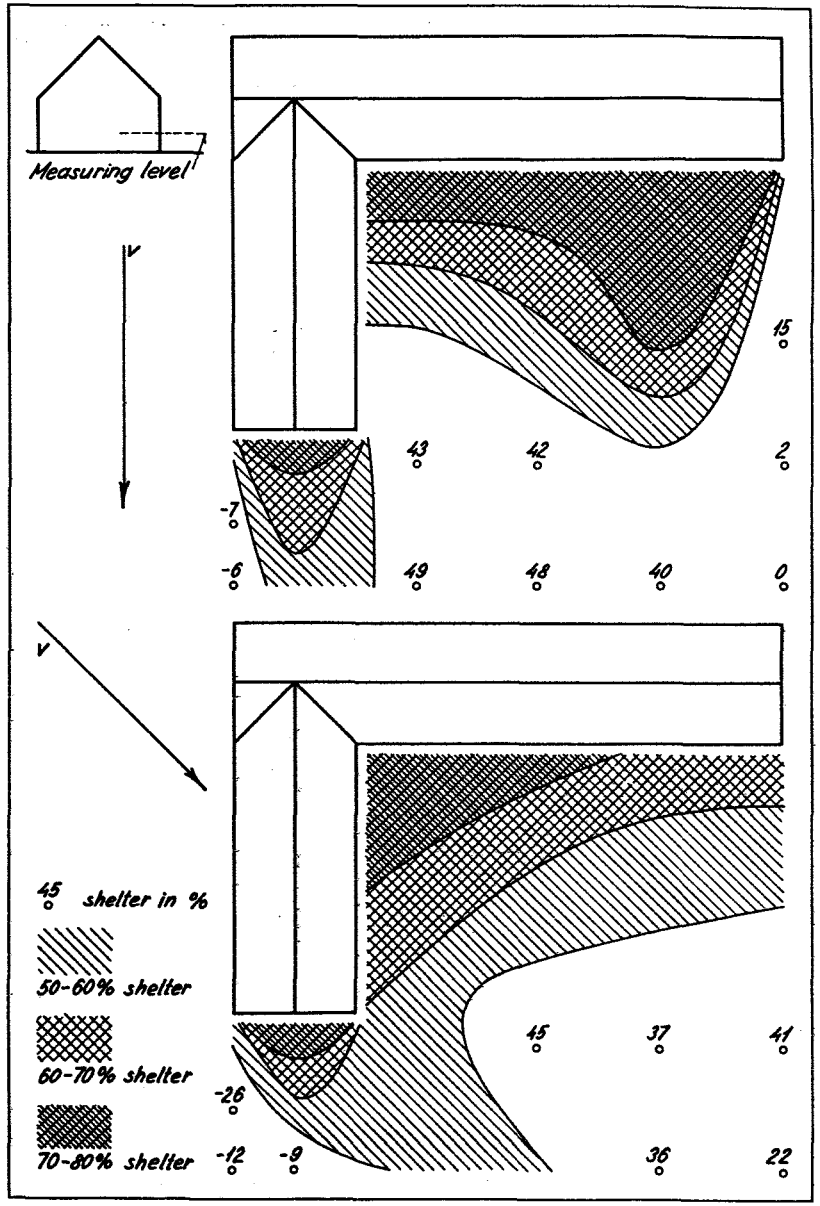

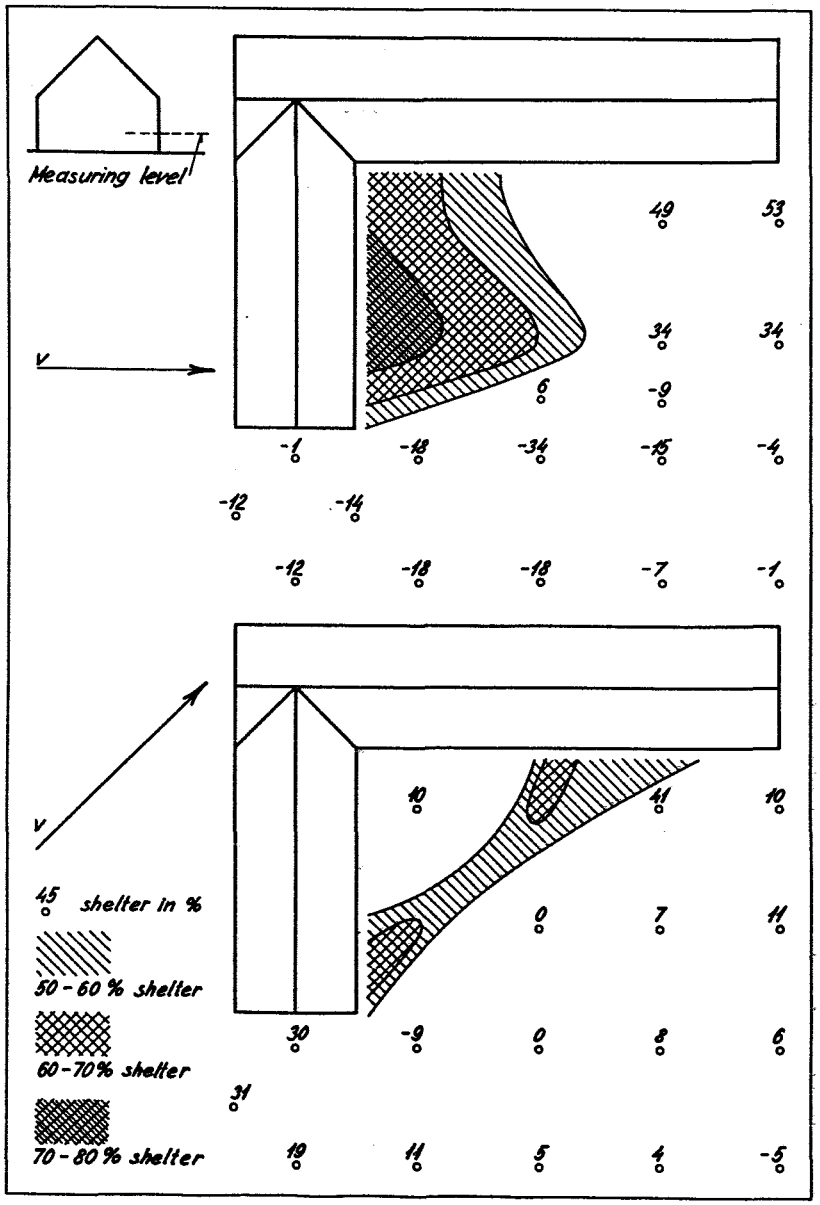
Measuring level
v
49
53
34
34
6
-9
-1
-18
-34
-15
-4
-12
-14
-12
-18
-18
-7
-1
v
10
41
10
0
7
11
30
-9
0
8
6
31
19
11
5
4
-5
45 shelter in %
50-60 % shelter
60-70% shelter
70-80 % shelter

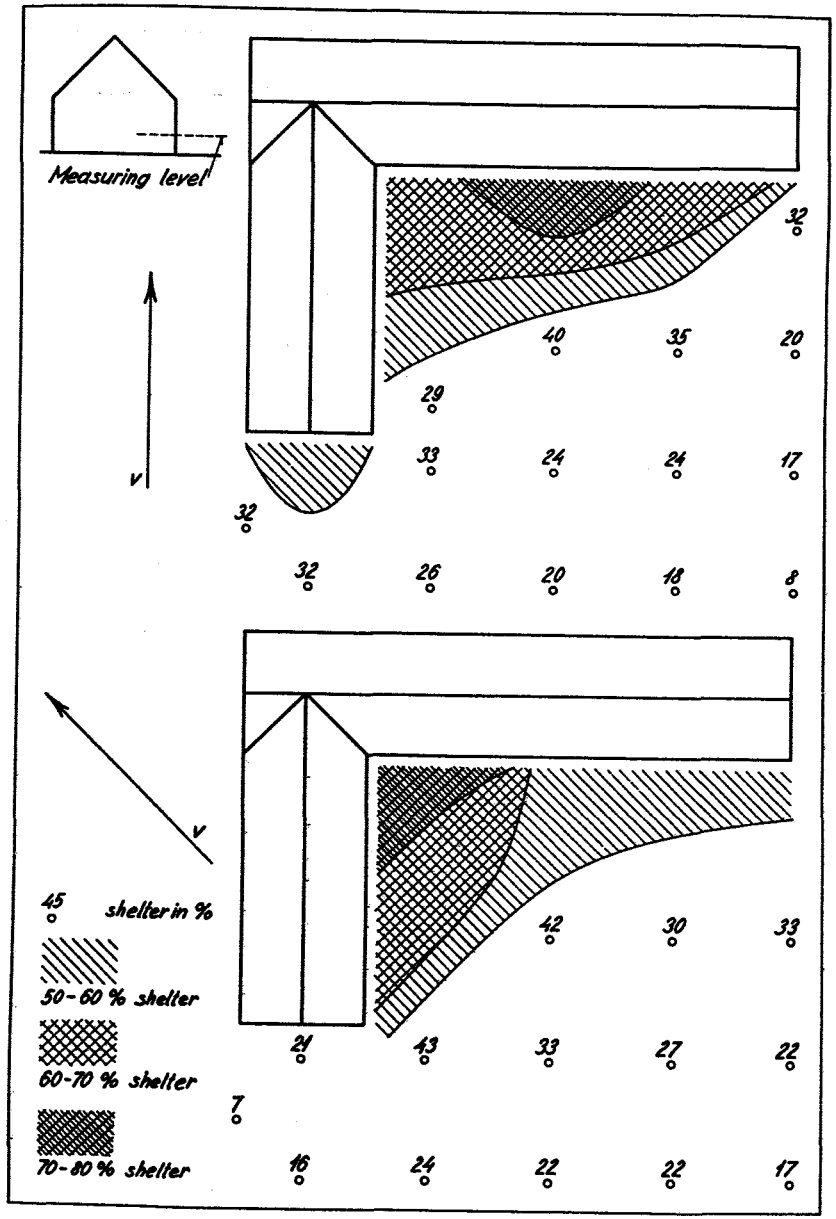
Measuring level
v
32
40
35
20
29
33
24
24
17
32
32
26
20
18
8
v
42
30
33
21
43
33
27
22
7
16
24
22
22
17
45 shelter in %
50-60 % shelter
60-70 % shelter
70-80 % shelter

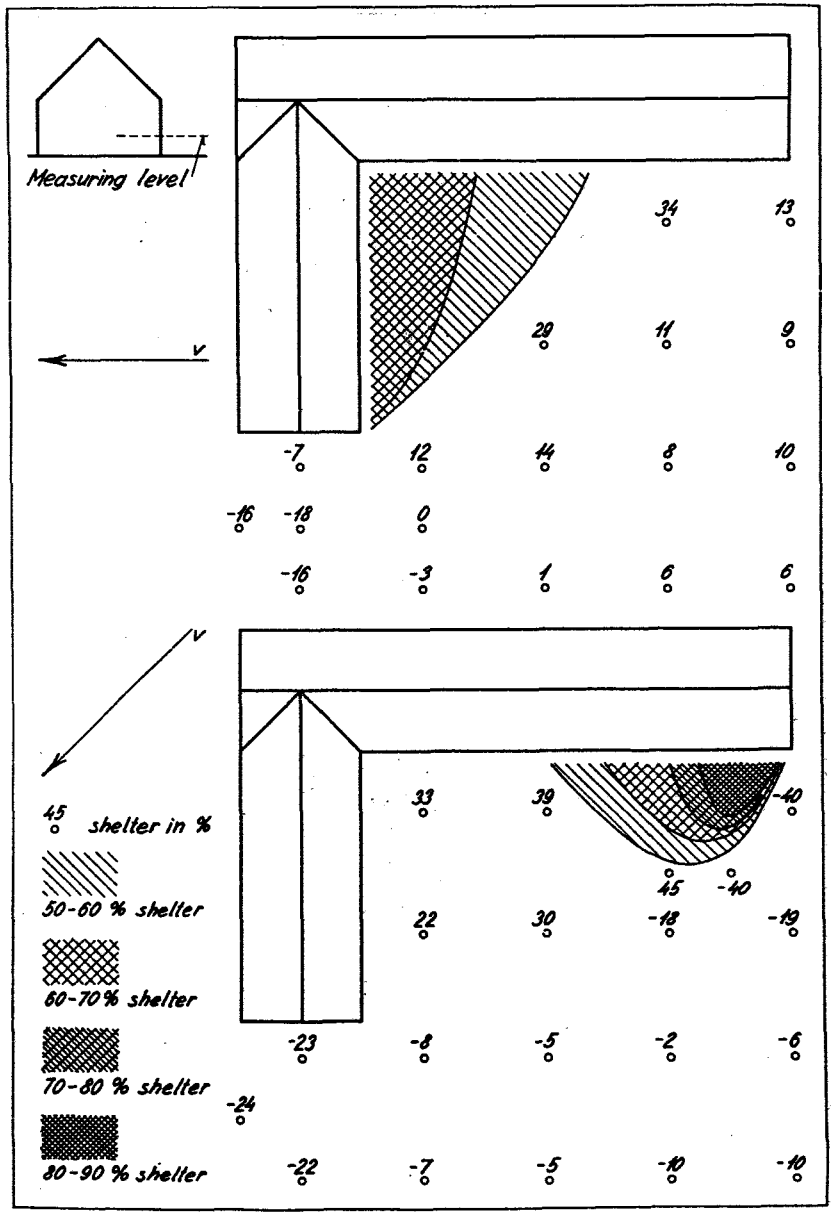
Measuring level
v
34
13
29
11
9
-7
12
14
8
10
-16
-18
0
-16
-3
1
6
6
v
45 shelter in %
50-60 % shelter
60-70 % shelter
70-80 % shelter
80-90 % shelter
33
39
-40
45
-40
22
30
-18
-19
-23
-8
-5
-2
-6
-24
-22
-7
-5
-10
-10

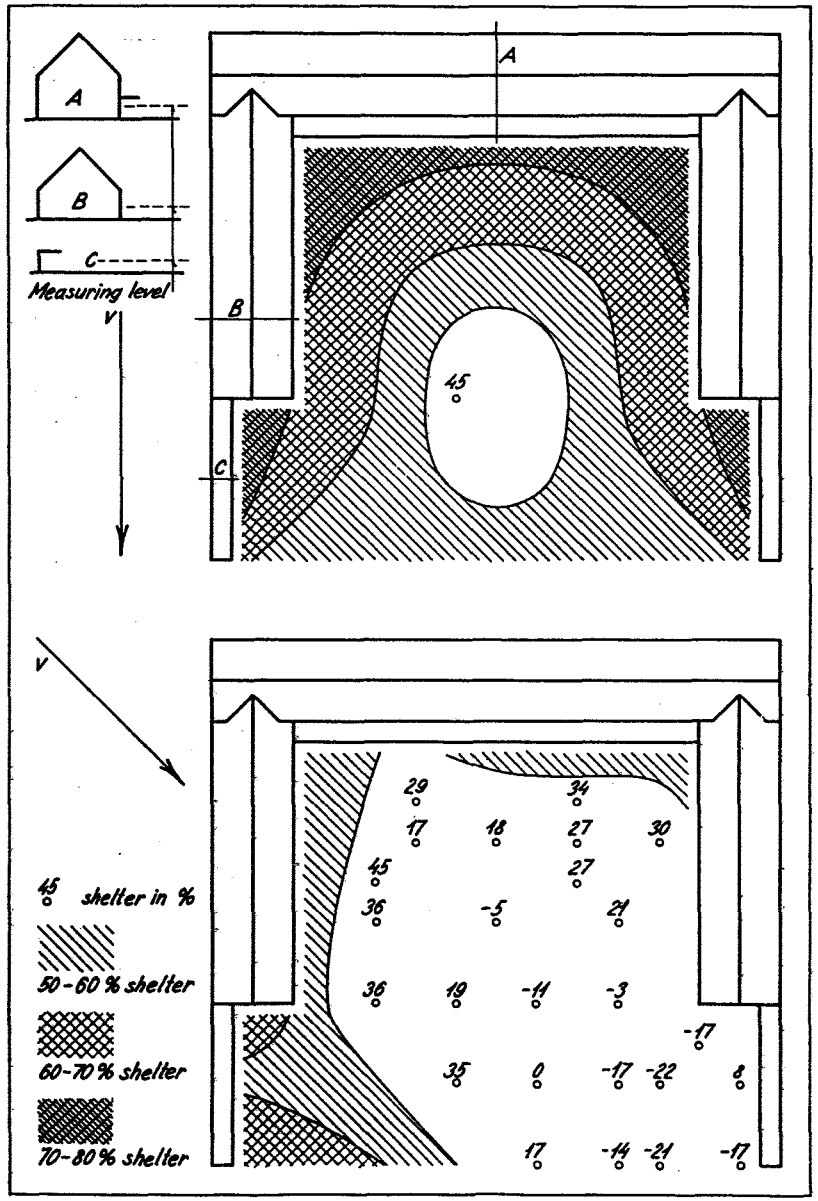
A
B
C
Measuring level
v
A
B
C
45
v
45 shelter in %
50-60 % shelter
60-70 % shelter
70-80 % shelter
29
34
17
18
27
30
45
27
36
-5
21
36
19
-11
-3
-17
35
0
-17
-22
8
17
-14
-21
-17

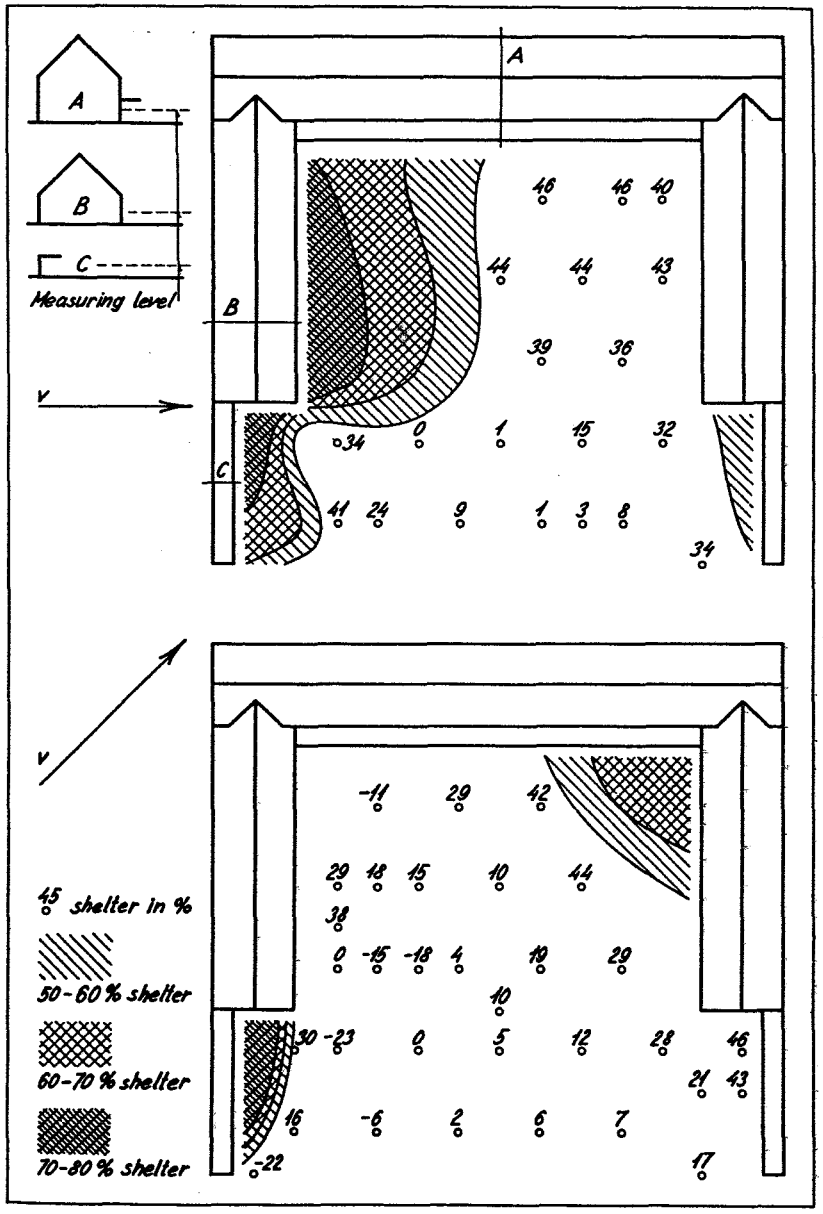

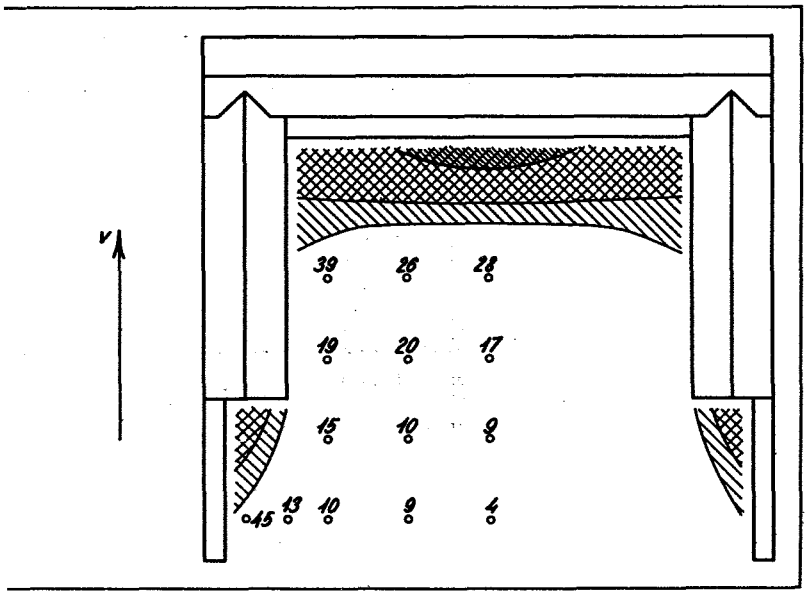

Figs. 64 65 66 and 67. Shelter at a four-wing building.
Isoskepes have been drawn for 50 60 70 and 80% shelter. Areas having more than 50% shelter are hatched with a density increasing with the shelter. In the remaining areas the shelter is given in %.

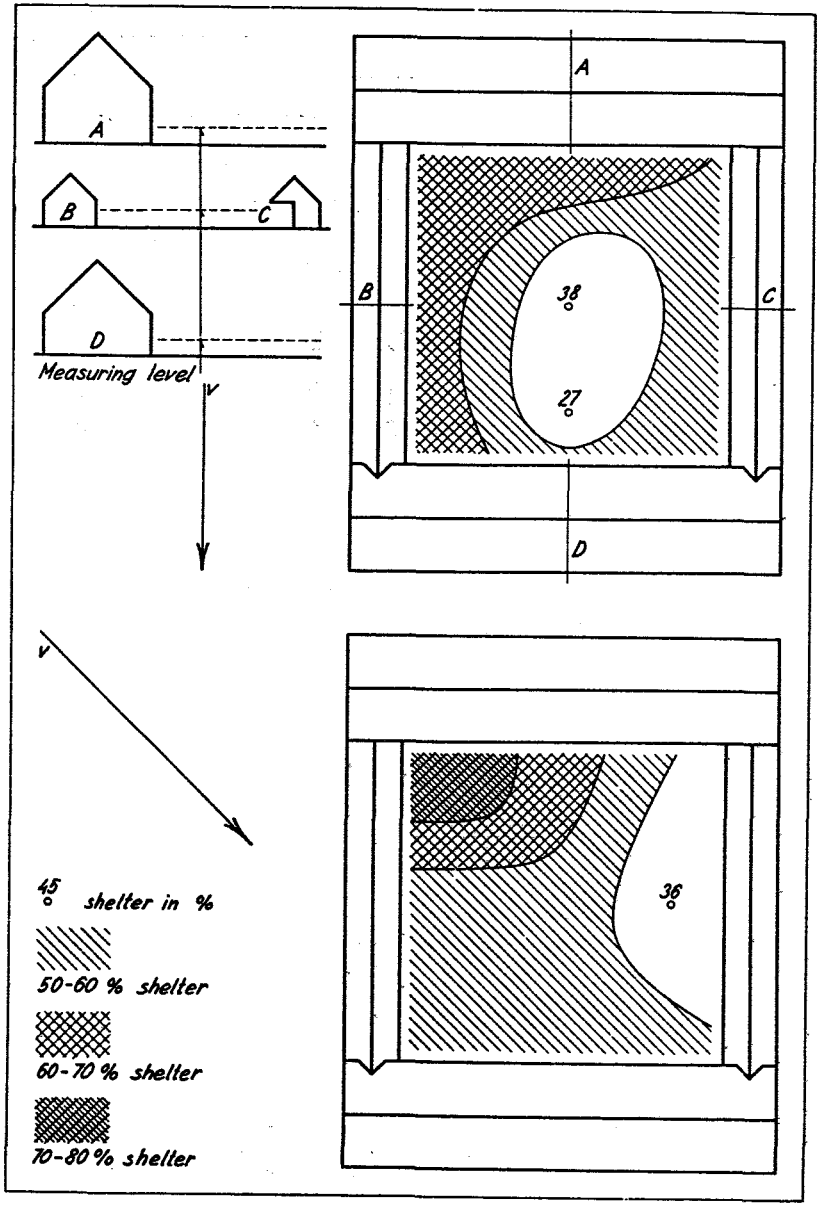
A
B
C
D
Measuring level
v
38
27
36
45 shelter in %
50-60 % shelter
60-70 % shelter
70-80 % shelter

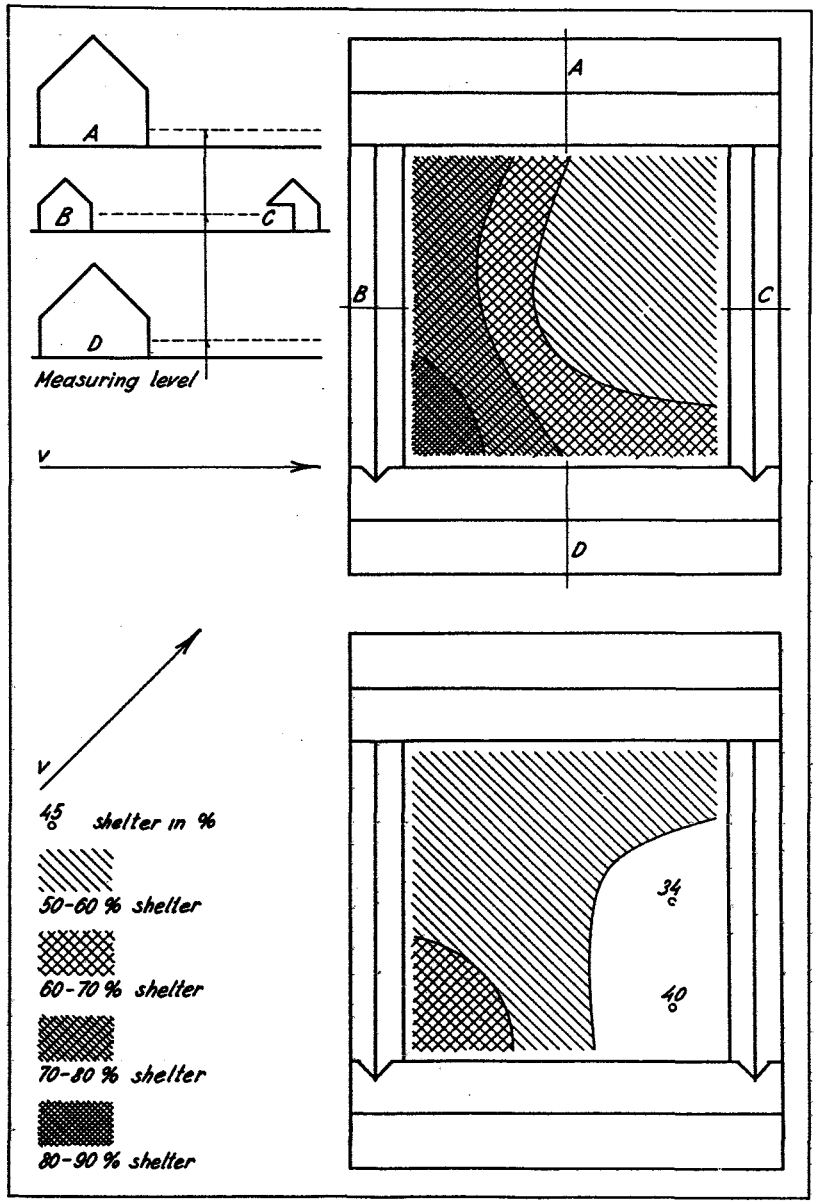
A
B
C
D
Measuring level
v
34
40
45 shelter in %
50-60 % shelter
60-70 % shelter
70-80 % shelter
80-90 % shelter

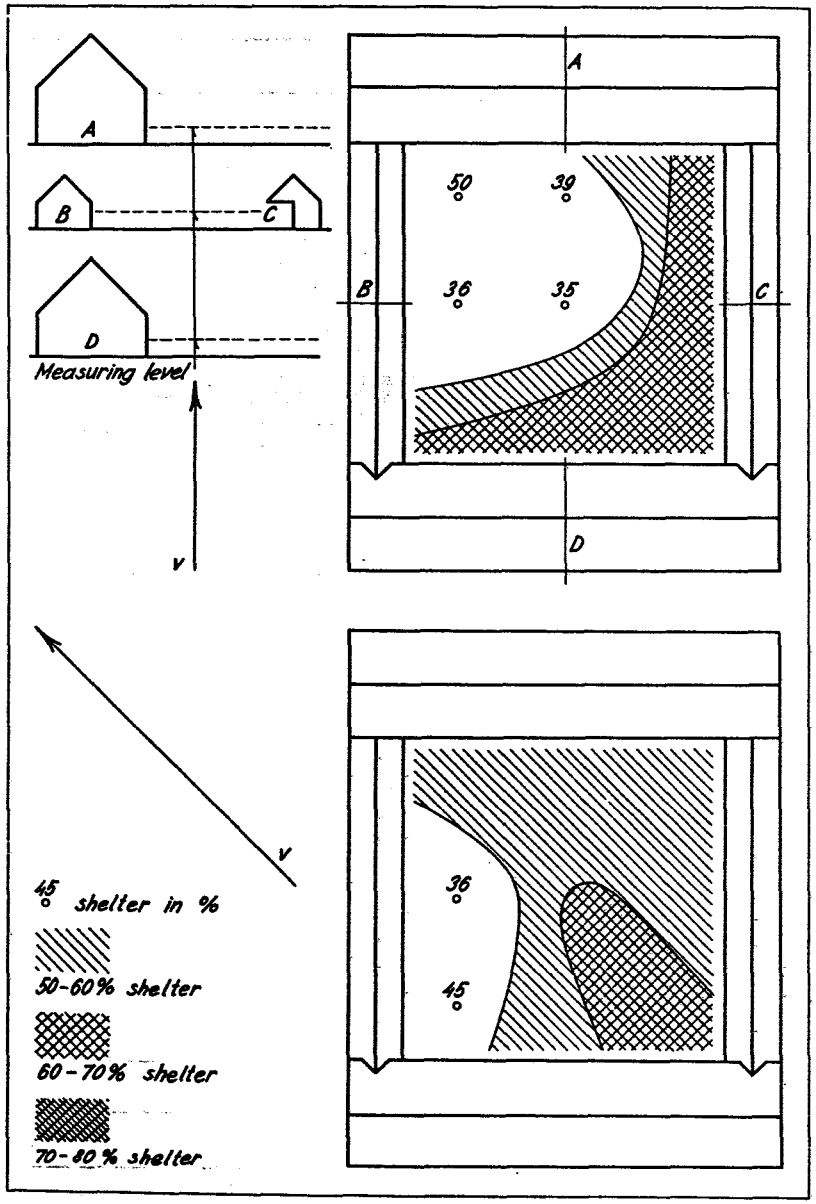
A
B
C
D
Measuring level
v
A
B
C
D
50
39
36
35
v
36
45
45° shelter in %
50-60% shelter
60-70% shelter
70-80% shelter

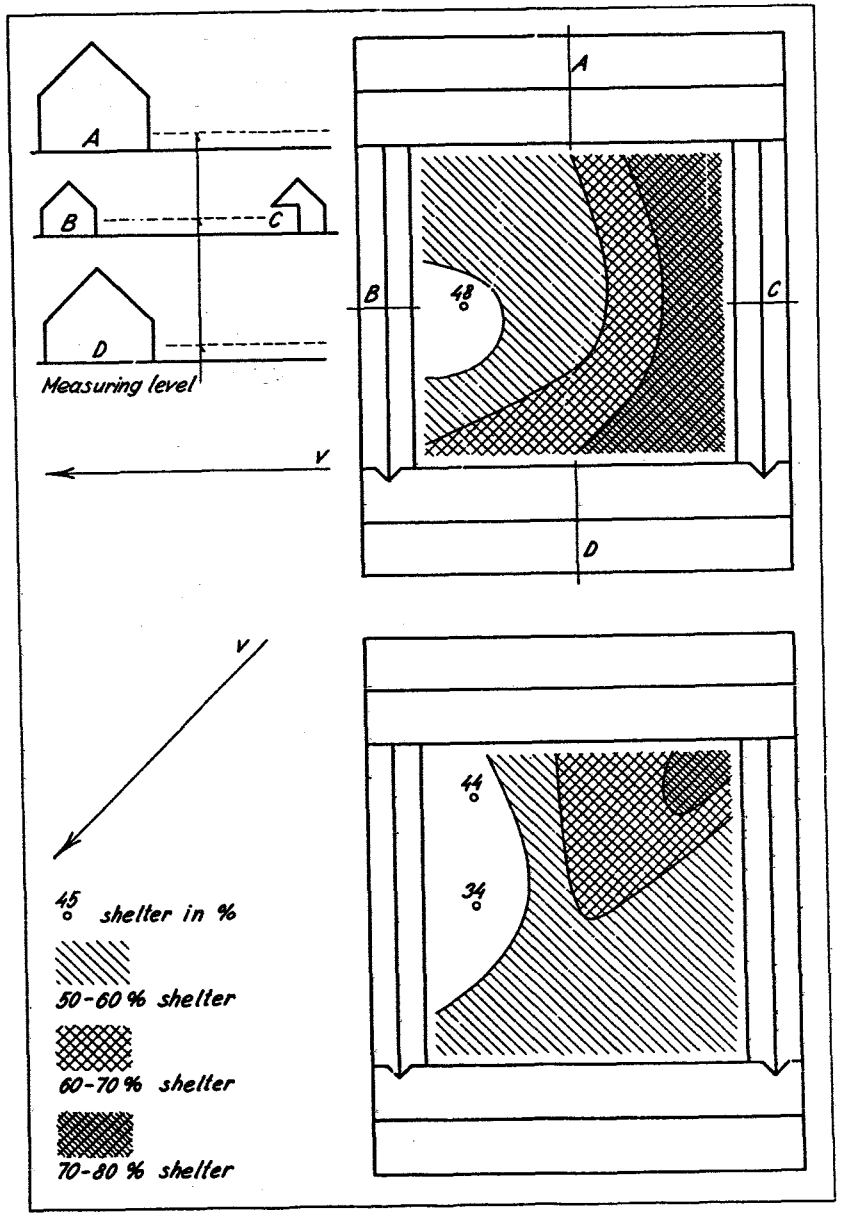
A
B
C
D
Measuring level
v
A
B
C
D
48
v
44
34
45° shelter in %
50-60 % shelter
60-70 % shelter
70-80 % shelter

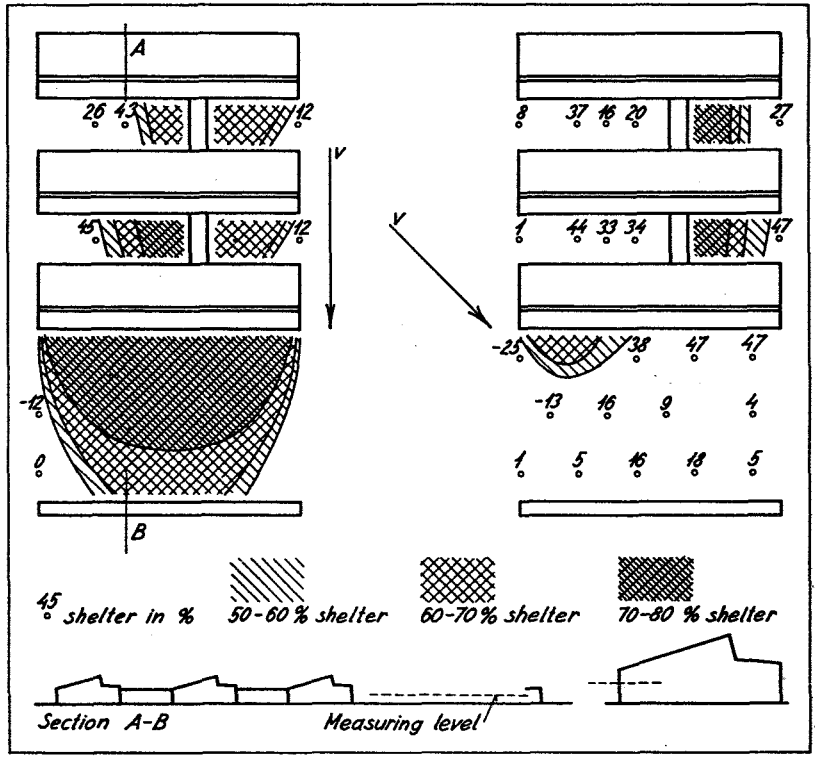

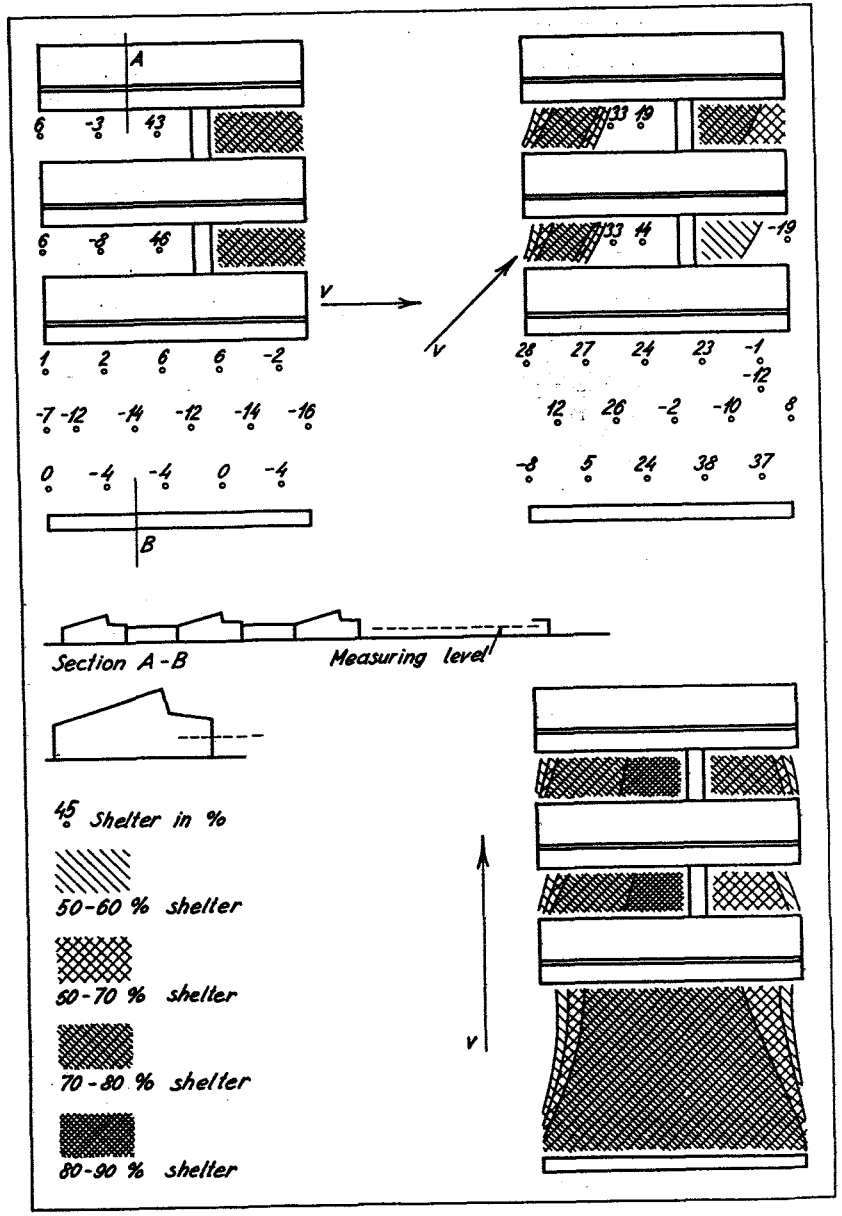

Figs. 68 and 69. Shelter at a school consisting of three parallel buildings and a lean-to parallel therewith.

Isoskepes have been drawn for 50 60 70 and 80% shelter. Areas having more than 50% shelter are hatched with a density increasing with the shelter. In the remaining areas the shelter is given in %.

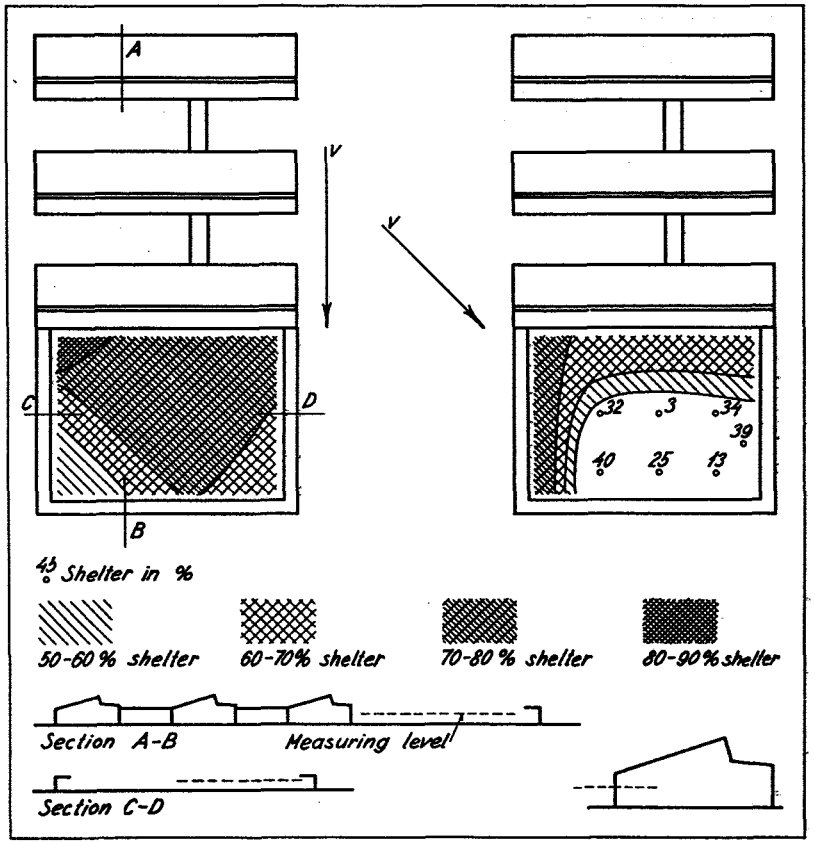

Figs. 70 and 71. Shelter at the same buildings as in Figs. 68 and 69, with lean-to shelters placed to the east and west of the playground.

Isoskepes have been drawn for 50 60 70 and 80% shelter. Areas having more than 50% shelter are hatched with a density increasing with the shelter. In the remaining areas the shelter is given in %.

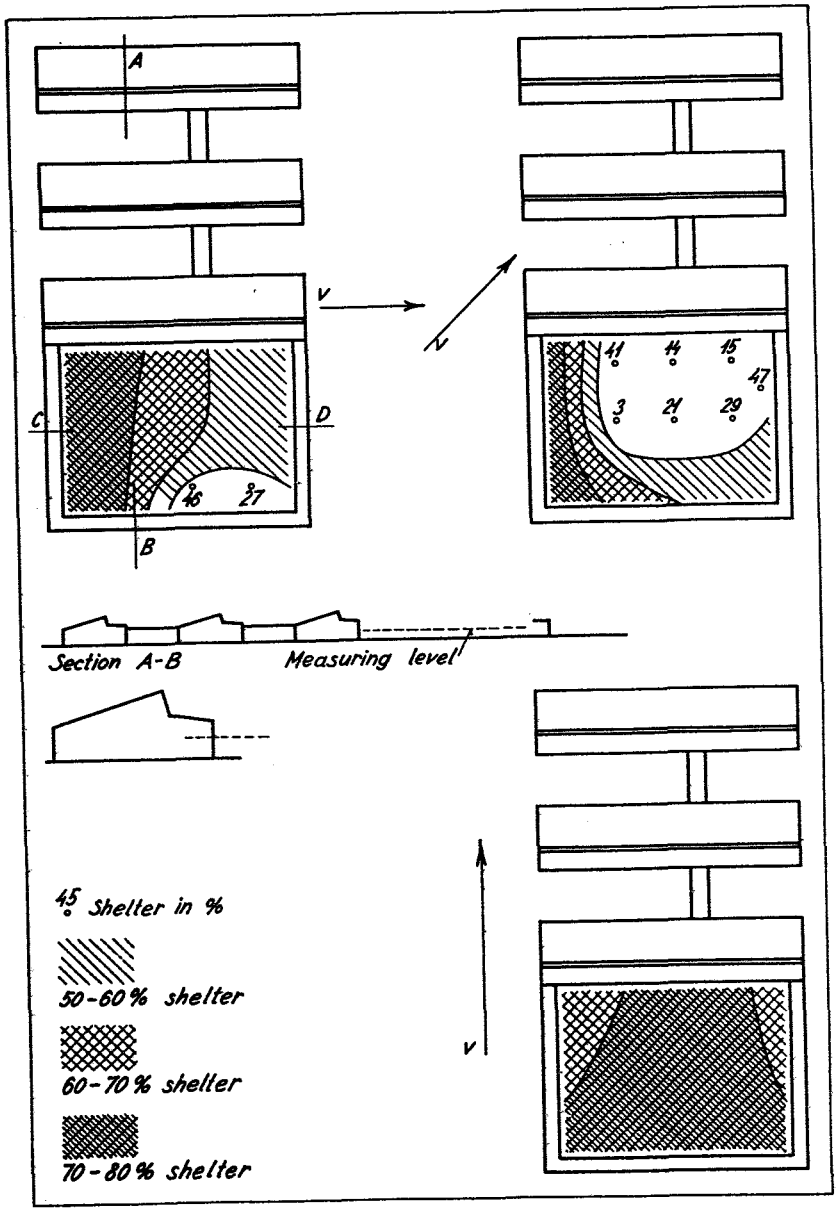

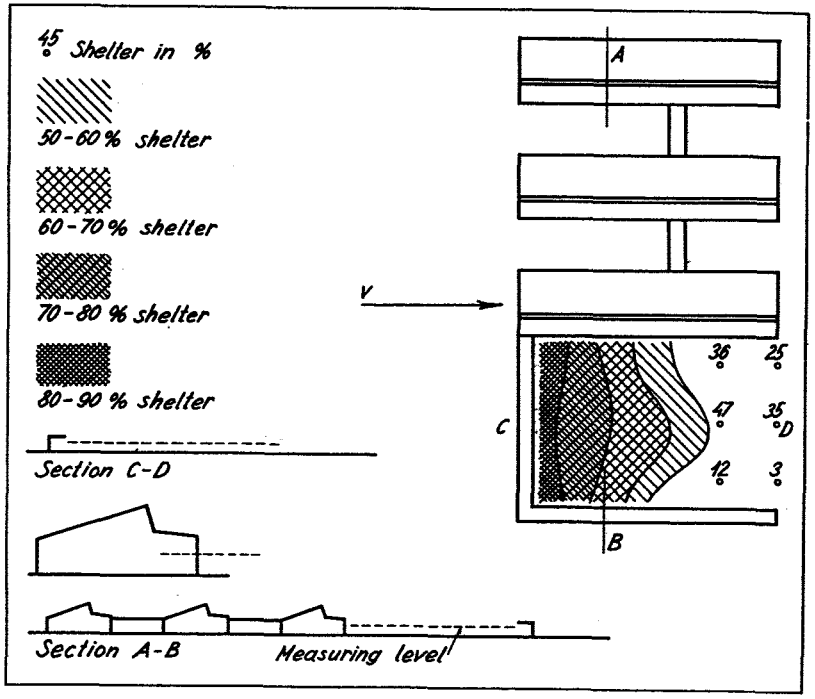

Fig. 72. Shelter at the same buildings as in Figs. 68 and 69 with a lean-to shelter placed to the west of the playground.

Isoskepes have been drawn for 50 60 70 and 80% shelter. Areas having more than 50% shelter have been hatched with a density increasing with the shelter. In the remaining areas the shelter is given in %.

Fig. 73. Shelter at the same buildings as in Figs. 68 and 69, a hedgerow having been placed to the east and west of the playground.

Isoskepes have been drawn for 50 60 70 and 80% shelter. Areas having more than 50% shelter have been hatched with a density increasing with the shelter. In the remaining areas the shelter is given in %.

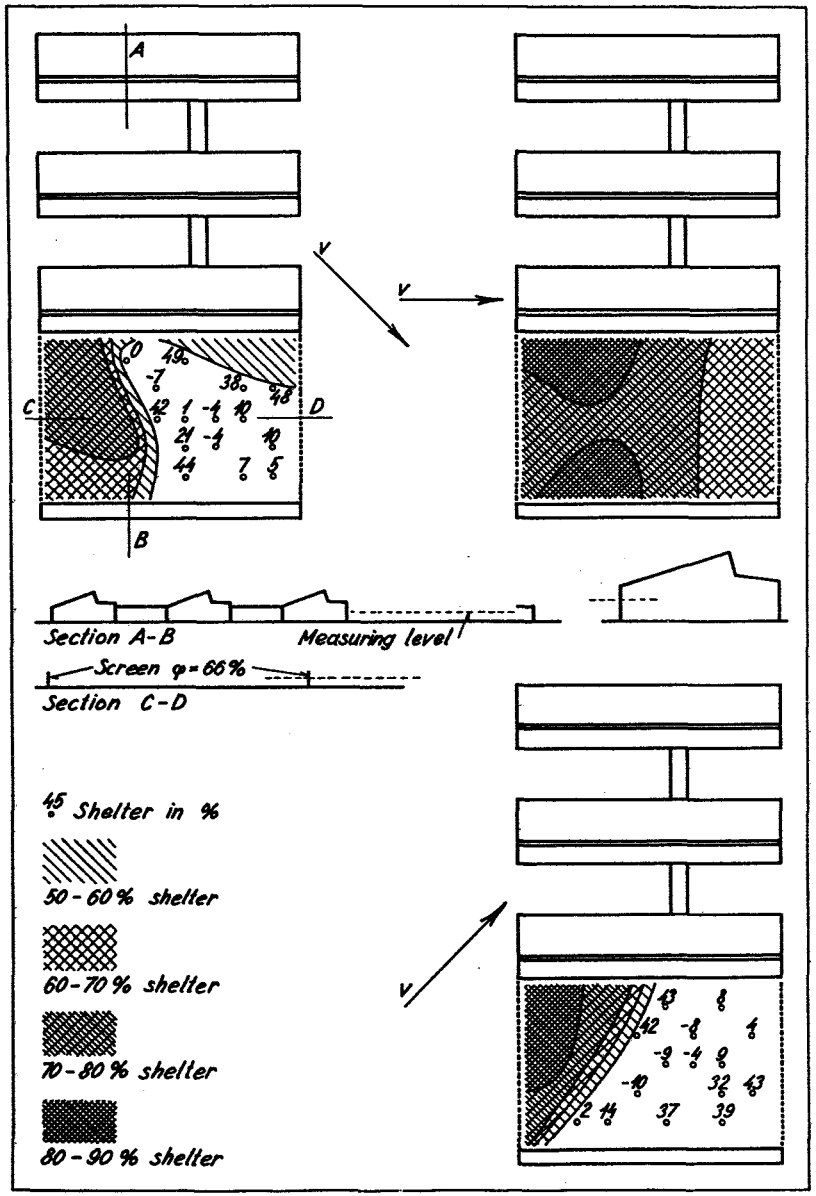

3.3 Discussion

Compared with hedgerows and perforated screens, houses – as will appear from the two preceding sections – afford poorer shelter, in the sense that only small areas with more than 50% shelter will occur.

Lean-tos with flat roofs seem to afford better shelter than normal houses with saddle-roofs.

As mentioned, only small areas having shelter of any importance will occur at houses, and as houses to a great extent cause large eddies in the wind, the shelter must be judged to be considerably inferior to that indicated by the hatched areas in the foregoing figures. At any rate, if the shelter is to afford possibilities for human comfort, it will, of course, be of importance to reduce the velocity of the wind, that is what is expressed by the shelter percentage. But it will also be of importance that the reduced wind is steady, particularly as regards direction. A wind which one moment blows into the face and the next moment into the back of the neck is felt to be highly disagreable even if it is rather light.

As regards the last-mentioned feature the wind in shelter areas at houses is very disagreeable. It changes direction with the unobstructed wind, but will frequently turn to an even greater degree when the free wind changes its velocity.

Figure 75a shows the flow over a house. The picture was taken at the starting of the flow and it will be seen that a small eddy has been formed to the leeward of the ridge. Figure 75b shows the air-current a little later and the eddy now fills the entire space over the leeward surface of the roof. A little later still the eddy has grown to the same size as the house and reaches the ground, as will be seen in Figure 75d. The eddy now passes on in direction with the wind, it has commenced to do so already in Figure 75d, leaving a shelter zone separated from the unobstructed flow by a discontinuity surface, as shown in Figure 75e. If the flow stops, the discontinuity surface will, however, at once be converted into a large eddy which will roll in over the leeward side of the house, as will be seen from Figure 75f.

The performance shown in Figures 75a – 75f will take place whenever the velocity of the wind rises or falls, with the result that at most places in the shelter zone

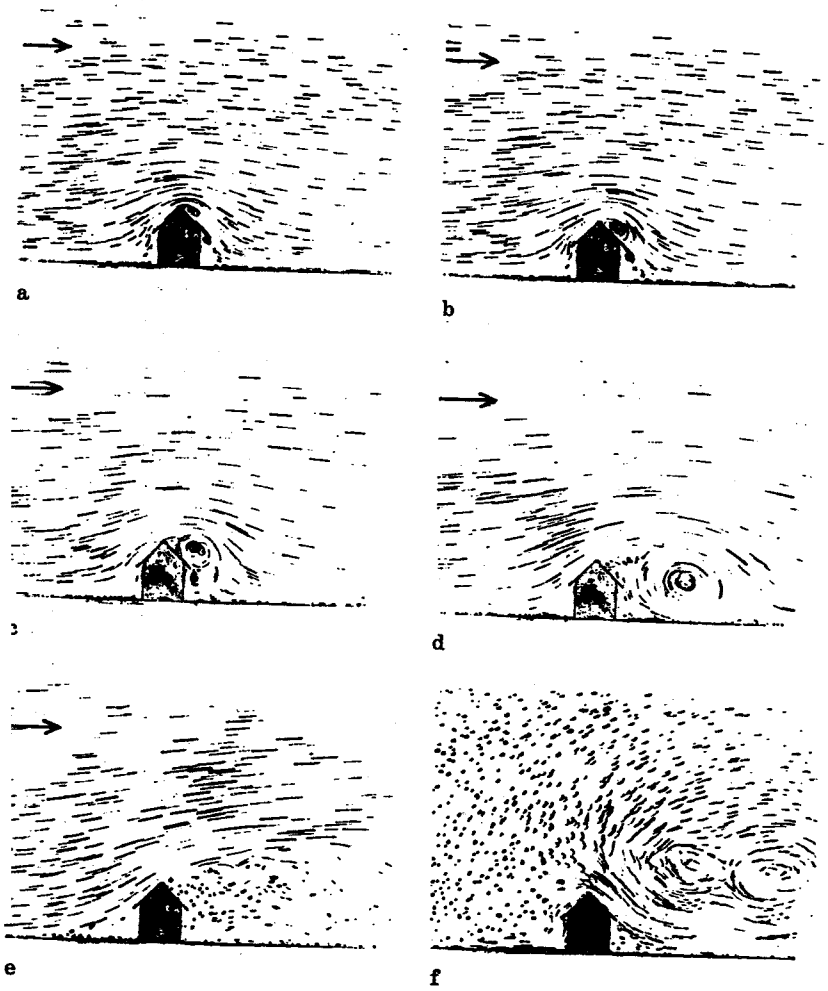

the direction of the wind will change 180°.

It can thus be established that houses afford poor shelter. When a good shelter is desired it will be necessary to employ hedgerows or perforated screens, or perhaps a lean-to.

4. DISPERSAL OF SMOKE FROM CHIMNEYS

4.1 Introduction

The smoke emerging from an isolated chimney will, as shown in Figure 77, undulate up and down in shapes that constantly change in the course of time. The plume will, however, remain within a parabolic envelope as shown in the figure. In the course of time the plume will sweep over the entire zone confined by the enveloping curve.

If the smoke is considerably lighter than the atmosphere, for instance because its temperature is high, it will rise on its way from the chimney. At very low speeds of the wind it may rise to a considerable height, but at only moderate wind speeds the rise will normally be of little importance.

The concentration of a noxious gas in the smoke at a given point in the surroundings will be in inverse proportion to the speed of the wind and will thus, ceteris paribus, constitute the greatest nuisance at small speeds of the wind.

In most places very low wind speeds will be of rare occurrence as compared with moderate speeds. In the solution of the problem of the dispersal of smoke we shall therefore here presuppose a certain moderate speed of wind, so that the rise of the smoke due to its lightness in relation to the atmosphere will be of little importance. The rise may be regarded as a welcome reserve in the rare cases when the speed of the wind is very low.

The smoke dealt with in this paper comprises all smoke gases, soot and the finest ash particles, all these components conforming to the laws for mass exchange. The coarser ash particles have, however, an appreciable rate of fall and will therefore reach the ground more quickly.

In Figure 77 the centreline of the enveloping curve has been drawn. At some distance from the chimney this centreline will be horizontal unless buildings or configurations of the ground influence the course of the smoke In the immediate zone, however, i.e. within the order of 50 times the cross-section of the chimney, the centreline may curve upwards or downwards, dependent upon the shape of the

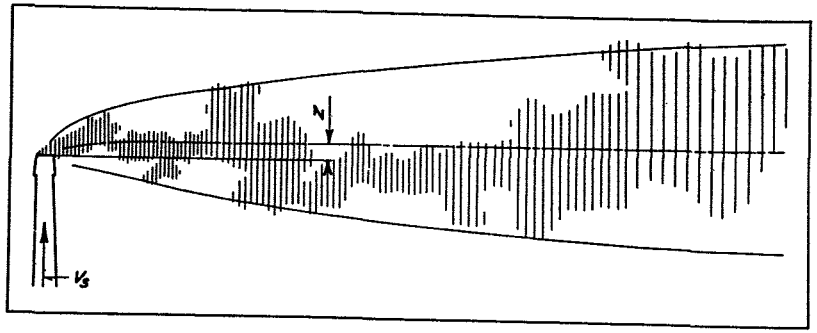

Fig. 77. Smoke plume from an isolated chimney.
The smoke plume ondulates upwards and downwards but remains within the parabolic envelope.

cross-section of the chimney and the ratio between the speed of the smoke inside the chimney and the speed of the wind. At a given height of chimney the centreline of the plume may be raised by a correct choice of cross-section and by the use of a great speed of the smoke. The turbulence of the air-current will also to some extent influence the level of the centreline, and the turbulence will be of material importance in determining the thickness of the enveloping curve of the plume.

When the atmosphere is in neutral equilibrium, the turbulence will be purely mechanical and depend on the roughness of the terrain. This may be considered the normal condition. This paper deals solely with conditions in an atmosphere in neutral equilibrium.

The following designations will be employed:

z_o roughness parameter of the terrain,
v_o speed of the unobstructed wind at the level of the top of the chimney,
A area of the clear opening of the chimney,
v_s mean speed of the smoke over the area A,
z rise of the plume in the immediate zone.

From these values a non-dimensional, characteristic set must be derived. The lengths are made non-dimensional by division with a length corresponding to the cross-section of the chimney; for this purpose the square root of the opening of the chimney will be used, $a = \sqrt{A}$.

The speed of the smoke, v_s, is, of course, made non-dimensional by dividing it with the speed of the unobstructed wind.

Thence, we obtain the following set of values:

$\frac{z_o}{a}$ non-dimensional roughness parameter,

$w = \frac{v_s}{v_o}$ non-dimensional speed of the smoke,

$u = \frac{z}{a}$ non-dimensional rise in the immediate zone.

Further,

H height of the chimney above the ground,

h height above the ground of a homogenous built-up area.

$\sigma = \frac{H}{h}$ non-dimensional height of the chimney above the groun

4.2 Immediate zone. Shape of chimney, turbulence, speed of smoke

The immediate zone is the area from the chimney to a distance of about 50a, a being the cross-section of the chimney.

In the experiments use was made of the three shapes of cross-section shown in Figure 79 all of which have the same area of clear opening. Smoke from the smoke generator described in Section 1.5 was sent up through the chimney in a quantity measured by the small venturimeter. The plumes of smoke were photographed and the pictures used for the measurement of the rise, z, etc.

The square chimney was placed with one side in the direction of the wind and also at an angle of 45°. The rectangular chimney was mounted lengthwise in the wind and at right angles to it.

The experiments were made both in wind with little turbulence and in a more turbulent air-current. In the former case the bottom of the tunnel was coated with corrugated paper with a roughness parameter equal to 0.07 cm. At the experiments with greater turbulence the model of a city with a roughness parameter of 3.5 cm was mounted on the bottom of the tunnel.

In the experiments a turbulence grate was used at the inlet end of the tunnel, so that at the place of measurement the thickness of the boundary layer was 45 cm. The chimney was placed in the front part of the 4th section with its opening 30 cm above the floor of the tunnel.

Figures 81a – 84b show examples of photographs of the smoke plume.

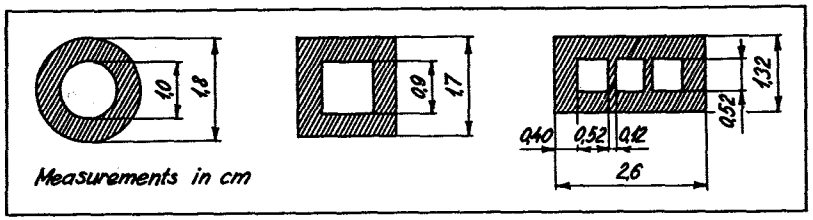

Fig. 79. Cross-sections through chimney models.

Shape of cross-section. The importance of the shape of the cross-section for the situation of the plume at the boundary of the immediate zone, i.e. at a distance of about 50a from the chimney, will appear from Figure 85. The non-dimensional rise of the plume u is plotted as an ordinate and is positive upwards. A negative u will thus mean that due to a downward suction behind the chimney the centreline of the plume will be below the level of the opening. The results are given for three different values of the non-dimensional smoke velocity, w, namely 0.5, 1.5 and 2.5 and for the two degrees of turbulence.

The figure shows that in all cases the rectangular cross-section placed lengthwise in the wind is the best one, i.e. the one giving the greatest rise or the least lowering of the plume. When, however, the rectangular chimney is placed at right angles to the wind, it will in all cases be the poorest one. The next best is the cylindrical chimney.

The two arrangements of the square chimney give only slightly different results, and it may therefore be presumed that the values of u for other angles between the side of the chimney and the wind will range between the values measured in these experiments. In other words, we may characterize the square chimney in terms of the arbitrary wind direction, as shown in the figure.

We can thus compare the round chimney with the square one at the arbitrary direction of the wind. The circular cross-section will always be the best one. At small turbulence and low smoke speeds the difference in value of u will be highest, namely 2.0, i.e. that a square chimney must be built twice its cross-section a higher in order to be as efficient as a round chimney in keeping the plume at a high level.

The rectangular chimney gives so different values of u in the two positions examined that it cannot on the

Figs. 81a – 84b. Smoke plumes in windtunnel.
The data for each figure is shown in the following table.

Fig.	Cross–section of chimney	Turbulence in tunnel	$w = \frac{v_s}{v_o}$
81a	rectangular, crosswise	small	2.18
81b	" , lengthwise	"	2.18
82a	circular	great	1.94
82b	"	small	0.49
83a	"	"	1.0
83b	"	"	2.0
84a	"	"	3.0
84b	"	"	4.2

The influence of the cross–section on the position and width of the plume is seen by comparing Figures 81a, 81b and 83b. Here the turbulence and the value of w are the same.

It is seen that the plume from the rectangular crosswise chimney is considerably lower than the plumes from the rectangular lengthwise chimney and the circular chimney.

The influence of the turbulence is seen from Figures 82a and 83b. Both figures are with circular chimneys and w = approx. 2. The great turbulence in Figure 82a causes plumes with larger widths than those in Figure 83b where the turbulence is small. It is seen that the centreline of the plumes lies a little lower in the case with great turbulence.

The influence of the smoke speed on the plume is seen from Figures 82b .... 84b which all concern a circular chimney in small turbulence, but with increasing values of the non–dimensional smoke–speed $w = \frac{v_s}{v_o}$. It can be seen that when w is increased the plume rises.

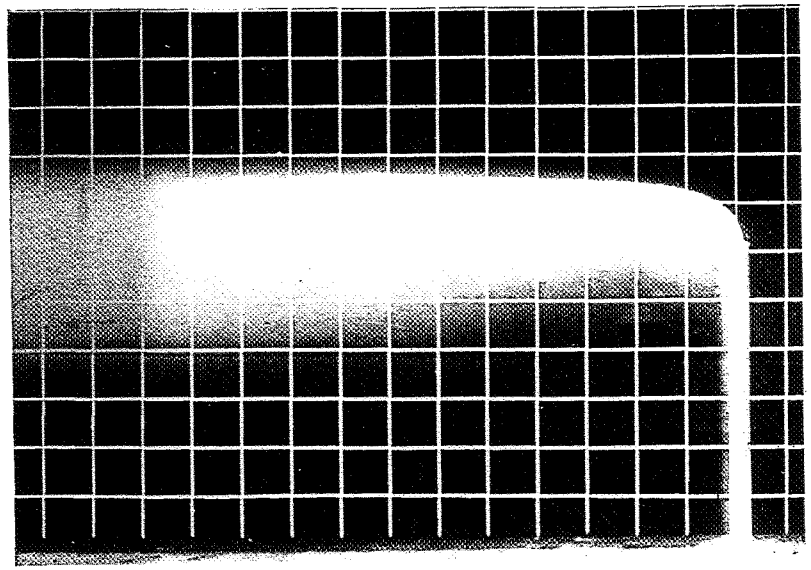

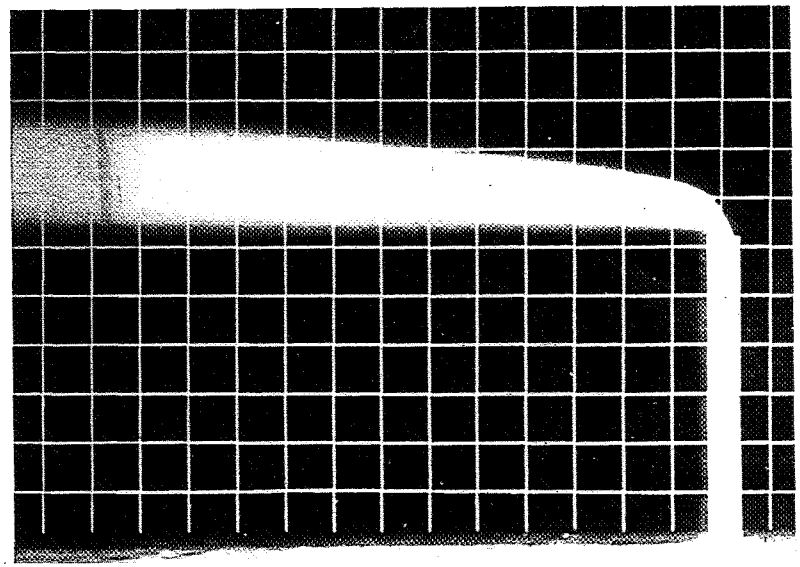

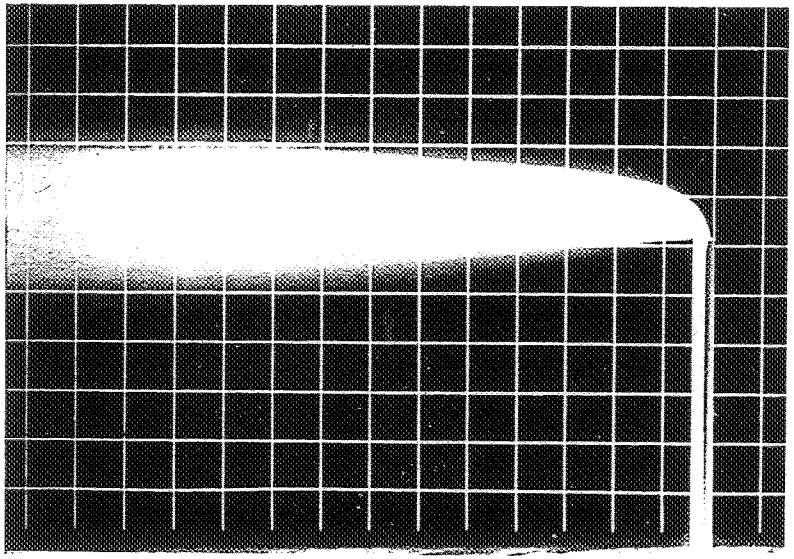

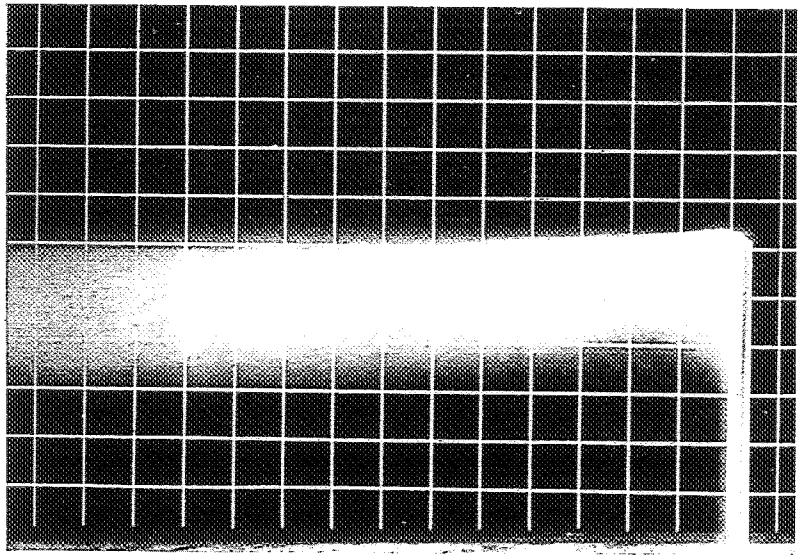

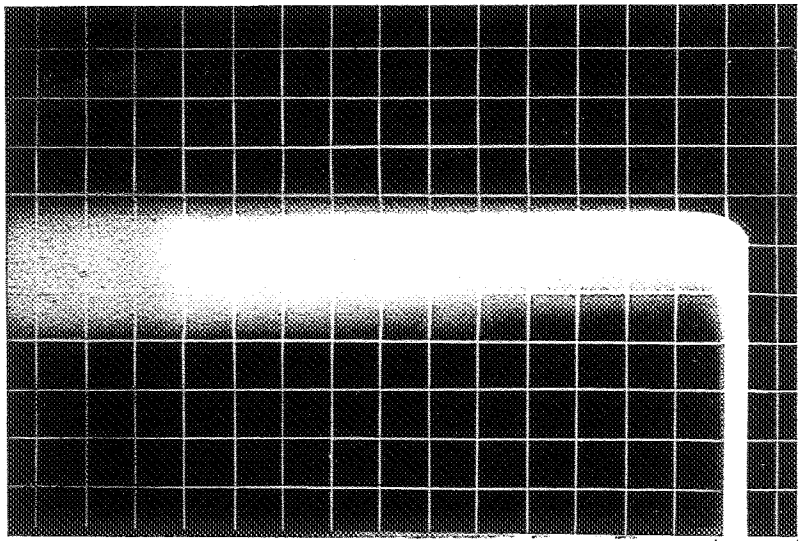

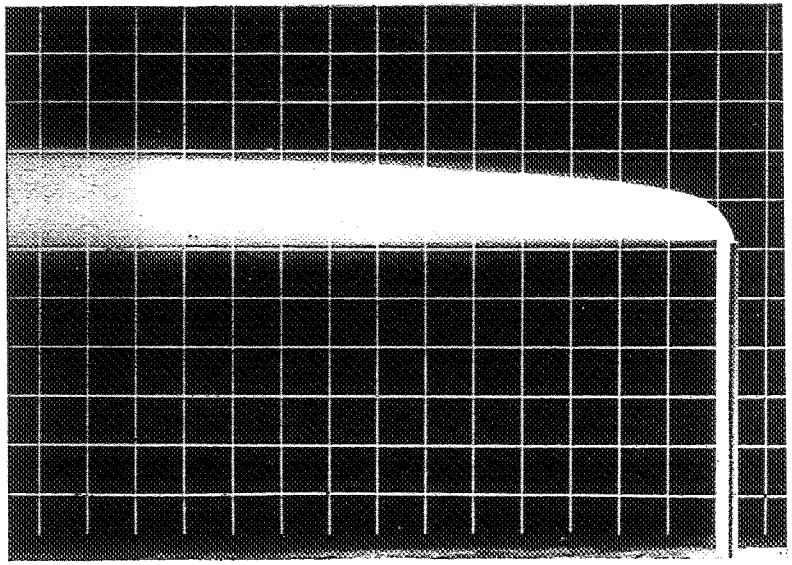

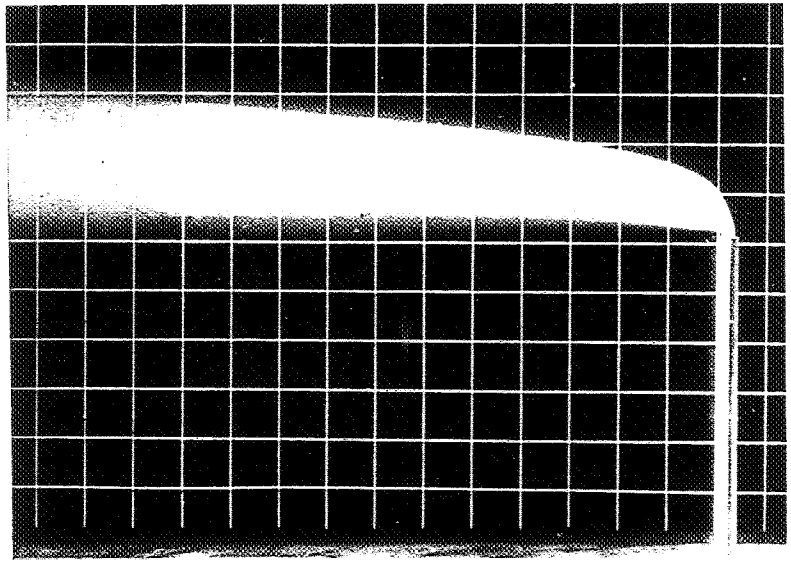

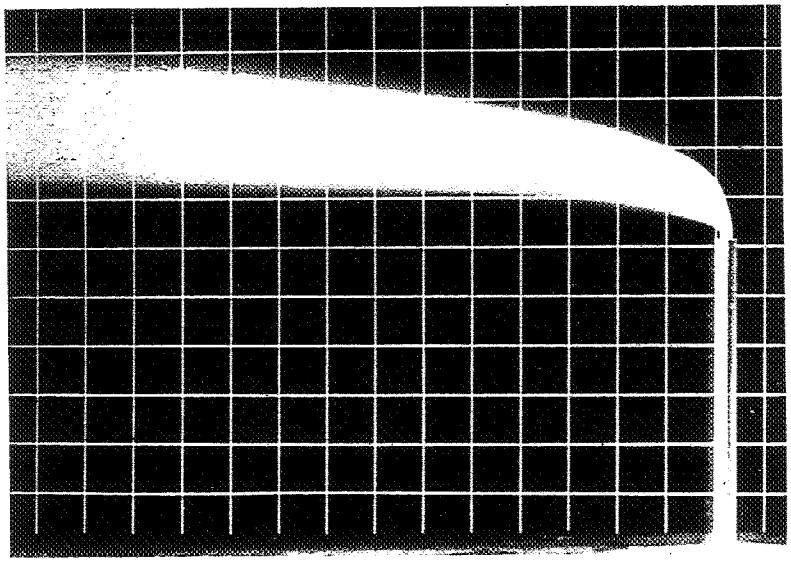

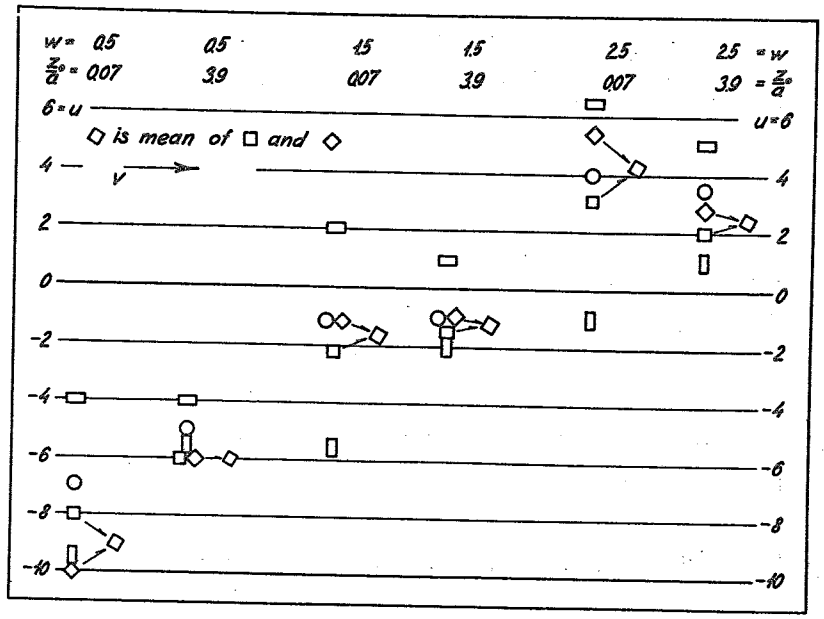

Fig. 85. Influence of the cross-section shape on the rising of the smoke.

The ordinate is the non-dimensional rise. The experiments were made for two values of the non-dimensional roughness and three values of the non-dimensional velocity of smoke.

basis of these experiments be evaluated for the arbitrary wind direction. It must, however, be noted that the favourable values of u obtained when the longer side is parallel to the wind will presumably apply only to a narrow margin of wind directions. It is to be presumed that, say, a 45° position will give as inferior a value of u as the transverse position – if not poorer. The highly favourable value of u when the longer side lies in the direction of the wind will therefore probably not be of much importance in practice.

The judgement given above of the qualities of the different cross-sections with regard to giving a high level of the plume will especially be of importance when the turbulence is slight. At high degrees of turbulence the importance of the cross-section shape will decline.

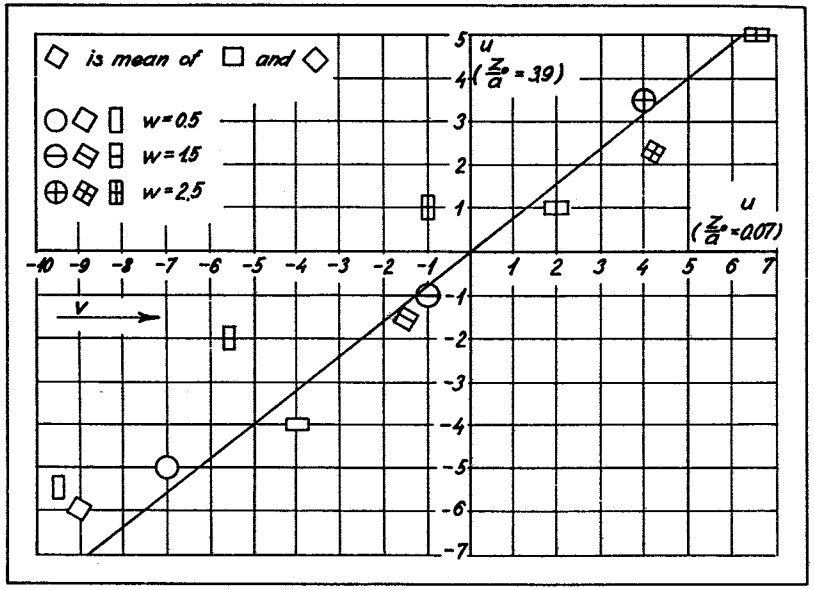

Fig. 86. Influence of the turbulence on the rise of the smoke plume.

The abscissa is the non-dimensional rise at small turbulence, the ordinate the rise at great turbulence. The experiments were made for three values of the non-dimensional velocity of the smoke, as will appear from the marks.

The turbulence. As mentioned above, the experiments on the course of the plume in the immediate zone were made at two degrees of turbulence. At low turbulence the enveloping curve of the plume will, of course, be a much more slender parabola than that obtained in strong turbulence, but that which is of interest to us in this connection is only where the centreline of the envelope is situated on the boundary of the immediate zone, i.e. at a distance of the order of 50a from the chimney.

Figure 86 shows how the non-dimensional rise u depends on the turbulence for the different cross-section shapes of the chimney. The ordinate represents the rise u in the flow with high turbulence, the abscissa the rise in the flow of small turbulence. The straight line drawn approximately through the points has a gradient of 0.8. Numerically the rise will thus be least in case of strong turbulence.

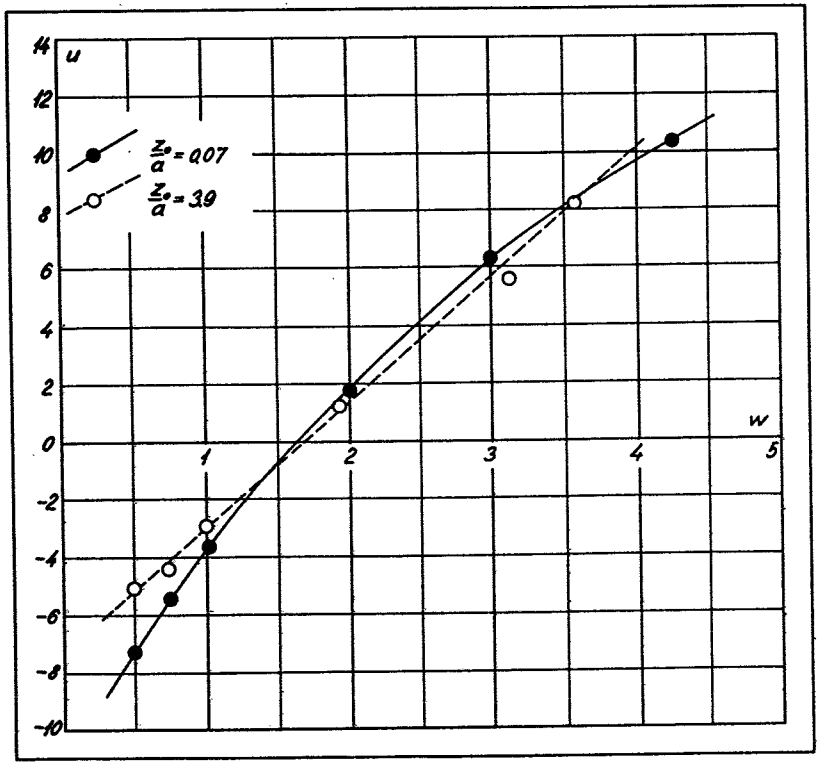

Fig. 87. Influence of the velocity of the smoke on the rise of the smoke plume from chimneys of circular cross-section.

The abscissa is the non-dimensional velocity of the smoke; the ordinate the non-dimensional rise. The solid curve and the solid marks correspond to the experiment at low turbulence. The broken curve and the open marks correspond to those at great turbulence.

The speed of the smoke. The most important factor with regard to the rise of the plume within the immediate zone is the ratio between the speed of the smoke and the speed of the unobstructed wind at the level of the opening of the chimney.

Figures 87, 88 and 89 show the results for the three different shapes of chimney. The abscissa is the non-dimensional speed w of the smoke, the ordinate the non-dimensional rise u at a distance of 50a from the chimney. Full-line curves and solid marks correspond to low turbulence, broken-line curves and open marks to high turbulence.

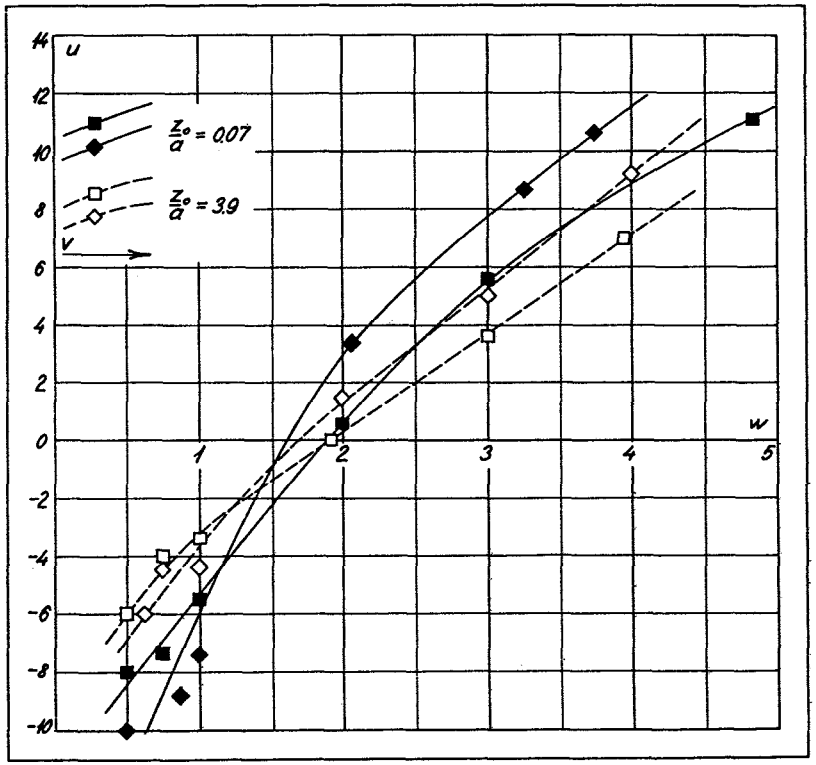

Fig. 88. Influence of the velocity of the smoke on the rise of the plume of smoke from chimneys of square cross-section.

The abscissa is the non-dimensional velocity of the smoke; the ordinate the non-dimensional rise. The solid curves and the filled in marks correspond to the experiments at small turbulence, the broken curves and open marks to experiments at great turbulence. As will appear from the marks the experiments were made both with the wind parallel to the side of the chimney and at an angle of 45°

In the case of the round chimney in Figure 87 the turbulence is of little importance. For w = 1.7 u is zero. At lower values of w u will be negative, at greater values positive. The curves are approximately rectilinear with a gradient of du/dw = 4.5, which means that an increase of w by 1.0 will compensate for a reduction in height of the chimney of 4.5 times the cross-section a.

As will be seen from Figure 88 the square chimney shows some difference according to whether the air is more

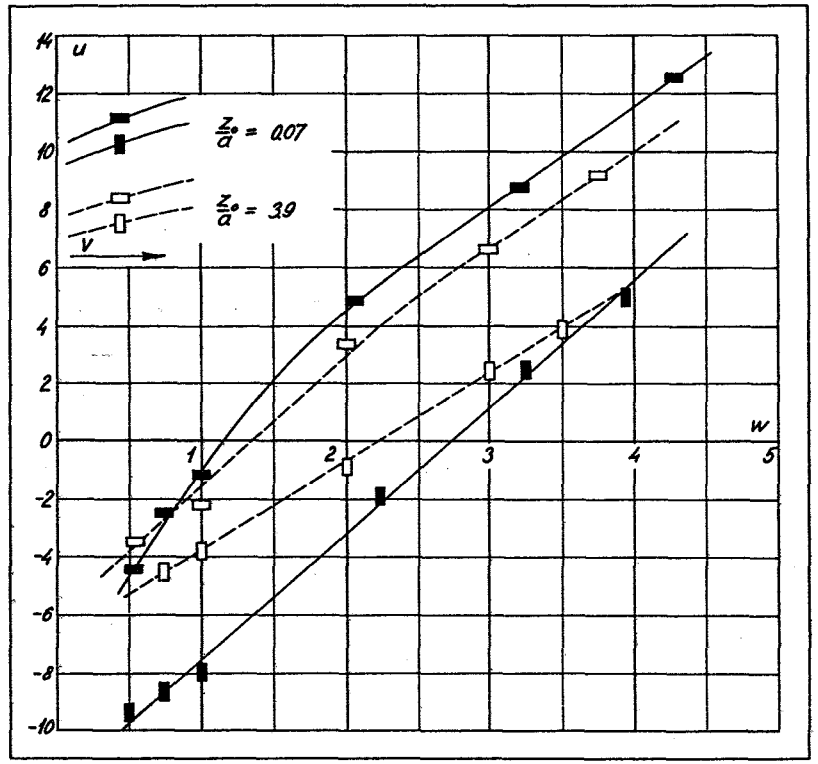

Fig. 89. Influence of the velocity of smoke on the rise of the smoke plume from chimneys of rectangular cross-section.

The abscissa is the non-dimensional velocity of the smoke; the ordinate the non-dimensional rise. The solid curves and the filled in marks correspond to experiments at low turbulence, the broken curves and open marks to experiments at high turbulence. As shown by the marks the experiments were made both with the wind blowing against the long and the short sides of the chimney.

or less turbulent. If, in the case of the greater turbulence, we take the mean of the two positions of the cross-section the gradient will be du/dw = 3.5. In the less turbulent flow the gradient is almost twice as great, namely du/dw = 6.5.

Figure 89 shows that the rectangular chimney in the position lengthwise in the wind gives considerably higher values of u than the same chimney at right angles to the wind. In the lengthwise position du/dw = 4 in both high and

low turbulence. In the transverse position the gradient will be greater in low turbulence, namely du/dw = 4, while in high turbulence du/dw = 3.

4.3 Isolated chimney

A systematic investigation was made in the wind tunnel of conditions at a house standing at varying distances from an isolated chimney.

The tunnel bottom carried a model of a built-up area and at the inlet end a turbulence grate was placed. Thereby the turbulent boundary layer at the place of experiment in the 3rd and 4th sections became 45 cm high; the velocity profile was logarithmic with a roughness parameter of 2.7 cm.

The chimney model was round with outer and inner diameters of 0.90 and 0.69 cm, respectively. Through the chimney a known quantity of CO_2 per unit of time was blown. The non-dimensional speed, w, of the smoke was about 1.5, ranging from 1.3 to 1.8, but its value is of relatively slight importance when conditions are investigated at so great distances from the chimney as was the case in this instance.

For the experiment the house shown in Figure 90 was

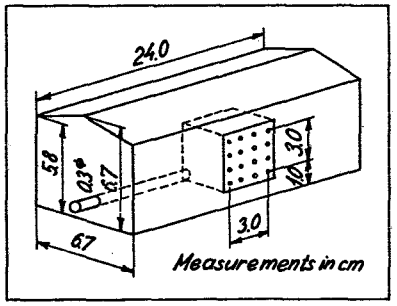

Fig. 90. Model of house for sampling of air for analysis.

Fig. 91. Contamination of air behind an isolated chimney.
The abscissa represents the distance from the chimney to the nearest house in proportion to the height of the house; the ordinate the height of the chimney in proportion to the height of the house. The curves correspond to the different levels of the non-dimensional smoke concentration. The solid curves represent conditions at the leeward front of the house, the dotted curves thus on the windward side. The maximum concentration, whether on the windward or leeward side is shown by a fat line.

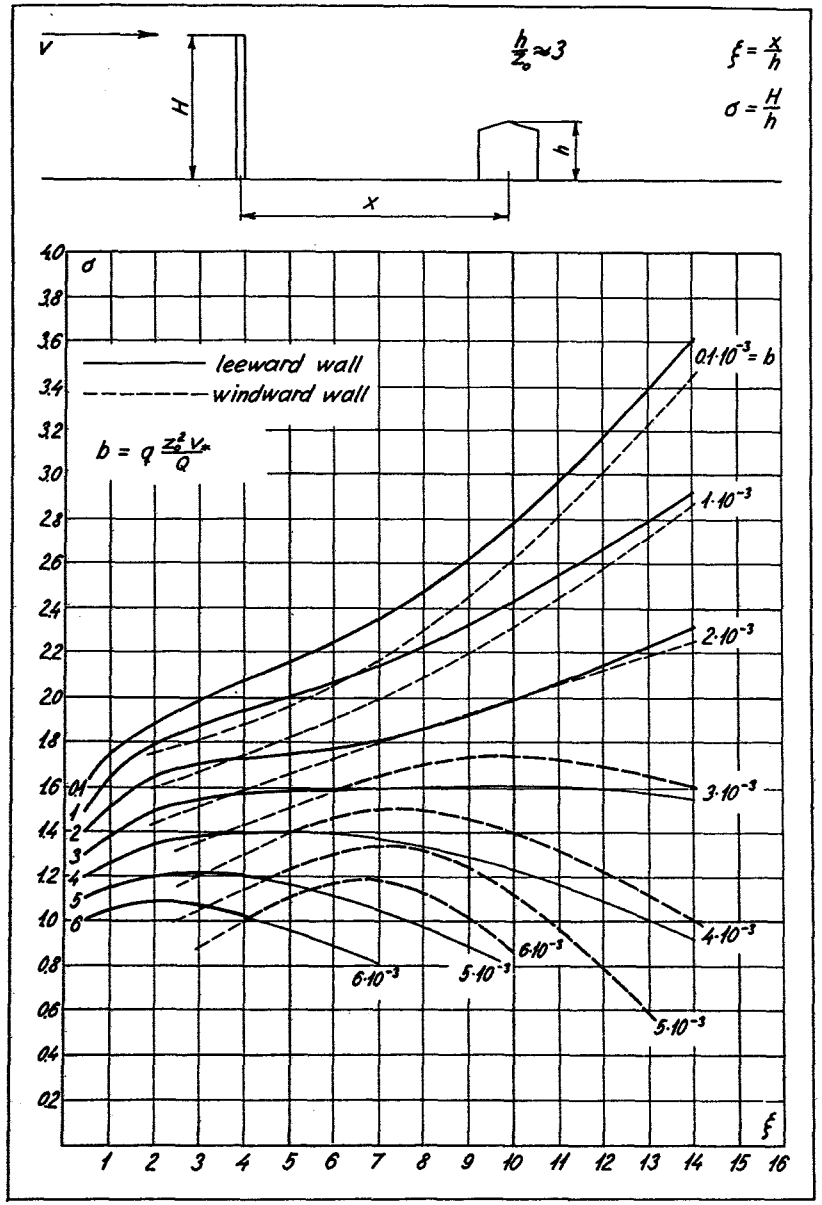

used. It is a model of a typical 3-storey dwelling-house on a scale of 1÷170. At the middle of one front of the house model a recess was cut and closed by a perforated metal plate. From the enclosed space air was sucked to the CO_2 analysis plant. Thus, the measurements give the mean CO_2 concentration in the area shown in Figure 90 at the middle of the facade of the building.

Otherwise the arrangement will appear from the upper part of Figure 91. The chimney is situated at a short distance from the last house in the 'roughness'. The house model is placed at distance x to the leeward of the chimney. The house was at all times placed with its front at right angles to the direction of the wind and with its centre, i.e. the point of suction, just below the chimney viewed in the direction of the wind.

Figure 91 shows the results of the measurements. The abscissa is the distance from the chimney to the house in proportion to the height of the house. The ordinate is the height of the chimney in proportion to the height of the house. The curves have been drawn corresponding to constant values of the non-dimensional concentration b, derived in Section 2.4. The full-line curves represent conditions on the leeward side of the house. The broken-line curves correspond to those on the windward side. The maximum concentration, whether on the leeward or the windward side, is drawn in heavy line, as solid and broken lines respectively.

It will appear from Figure 91 that the concentration is greatest on the leeward side of the house when the distance between the chimney and the house is less than 4-6 times the height of the house, except as regards small concentrations when the leeward side will always be the more exposed.

Fig. 93. Contamination of air behind the chimney on a house.
The abscissa represents the distance from the chimney to the nearest house in proportion to the height of the house, the ordinate the height of the chimney in proportion to the height of the house. The curves correspond to different levels of the non-dimensional smoke concentration. At the ordinate axis the conditions prevailing on the leeward side of the house bearing the chimney are shown. The curves show conditions at the windward front of the next house of the group; at the leeward front the concentration is a trifle smaller.

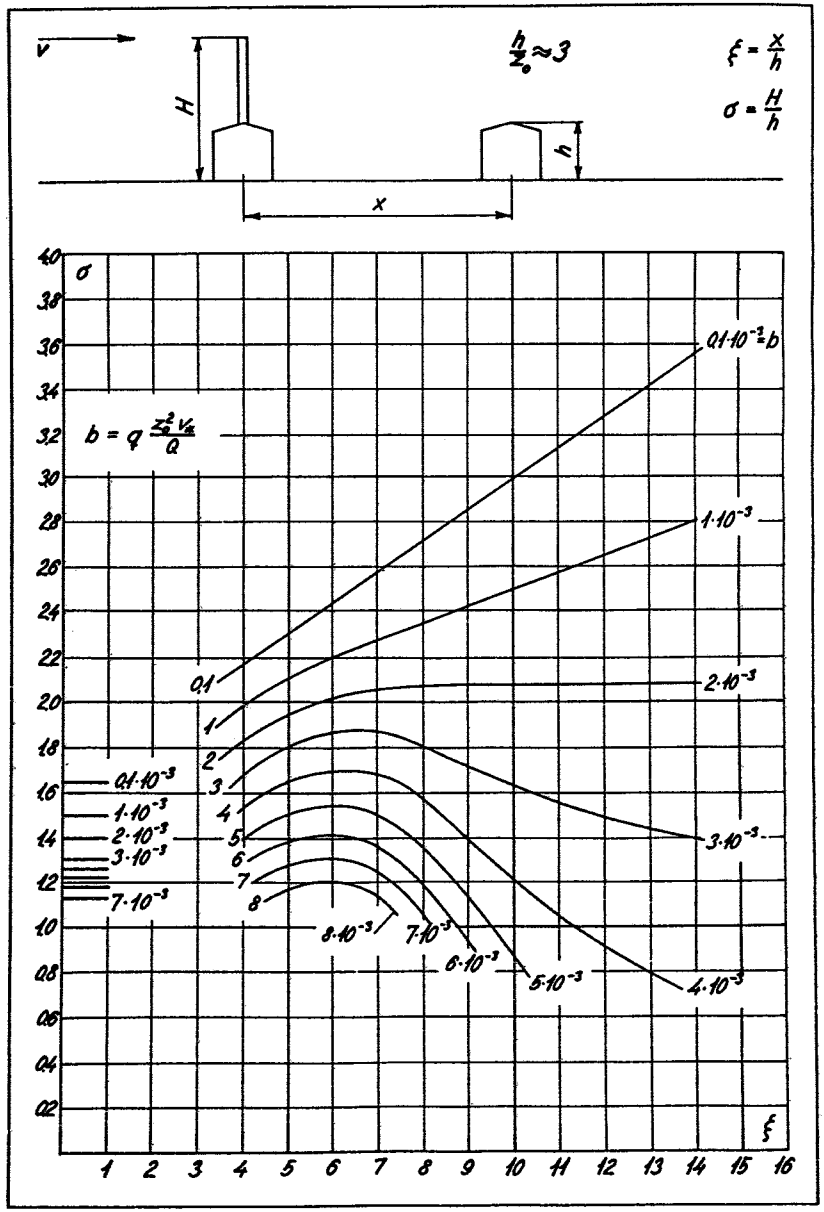

4.4 Chimney on a house

A systematic investigation was made in the wind tunnel of conditions at a house placed at varying distances from a chimney on another house.

The upper part of Figure 93 shows the arrangement. The experiments were exactly like those described in Section 4.3. The chimney was, however, og square cross-section with a clear opening of 0.6 cm and an external cross-section of 1.0 cm.

The results appear from Figure 93. The abscissa is the distance from the chimney to the house under measurement in proportion to the height of the house. The ordinate is the height of the chimney in proportion to the height of the house. The curves have been drawn to correspond to constant values of the non-dimensional concentration b derived in Section 2.4. The concentration is nearly equal at the windward and leeward fronts, but sligthly greater at the windward facade. The measurements shown in Figure 93 origins from the windward facade. On the ordinate axis the concentrations at the leeward front of the house carrying the chimney are shown.

4.5 The distant zone

The two preceding Sections dealt with conditions at the houses nearest to the chimney. This Section will deal with smoke conditions in general in an extensive, homogeneous built-up area around a tall chimney. The experiments aim solely at indicating how tall the chimney must be in order that excessive concentrations may be avoided anywhere within the built-up area.

For these experiments the tunnel was lengthened by 2 m, so that the working sections were of a total length of 7.5 m. The extension was interposed between the 1st and 2nd sections.

The tunnel bottom had a homogeneous roughness in the form of a model of an urban district extending of the full length of the tunnel. In the 3rd and 4th sections the velocity profile was logarithmic with $z_0 = 1.9$ cm. The chimney model, which was of circular cross-section with internal and external diameters of 0.8 and 1.0 cm, respectively, was placed in the forward part of the 3rd section. The non-dimensional velocity of the smoke in all the experiments was w = 1.0.

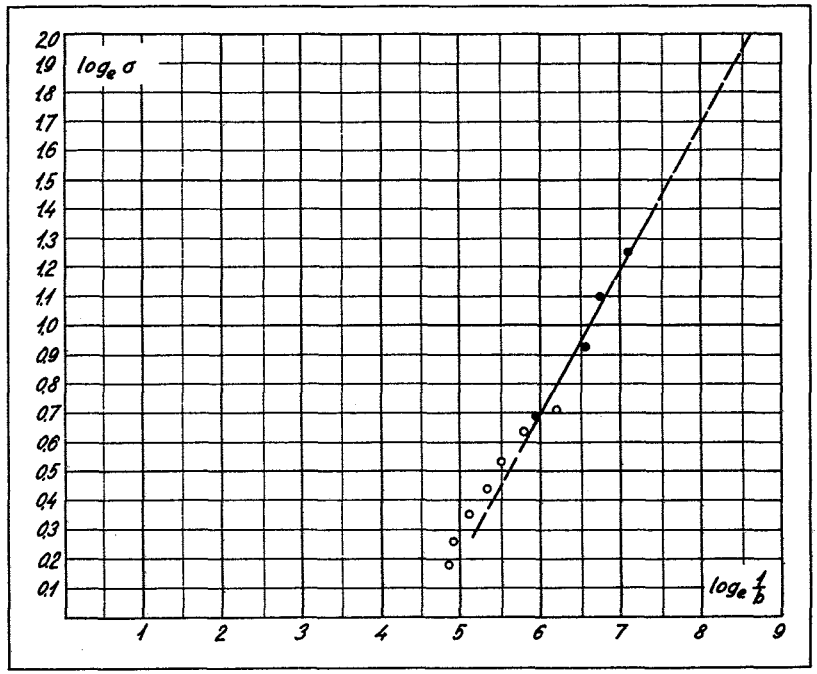

Fig. 95. Smoke contamination in the distant zone.
The abscissa is the logarithm of the non-dimensional strength of the source; the ordinate the logarithm of the non-dimensional height of the chimney. The curve corresponds to the maximum concentration at roof level and is to be found at a distance of 10-12 times the height of the chimney above the buildings.

At the level of the ridges of the houses air was sucked out for CO_2 analysis. To neutralize local effects suction was made through four tubes distributed over 10 cm of the width of the tunnel, 5 cm on each side of the centreline. The chimney was placed in the centreline of the tunnel.

For each height of chimney the concentration at ridge level was measured at different distances from the chimney. From these measurements the maximum was determined to be at a distance from the chimney of 10-12 times the height of the chimney above the roofs.

The results are shown with solid marks in Figure 95. The abscissa is the logarithm of the non-dimensional strength of source $\frac{1}{b}$; the ordinate is the logarithm of the

non-dimensional height of chimney σ.

From Sections 4.3 and 4.4 it appears that out of regard to the nearest house a chimney must be higher when placed on a house than when it is isolated; these are the conditions shown in Figure 93. If in that figure we consider the curve corresponding to $b = 3 \cdot 10^{-3}$, it will be seen that the maximum height of chimney, i.e. $\sigma = 1.9$ will be required when the nearest house is at distance $\xi = 7$. $\text{Log}_e\ \sigma = 0.64$, $\log_e \frac{1}{b} = 5.8$. This point is indicated by an open circle in Figure 93. The other curves in Figure 93 have given the open circles in Figure 95.

It will be seen that the investigations in the intermediate zone pass into the distant zone in a quite natural manner. The straight line in Figure 95 is not theoretically motivated but is in excellent conformity with the experimental results. The line has a gradient of 1/2 and the equation

$$\log_e \sigma = \frac{1}{2}(\log_e \frac{1}{b} - 4.6), \text{ whence}$$

$$\sigma = \frac{1}{10}\sqrt{\frac{1}{b}}.$$

BIBLIOGRAPHY

JENSEN, MARTIN: Shelter Effect. Investigations into the Aerodynamics of Shelter and its Effects on Climate and Crops. – Copenhagen 1954.

JENSEN, MARTIN: The Model-Law for Phenomena in Natural Wind. – Ingeniøren, International Edition, Vol. 2, No 4, 1958.

LETTAU, H.: Atmosphärische Turbulenz. – Leipzig 1939.

NIKURADSE, J.: Gesetzmässigkeiten der turbulenten Strömung in glatten Rohren. – V.D.I. Forschungsheft 356, 1932.

NIKURADSE, J.: Strömungsgesetze in rauhen Rohren. – V.D.I. Forschungsheft 361, 1933.

PRANDTL, L.: Ergebnisse der Aerodynamischen Versuchsanstalt zu Göttingen. III Lieferung, Berlin 1927. IV Lieferung, Berlin 1932.

SCHLICHTING, H.: Neuere Untersuchungen über die Turbulenzentstehung. – Naturwiss. 22, 1934.

SCHLICHTING, H.: Experimentelle Untersuchungen zum Rauhigkeitsproblem. – Ing. – Archiv, 7, 1936.

SCHMIDT, W.: Der Massenaustausch in freier Luft und verwandte Erscheinungen. – Probleme der kosmischen Physik VII. Hamburg 1925.

SUTTON, O.G.: Micrometeorology. – New York, Toronto, London 1953.